Alloxan-induced pulmonary edema in a canine model: Respiratory dynamics, blood gas analysis, alveolar fluid composition and surface tension characteristics

by

Ann Maureen Nielsen

A Thesis Submitted to the
Graduate Faculty in Partial Fulfillment of
The Requirements for the Degree of
MASTER OF SCIENCE

Department: Veterinary Anatomy, Pharmacology and Physiology
Major: Physiology

Iowa State University
Ames, Iowa

1977

TABLE OF CONTENTS

LIST OF TABLES

LIST OF FIGURES

Page

LIST OF ABBREVIATIONS

a	arterial
A	area
A-a	alveolar-arterial gradient
BE	base excess
Ch	cholesterol
C_L	dynamic lung compliance
E	expiratory
f	frequency of respirations
$\dot{F}$	rate of airflow
HCO_3^-	bicarbonate ion
I	inspiratory
k	compressibility coefficient
LPC	lyosophosphatidyl choline
N	neutral lipids
P	pressure
PC	phosphatidyl choline
PE	pulmonary edema
PI	phosphatidyl inositol
ΔP_{es}	esophageal pressure gradient
PS	phosphatidyl serine
RAW	airway resistance
RLW	relative lung weight
$\bar{s}$	stability index
Sph	sphingomyelin

ST or γ	surface tension
UnP	unidentified phosphatide
v	venous
V	gas volume
$\dot{V}$	gas volume per unit time
$\dot{V}_A$	alveolar ventilation
$\dot{V}_A/\dot{Q}$	ventilation-perfusion ratio
$\dot{V}_D$	dead space ventilation
$\dot{V}_e$	total pulmonary ventilation
V_t	tidal volume
W/D	wet weight/dry weight ratio
W_{El}	elastic work

ACKNOWLEDGMENTS

A written paragraph that has been edited is not an adequate way to recognize and thank some very special people that have helped me with this project. I would be disappointed in myself if I thought these people did not already sense their importance to me.

"Clothesline lungs and Willie curves; she knows them oh so well,
A patient lady who kept me sane, but Lucy would never tell.
Virgil found my Rottinghouse and saved the 32's,
He 'loaned' me tubes, gave me pent. and fixed the P_{O_2}.
Rose and Grace cleaned up the wax and gave me my first knife,
And big Doug Bates held the dogs which surely saved my life.
Downstairs Art would prime the Wang and watch me 'Error' my means,
While Bud built shelves and drilled the holes--all in those green jeans.
Without their help its plain to see; grad date wouldn't be for eons,
Most important of all, I claim them as friends, good people,
hard workers, NOT PEONS!"

Dr. Cholvin, I thank you for giving me a long chance at succeeding in graduate school in the first place in spite of my shaky background and then for encouraging me NOT to give up three weeks after beginning. Dr. Engen deserves a medal for his steady involvement and interest in my immediate and future progress. His patience with me in learning as well as in laughing is a virtue. And with a Dad who says ". . . just do your best honey . . ." and a Mom who encourages me to ". . . follow my own star . . .", everything is easy and well worth it.

INTRODUCTION

Pulmonary edema is the progressive filling and subsequent storage of fluid in the bronchial tree and alveoli which impedes gaseous exchange in the lungs. The prevalence of this disease under widely varying circumstances, i.e., cardiac disease, cerebral trauma, and multiple fractures, has promoted numerous investigations into its pathogenesis and sequalae of events during development. We believe that most of the confusion that exists concerning acute lung edema has arisen from the failure to realize explicitly that water movement is a physio-chemical process and can be accounted for in those terms. Our study was aimed at describing precisely several aspects of physical and chemical respiratory variables related to pulmonary edema.

Pulmonary mechanics, blood gas analysis, and qualitative and quantitative characterization of alveolar lining material were studied in five normal and 4 alloxan-induced pulmonary edema dogs. The rationale for using alloxan as a model of acute edema was based on its production of microcirculatory injury with subsequent contact between serum components and extravascular tissues (12, 53, 226). Respiratory mechanics were studied in hopes of selecting early dependable measurements of edema formation. We further attempted to relate the physiological action of alveolar lining material to respiratory dynamics in an effort to show how alterations in the physical and chemical properties of the lung lining are involved in edemagenesis.

The review of literature and details of our study which follow is an attempt to describe the clinical symptoms, morphological alterations, and

physiological consequences of abnormal water movement from the capillary to the alveolar lumen. We intend to provide the theoretical and historical evidence for information concerning the genesis and development of acute pulmonary edema.

LITERATURE REVIEW

Pulmonary edema (PE) may be described as abnormal extravascular water storage in the lungs. To determine the intricacies and complexities between cause and effect in the mechanisms by which lung edema occurs in disease or by experimental induction is a difficult task. Two hundred years of literature attest to this in that the condition is yet unresolved. In 1878 Welch (245) described the major mechanism in acute PE, namely ". . . a disproportion between the working power of the left ventricle and the right ventricle of such a character that, the resistance remaining the same, the left heart is unable to expel in a unit of time the same quantity of blood as the right heart . . . ." He further implicated osmotic pressure, alterations in capillary endothelium, and impaired lymphatic drainage in contributing to edemagensis.

In the past one hundred years it has become widely accepted that the development of lung edema can be primarily attributed to hemodynamic changes or to increased capillary permeability. For a complete review, see Robin, Cross, and Zelis (201). Hemodynamic edema may arise in association with elevated left atrial pressures as in congestive cardiac failure (15) and pulmonary emboli (215); while chemicals such as alloxan (12,53 69,87,226) and alpha-naphthylthiourea (65,152,219,252), hyperoxygenation (24,118), and bacterial toxins (82,99) may induce lung edema following direct damage to capillary endothelial cells. The symptoms of such pulmonary diseases as high altitude edema (124), shock lung (166), and heroin induced edema (5,111,112) do not fit nearly into the classical hemodynamic or permeability definitions of pulmonary edema. The prevalence

of these disorders has stimulated a new surge of investigations into the factors that predispose lung edema as well as reexamination of conventional ideas about water exchange within the lungs.

Visscher et al. (237) published a list of indirect determinants of experimental pulmonary edema to acknowledge the extremely wide variety of conditions and agents which are directly or more remotely associated with induction of lung edema. No single mechanism is responsible for all forms of PE, unless it be said simply that such edema is a result of an excessive rate of water movement out of the blood vessels of the lung over the rate of fluid return into the systemic circulation.

Fluid Exchange in the Lungs

According to Starling's (221) hypothesis for bulk capillary water transfer there are several factors that could lead to pulmonary edema: elevated capillary hydrostatic pressure, decreased plasma colloid osmotic pressure, increased capillary permeability to plasma proteins, increased capillary surface area, and decreased lymphatic drainage.

Starling's law of fluid exchange is expressed as $K = (P_c + \pi_{if} - P_{if} - \pi_{pl})$ where K is the filtration coefficient in ml/min/cm^2/torr, π_{pl} and P_c are capillary colloid osmotic and hydrostatic pressure, while π_{if} and P_{if} are interstitial fluid colloid osmotic pressure and hydrostatic pressure, respectively. Strict application of this law is difficult when used in studying fluid filtration within the lungs. Pulmonary capillary hydrostatic pressure is at best an estimated value in Starling's law as applied to the lungs and is most often taken to be 1 torr greater than

left atrial pressure (54). However, the effects of gravity promote a regional gradient of increasing hydrostatic pressure in dependent portions of the lung. Also, pleural forces of the lung are nonuniformly transmitted within the parenchyma promoting more subatmospheric pressure around extra-alveolar vessels than around pulmonary capillaries (107,146). A more difficult problem is that direct measurements of effective perimicrovascular fluid protein and alveolar tissue pressures have not been satisfactorily accomplished and thus are most often mere estimates based on lymph collection. Warren et al. (241) pointed out the difficulties in collecting lymph specifically of lung origin. Collection from the right cervical lymphatic duct as is often used in describing pulmonary lymph, was shown to contain intestinal chyle in 50% of the dogs they cannulated. Others (151) have concluded that collection of true lung lymph for estimating perivascular fluid parameters requires thoracotomy for visual access to efferent lung lymphatics. This is not usually practical in studying lung mechanics. However, a recent method for determining the fraction of lung lymph in the thoracic duct based on oxygen content lends some optimism to this dilemma (149). Regardless of the foregoing, Staub (224) and Taylor et al. (232) measured the protein concentration and osmotic pressure of "pulmonary lymph" and assumed that it represented perimicrovascular fluid. Others (88,130) have measured the plasma protein concentration in lung interstitium by microelectrode and concluded that the total quantity of protein is evenly distributed in the interstitial compartment. However, the protein compartment is known to be composed of two contiguous regions, a peribronchiolar space and a poten-

tial space between the basement membranes of the alveoli and their respective capillaries (162). This anatomical separation presents possible differences in fluid content which were not assessed by the previously cited studies. It is evident that irregularities in interstitial hydrostatic pressure and pericapillary protein concentration are capable of influencing fluid filtration.

Regarding tissue pressure, early investigations (100,130,135,146,187, 222) and more recent studies (89,225) present evidence that a negative interstitial pressure in the lung unlike that of other body tissues, may play a major role in directing fluid transfer from the intercellular spaces toward the lymphatic channels. Howell et al. (104) even suggest that the pressure around extra-alveolar vessels is more subatmospheric than pleural pressure. Therefore, the forces across the pulmonary capillary present a slight positive pressure gradient outward into the interstitium with the fluid then being cleared by the lymphatics. The influence of extravascular negative pressure in producing transudation of fluid from the lung capillaries into lung parenchyma was observed 35 years ago by Warren and coworkers (241).

Another theory involved in fluid movement within the lungs is the existence of an uncompensated osmotic gradient across alveolar membranes. Clements (42) further presented the idea that fluid which normally enters alveoli acts as a diluent causing a temporary osmotic gradient sufficient to enhance fluid reabsorption.

The rate of accumulation of fluid in the lungs and the ability of the lungs to maintain a "dry" state is influenced by the difference between

capillary hydrostatic pressure and the osmotic pressure of the plasma proteins (72). Guyton and Lindsey (89), studying PE induced via elevated left atrial pressure with and without reduced plasma proteins, observed that the rate of fluid transfer from capillaries to alveoli was approximately proportional to the gradient between pulmonary capillary pressure and plasma colloid osmotic pressure. Recently, Rabinovitch et al. (193) observed in patients recovering from acute myocardial infarction, a moderate increase in pulmonary wedge pressure and a reduction in plasma colloid osmotic pressure after the onset of pulmonary edema. They further reported that in the absence of lung edema, the mean gradient between these parameters was 9.7 torr which was reduced to 1.2 torr following appearance of pulmonary edema. In contrast, Levine et al. (130) observed a slow initial increase in extravascular water followed by a rapid increase, although the hydrostatic osmotic gradient remained constant; suggesting to them that lung edema does not develop at a constant rate proportional to the imbalance of forces in Starling's equation.

It has been suggested (42,86) that alveolar interfacial surface tension should be considered in the balance of forces determining normal and abnormal water exchange in the lungs. Drinker (64) provided the original theoretical background for the significance of the lining film in preventing alveolar transudation. Favoring fluid movement into the alveoli, he listed hydrostatic pressure of small blood vessels and the negative intrathoracic pressure. He considered the plasma protein osmotic pressure as the pressure opposing alveolar flooding. These factors led to a balance in favor of dry alveoli. Drinker further considered that

if hemispherical alveoli with 50 μ radii existed with a 55 dyne/cm surface tension as suggested by duNouy (66) producing a negative pressure around small blood vessels, the gradient favoring dryness would be replaced by a gradient favoring transudation. Part of the discrepant behavior of the lungs with respect to water accumulation seems attributable to the layer of surfactant lining the alveoli which will be discussed in more detail later. Accordingly, the pulmonary blood-gas barrier also exhibits several unique permeability characteristics (38) such as its relative impermeability to sodium (185) which are directly involved in the lung's water exchanging function.

Pathways of Fluid Movement within the Lungs (Figure 1)

The pathways of normal and edema fluid movement are as unclear as the driving forces previously discussed. Drinker (64), assuming a discontinuous alveolar epithelium, thought that capillary leakage filled alveolar walls and spaces simultaneously before lymphatic vessels were completely filled. Several years later, Macklin (137) proposed that bulk alveolar fluid was exhaled, although some regional lymphatic drainage was acknowledged. In contrast, Visscher, Haddy, and Stephens (237) proposed the fluid transudation sequence: intracellular (endothelial), interstitial, and alveolar, but did not discuss the temporal interrelationships among the various phases. Physiologic observations indicate that the alveolar epithelium is the least permeable component of the alveolocapillary barrier (39,56) suggesting that interstitial edema and increased pulmonary lymphatic flow must be antecedents of alveolar edema.

Figure 1. Drawing of a typical alveolo-capillary barrier illustrating the pathway of normal fluid movement within the lung.

Capillary fluid-CAP and red blood cells-RBC pass primarily through: (1) attenuated capillary endothelium-END, (2) capillary basement membrane-BM_c, (3) interstitial space-IS containing an extensive network of lymphatic vessels-Lp, collagen-C, and elastic fibers-El, (4) epithelial basement membrane-BM_{ep}, and (5) epithelial cells-EP, into the alveoli-ALV on the thick side of the alveolo-capillary barrier. The thin side of the barrier is shown to be composed of the same membranes, although the IS is generally thinner and occasionally absent in places where the capillary endothelial and alveolar epithelial basement membranes are fused (arrow).

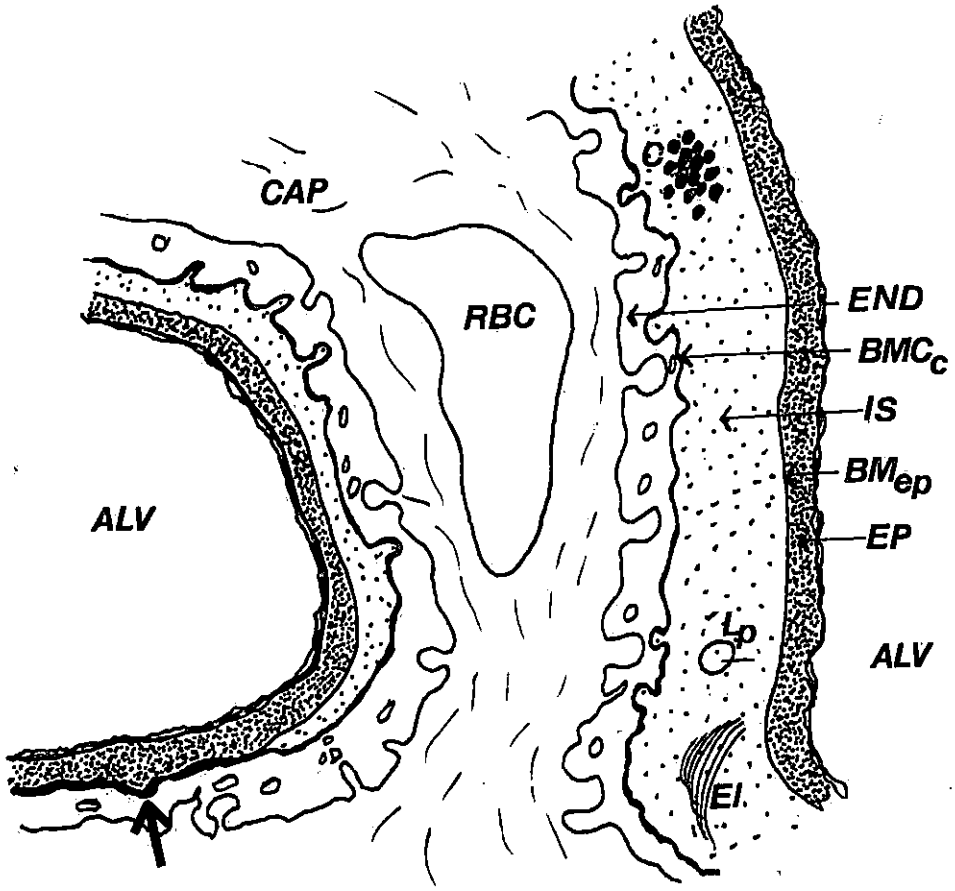

GAS EXCHANGE
(thin side)

WATER EXCHANGE
(thick side)

Based on studies of rapidly frozen lungs, Staub and workers (226) showed that the sequence of fluid accumulation in various compartments of the lungs was the same in hemodynamic and permeability types of edema. Cottrell et al. (53) reported that hemodynamic pulmonary edema results from merely an acceleration of the normal process of fluid exchange within the lung.

Fluid leaving preferential pulmonary vessels (19,190) passes into the interstices of the alveolar walls where fluid moves under the direction of a subatmospheric pressure within the interstitial space reaching the systemic veins via the lymphatics (216). Cytoplasmic swelling and fragmentation of endothelial cells has been observed in the early stages of edema (118). Szidon and coworkers (229) describe expansion of perivenous and peribronchiolar sheaths and distension of the septal lymphatics during this stage. As a result of hydrodynamic gradients and septal "sumps," edema fluid in the lung tends to collect in the interstitial spaces surrounding the bronchioles and blood vessels. When interstitial fluid pressure increases within these limiting membranes as a result of fluid accumulation, vascular congestion and/or small airway collapse are observed.

Alveolar wall edema follows the interstitial phase with expansion of the alveolo-capillary membrane as seen by electron microscopy (53,117, 211). Necrosis of Type I and Type II epithelial cells has also been observed during this stage (204). Only during the late stages of severe lung edema does fluid fill the alveoli (72). Events at the pulmonary microvascular level have been elucidated by electron microscopy using saccharated iron oxide, ferritin, and carbon black labelling to delineate

sites of fluid leakage (58,234). Possible routes of final alveolar flooding include physical rupture of epithelial cells (227), fluid passage through tight junctions (168), or fluid leakage into alveoli from an upstream site such as the small bronchioles (249). The most striking and perhaps most difficult to explain is the observation that individual alveoli of the edematous lung are either completely normal, i.e., air-filled, or completely filled with edema fluid. The lack of intermediate forms suggests that alveoli fill independently of one another (50) and in an "all-or-none" fashion as originally suggested by Drinker (64).

Pulmonary Lymphatics

To cope with leaks that occur normally and pathologically from capillaries into the alveolar septum, the lung is drained by an elaborate system of lymphatics (155) that return water and protein from the pulmonary interstitial space to the systemic veins (126). The importance of lymphatic drainage in preventing lung edema is a controversial topic. Thirty years ago, Cameron and Courtice (34) observed a significant reduction in lung lymph flow during edema which occurred simultaneously with protein accumulation in alveoli. Visscher et al. (237) reported lymph flow during acute lung edema in dogs to be about 1 ml/min, which did not even approach the 15 ml/min rate of fluid accumulation in alveoli. From these observations, they minimized the importance of lung lymphatics in maintaining dry lungs and further stated that even complete obstruction of lymphatic drainage would be capable of producing only a barely detectable edema in six hours. Three years later, Guyton and Lindsey (89) contrastingly

stressed the importance of lymphatic drainage in preventing elevated tissue colloid osmotic pressure which would lead to pulmonary edema.

The discrepancy between the amount of water that normally necessitates draining and the capacious drainage system lends credence to the idea that the major role of the pulmonary lymphatics is to return protein, rather than water, to the systemic circulation (72). Protein accumulation in the interstitial space could affect the osmotic gradient between plasma and tissue fluid in the perivascular spaces and thereby promote edemagenesis.

Unfortunately, the pathways of protein reabsorption from pulmonary alveoli have not been adequately assessed. Because lymph vessels are not present at the alveolar level (155), plasma derived proteins must travel a considerable distance in the interstitial space to penetrate lymphatics if they are to be removed from alveoli via this pathway. In fact, the delay of protein reabsorption from the alveolar lumen appears to occur in removal of protein from the interstitial space rather than in its passage through the alveolar epithelium (17).

Whether or not ultrafiltration is a normal characteristics of the alveolo-capillary barrier still remains a question. Low protein concentrations in tracheal fluid samples of cats and rabbits as compared to simultaneously collected interstitial protein content seems to bear this out (25,192). However, results are conflicting as to this functional characteristic in pulmonary diseases. Wilen et al. (251) compared total protein concentrations of blood serum and tracheal fluid of 7 cardiac patients and 8 noncardiac drug overdose patients with pulmonary edema. He found no

difference between serum protein and edema fluid protein in the noncardiac patients, while the cardiogenic edemic patients had 32% less protein in edema fluid than in serum, suggesting to them that protein movement appears to play a role in the severity and duration of PE, rather than in the initiating factor. In a similar study, Katz et al. (112) reported 60% less protein in edema fluid than in serum of cardiac patients while drug overdose patients presented with equal total protein in both compartments. Along these same lines, Aviado (13) showed that edema fluid of alloxan induced pulmonary edema in dogs resembled edema fluid of burn victims and was capable of clotting. Recent studies by Staub et al. (227) report similar findings suggesting the presence of serum protein accumulation in edematous lungs. In contrast, Koenig and Koenig (122) measured a very low protein content in cat and guinea pig edema fluid from which they concluded that excessive permeability to protein was not a requisite for lung edema.

It is possible that protein content of edema fluid may provide distinction between hemodynamic and permeability pulmonary edema, although the loci of vascular leakage in edema coupled with normal ultrafiltration sites may partially determine protein content of lung fluids (191).

Gas Exchange in Pulmonary Edema

The practical situation of unique importance in lung edema is the filling of alveoli, alveolar ducts, and the bronchial tree with fluid (205,252). Such fluid impedes or prevents aeration of alveoli and thus of the blood flowing through their capillaries. The major physiological

processes affecting the exchange of oxygen and carbon dioxide between the gas and blood of the lungs can be classified into four broad categories: (1) diffusion, (2) distribution, (3) circulation, and (4) ventilation.

The initial theoretical and technical studies in the analysis of alveolar gas and alveolar capillary blood (194,198) and the O_2-CO_2 diagram of Rahn and Fenn (195) are still employed as useful analytical tools. Prior to the 1950's, anoxemia which often accompanies pulmonary edema was attributed to impaired diffusion resulting from tissue damage. Riley and Cournand (198) showed that by measuring the alveolar-arterial oxygen tension gradient (A-a O_2) at normal and at low levels of oxygenation, one can assess the effects of impaired distribution and/or diffusion in causing arterial unsaturation. Impaired diffusion due to tissue damage at the blood-air barrier membranes causes an increase in the oxygen partial pressure gradient between alveolar gas and the blood leaving the alveolar capillaries without producing a significant carbon dioxide gradient. This effect is a manifestation of the fact that the CO_2 diffusion rate per torr gradient is approximately 25 times that of the O_2 diffusion rate in the liquid state (96). However, impaired distribution regularly affects both the O_2 and CO_2 gradients. Theoretically, the presence of a A-a CO_2 gradient should distinguish diffusion from distribution abnormalities (194).

Williams (252) concluded from studies of alveolar-arterial oxygen differences in dogs breathing various oxygen mixtures that arterial unsaturation exemplified by elevated A-a O_2 gradients during lung edema was chiefly due to altered distribution of ventilation and perfusion, i.e., $\dot{V}_A/\dot{Q}$ mismatch, in the lungs. They explained that airway obstruction

occurring in PE acted to remove large numbers of alveoli from effective ventilation such that blood flow through those areas remained venous in character.

Rahn and Fenn (195) demonstrated that if the presence of an A-a O_2 gradient while breathing room air was due to true venous admixture as proposed by Williams (252), an increased inspired oxygen should raise the A-a O_2 difference. This was shown by Gil and Weibel (80) who attributed progressive arterial hypoxemia in edemic patients to an increasing veno-arterial admixture as blood circulated through poorly ventilated or non-ventilated regions in the lung.

Several years later, Addington et al. (5) cited clinical cases of lung edema in which positive end-expiratory pressure (10 cm H_2O) coupled with 100% oxygen breathing was not effective in maintaining arterial oxygen saturation which indicated to them the presence of excessive intrapulmonary shunting. Similarly, measurements of total water content in severely edematous lungs following administration of alloxan have revealed areas of reduced perfusion (186).

The oxygen and carbon dioxide partial pressure in any alveolus may vary between that of the inspired air and mixed venous blood depending upon the ventilation-perfusion ratio ($\dot{V}_A/\dot{Q}$) which is most often measured by inert gas elimination techniques. High $\dot{V}_A/\dot{Q}$ ratios indicate equilibration of blood with inspired gas, i.e., $P_{A_{O_2}} = P_{I_{O_2}}$, whereas low $\dot{V}_A/\dot{Q}$ ratios reflect reduced gaseous exchange. In the latter case, the arterial oxygen content becomes more equal to the venous oxygen content and the alveolar P_{O_2} reflects oxygen tension in mixed venous blood. However,

overventilated regions do not make up for those which are underventilated; hence the mismatch of ventilation and blood flow results in raised arterial P_{CO_2} (246).

The idea that obstructed alveoli may exchange gas via collateral pathways from neighboring alveoli infers that carbon dioxide output can be more impaired than oxygen uptake (30,246). In such cases, pulmonary edema with hypercapnia could occur while the calculated A-a O_2 gradient would not be increased (60). In fact, C_{O_2} retention has been observed in some cases of severe lung edema (8,11). However, hypercapnia in PE is an unlikely occurrence until water has accumulated to the point of obstructing terminal airways, or ventilatory depression begins (72).

Augmenting the distribution defect, diminished ventilatory response to hypoxia has been observed in persons who have had prolonged hypoxemia (33,220). In these cases, CO_2 elimination would be impaired consequent to $\dot{V}_A/\dot{Q}$ abnormalities rather than to impaired diffusion (205,252).

Events leading to the unusual combination of metabolic acidosis with reduced alveolar ventilation were surmised by Schaaf et al. (209) studying methadone abuse patients with pulmonary edema. Respiratory center depression in these patients produced alveolar hypoventilation with development of hypercapnia, hypoxemia, respiratory acidosis, and eventually lung edema. Severe $\dot{V}_A/\dot{Q}$ mismatch due to the lung fluid accumulation alone causes hypoxemia. The magnitude of reduced blood oxygen becomes even more severe if development of metabolic acidosis due to lactic acidemia accompanies the distribution defect. There is a subsequent increase in alveolar ventilation and return of arterial P_{CO_2} to normal or even subnormal

values. Low partial pressure of CO_2 associated with low arterial pH suggest the presence of metabolic acidosis and a blunted ventilatory response to the increased hydrogen ion concentration. However, in acute lung edema, all combinations have been reported: hypercapnia with acidosis, metabolic acidosis with normal arterial P_{CO_2}, and so on. The retention of CO_2 can also be enhanced by the metabolic alkalosis that follows administration of therapeutic diuretics.

Pulmonary Hemodynamics in Lung Edema

Perfusion of lung parenchyma which affects alveolar and blood gas partial pressures depends to a large extent on the systemic and pulmonary blood pressure, volumes, and flows. Takino (230) has published the most comprehensive study on the general anatomy of the pulmonary vasculature. He reports a species specific range in muscular wall thickness which is vital to understanding the mechanism by which capillary pressures are controlled by bore size. Visscher et al. (237) outlined some of the indirect determinants of hemodynamic and/or permeability lung edema upon pulmonary capillary pressures (Table 1).

In a study concerning the local mechanisms involved in alloxan-induced pulmonary edema, Aviado (12) reported that pulmonary hypertension and congestion occurred in two stages. Using P^{32} labeled erythrocytes and I^{131} labeled albumin they detected an initial fall in pulmonary blood volume followed shortly by a massive increase in pulmonary blood volume. The first effect was attributed to arteriolar constriction with the latter due to venular constriction. Accordingly, Haddy et al. (92) observed that

Table 1. Determinants of pulmonary capillary pressure considering in each case a change in only one variable at a time[a]

Variable	Direction of change	Direct effect on capillary pressure	Effect on pulmonary venous pressure
1) Pulmonary arteriolar bore	Constriction	Fall	Fall
	Dilation	Rise	Rise
2) Pulmonary venule bore	Constriction	Rise	Fall
	Dilation	Fall	Rise
3) Pulmonary artery pressure change without bore change	Rise	Rise	Rise
	Fall	Fall	Fall
4) Pulmonary venous or left artrial pressure change	Rise	Rise	Pulmonary venous pressure is determining factor.
	Fall	Fall	

[a]Adapted from original table by Visscher et al. (237).

pulmonary venous pressures greater than 15 torr were associated with significantly higher lung weight/heart weight ratios indicating to them that excessive water had accumulated in the lungs. More precisely, Guyton and Lindsey (89) found that the rate of lung fluid accumulation assessed by lung weight/body weight ratios was directly proportional to the rise of left atrial pressure above a "critical flooding" pressure which they determined to be 24 torr in a canine model. In contrast, McHugh and coworkers (142) reported that left ventricular filling pressure did not always correlate with radiographic signs of pulmonary edema. Similarly, Staub et al. (227) have recently shown that alloxan-induced pulmonary edema occurs in the presence of a constant left ventricular end-diastolic pressure.

Until recently, mitral stenosis and aortic obstruction which are disorders associated with lung edema were thought to be due to retrograde pressure elevation experienced by the pulmonary vascular bed. However, Gorlin et al. (85) deduced that elevated pulmonary vascular volume contributes to edemagenesis in these diseases as well. Systemic hypervolemia has also been implicated in the development of PE and is even thought to be the major precipitating factor in "shock lung" (191). Opdyke et al. (173) was the first to report that left atrial pressure increased more than right atrial pressure by infusion of blood or saline resulting in lung edema. Two years later, Haddy et al. (91) observed the identical response. Excess intravascular volume resulted in increased right heart filling which was associated with increased pulmonary artery pressure such that pulmonary venous pressure was also elevated. Staub et al. (226) reported that increased vascular volume due to transfusion caused edema only in the dogs with a persistent left ventricular end-diastolic pressure greater than 20-25 torr. About the same time, Levine et al. (130) induced pulmonary edema in dogs by a combination of increased pulmonary capillary pressure and hemo-dilution lending further credence to the importance of systemic vascular volume in the pathogenesis of lung edema. Recent studies by Brigham and Snell (27) report that such volume overload results in an elevated systemic blood pressure with elevated pulmonary vascular pressures as well.

Low oxygen tension has also been implicated in causing small pulmonary arteries to constrict resulting in pulmonary hypertension and edema although the results are conflicting. Relying primarily on serial measurements of lymph flow, Drinker (64) stressed the importance of hypoxia in

causing fluid exchanging pulmonary vessels to leak. Seven years later, Courtice and Korner (55) demonstrated that hypoxia alone had no edemagenic effect on rabbits, but that if low oxygen breathing occurred concomitantly with fluid infusion pulmonary edema ensued. They suggested that hypoxia caused a reduction in cardiac output with a compensatory systemic vasoconstriction resulting in a shift of systemic blood volume into the pulmonary vascular bed with elevated pressures resulting.

Along these same lines, Rivera-Estrada et al. (199) produced an increased hydrostatic pressure gradient across the pulmonary vascular bed by administering 5% oxygen in nitrogen to dogs anesthetized with pentobarbital. They hypothesized post-capillary (venular) resistance to be the cause of the pressure gradient based on their observation of a significant gradient between pulmonary veins and left atrium in the absence of left ventricular failure. They simultaneously measured a decline in the pressure gradient between mean pulmonary artery pressure and mean arterial wedge pressure which they explained was the result of arteriolar dilation. Viswanathan et al. (238) showed that high altitude pulmonary edema patients show more pulmonary hypertension and hypoxemia during low oxygen breathing than controls, which suggested a tendency to pulmonary vasoconstriction in response to hypoxia in subjects prone to altitude PE. Wood and Roy (253) have shown that hypoxia causes peripheral vasoconstriction with a shift of blood from the systemic circulation to the pulmonary circulation such that capillary pressure increase promoting a tendency toward fluid transudation into alveoli. Recent studies by Kleiner and Nelson (121) indicate that the most plausible explanation of high altitude PE is nonuniform arteriolar vaso-

constriction in some lung fields resulting in hyperperfusion and pulmonary hypertension with exudation of fluid into the interstitial spaces and alveoli. In addition to the capillary bore changes, low oxygen tension causing increased capillary permeability must be considered (101,125).

Pulmonary Mechanics

Routine clinical tests of lung function involve diffusing capacity determination, lung volume subdivisions by spirometric analysis, and morphometric point counting (243) to determine conductive (broncho-vascular) and nonconductive (respiratory) volume fractions. Nicoloff et al. (169) reported that heroin-induced edemic patients presented with reduced lung volumes and diffusing capacities. Karliner et al. (111) evaluated lung function in edemic patients during the recovery period and at 10 and 12 weeks later, reporting that although airway obstruction was effectively cleared, vital capacity and total lung capacity were still severely impaired. Schaaf et al. (209) similarly observed reduced functional vital capacity and total lung capacity coupled with impaired gas transfer during a five month recovery period. Morrison et al. (160) reported a 50% reduction in lung volume after an acute bout of lung edema.

Respiratory patterns observed during the pathogenesis of lung edema include apnea, dyspnea, orthopnea, hyperpnea, and tachypnea. The characteristic pattern observed in pulmonary edema induced by alloxan is a brief period of apnea immediately following the injection with progressively increasing polypnea (14). Unfortunately, few studies have been undertaken to relate cyclic respiratory patterns to the severity or stage of edema

let alone to understanding the physiological mechanisms underlying the mechanical ventilatory responses observed in pulmonary edema. Mead and Collier (144) proposed that intermittent single large inflations during tidal breathing, as are often observed in acute lung edema, could restore compliance to its normal value by increasing internal surface area such that more surface active material could be recruited to the alveolar surface thereby enhancing its stability. Fishman (72) suggests that the anatomical location of juxtapulmonary capillary receptors (J-receptors) in the interstitial space are such that excess pericapillary fluid accumulation in PE acting to stimulate these J-receptors theoretically promotes increased ventilatory activity particularly during the "interstitial stage" of lung edema. Paintal (176) reported that administration of alloxan was followed by bursts of excitation by these receptors.

Recently more quantitative and meaningful information concerning the mechanical performance of the lung has been obtained from determinations of pulmonary compliance and airway resistance. Otis et al. (175) found that in the presence of airway obstruction, lung compliance (C_L) falls as respiratory rate increases. Hughes et al. (105) studied lung compliance in pulmonary congestion and edema in rabbits and cats and related changes in C_L to perfusion pressures as well as to increased lung weights. Guyton and Lindsey's (89) calculations of compliance revealed that the intrapulmonary pressure required for a given change in volume was considerably greater in the case of edematous lungs than in nonedematous lungs. He warned that this was a general trend in extreme cases, occurring with so much overlapping that its use in assessing PE clinically was

probably not reliable. Regardless of this, elevated as well as reduced dynamic compliance have been reported in a variety of species as the indice of lung edema. Part of the inconsistencies in the absolute values reported for C_L as well as the changes (increase or decrease) observed in C_L during edemagenesis may reflect the variables used to calculate or measure direct compliance. Intrapleural, intraesophageal, transpulmonary, and alveolar pressures have all been used. The compliance value calculated as tidal volume divided by the change in pressure includes the elastic components of the chest well, diaphragm, airways, and connecting tubing as well as the lung tissue itself. This offers further evidence for inconsistent changes in C_L.

Whether reduced compliance reflecting increased lung stiffness is due to congestion and interstitial edema fluids and/or to loss of alveolar lining material is a controversial matter. Early studies by Cook and coworkers (50) proposed that a large fall in compliance out of proportion with lung volume was the pattern of abnormal mechanics which suggested alveolar closure. He further showed that since edematous lungs manifest marked static hysteresis during respiratory maneuvers at distending pressure of 30 cm H_2O beyond the tidal range that surface phenomena were responsible for the mechanical behavior of the diseased lungs. Two years later, Clements (42) studied alveolar stability from expansion index determinations at 5 cm H_2O transpulmonary deflation pressures which corresponds to resting end-expiratory pressure. They deduced from their work that smaller expansion indices resulted from unstable lungs having relatively more alveoli that have prematurely closed, hence a smaller alveolar

$$\text{Expansion Index}^{1} = (V_{FR} - V_D)/(V_{max} - V_D)$$

volume relative to maximal volume. About the same time, Colebatch and Halmagyl (48), studying the effects of fluid in the lungs, found that there was a large fall in lung compliance within two minutes after introducing as little as 1 ml/kg water into the lungs. Widespread closure of terminal air units thereby reducing the number of distensible alveoli participating in volume change was again suggested. Johnson et al. (109) observed premature closure during pressure-volume studies of fluid filled lobes such that on deflation while still at relatively high transpulmonary pressure, many alveoli closed. Frazer and Weber (74) have recently shown that premature closure and gas trapping can be illustrated by the fact that pressure-volume curves do not form closed paths at zero or even negative transpulmonary pressures.

Airway obstruction is a major complication in pulmonary edema and is manifested in breathing resistance. The vicious cycle is begun whereby edema fluid obstructs or compresses conducting airways causing breathing resistance to become apparent which in itself enhances fluid transudation into alveoli. Reichsman (197) was the first to show that inspiratory resistance in dogs and rats was followed by lung edema. Two years later, Zinberg et al. (257) demonstrated that expiratory resistance over a long period of time had the same effect of producing lung edema. Shortly thereafter, Haddy and coworkers (91) clarified the mechanism of resistance breathing in producing pulmonary edema. By using a flexible catheter system to measure pulmonary artery and pulmonary venous pressure, they

---

[1] Functional residual volume (V_{FR}), dead space volume (V_D) and maximum lung volume at peak inspiration (V_{max}) are measured in ml.

found that edemagenesis associated with airway resistance breathing was apparent only when pulmonary vein pressures were greater than 15.5 torr. Visscher et al. (237) offered a theoretical explanation for edema resulting from inspiratory and expiratory resistance to airflow. The former causes a more negative pleural pressure with increased right heart filling such that pulmonary arterial and thus capillary pressures become elevated, conditions which lead to PE. Expiratory resistance on the other hand causes elevated pleural pressures with a decreased right heart filling, such that a temporary fall in pulmonary microvascular pressure is observed. However, prolonged reduction in right heart return results in cardiac asphyxia with subsequent cardiac failure which ultimately causes elevations in pulmonary vascular pressures leading to lung edema.

Alveolar Surface Tension in Pulmonary Edema

By comparing pressure-volume characteristics of lungs inflated with gum arabic solution and of the same lung inflated with air, Von Neergard (239) estimated that 2/3-3/4 of the lung's elasticity was derived from interfacial forces. In the summary of this classical paper he wrote: "It is possible that the surface tension of the alveoli is decreased below that of other physiological fluids by accumulation of surface active material, in accordance with Gibbs-Thomsen's law." Von Neergard was correct in his prediction of the presence of alveolar surfactants, but these substances are not reversibly adsorbed Gibb's films; rather they are insoluble films (43). Unfortunately his (Von Neergard) work attracted very little attention for 25 years; then a variety of methods evolved for

studying surface tension phenomena, such as pressure-volume relationships in bubbles (179) and in whole lungs (30) from which static and dynamic compliance determinations are made, Langmuir-Adam troughs and the Wilhelmy surface tension balance (40,41,128,193,235), and microscopic observations of bubbles in air-saturated water (178,179,180,181) from which stability ratios for lung fluids have been determined.

A wide variety of preparations have been used as sources of surface active material. These include extracts of homogenized whole lung, saline removed from lungs by lavage, bubbles squeezed from the cut surfaces of lungs at autopsy, and pulmonary edema fluid. In 1960, Bondurant et al. (21) developed a method for the large scale extraction of surfactant from the lungs. This important step made possible unequivocal studies of the chemical composition of the material and greatly extended the vista for investigation of its function, although some inferences had already been made concerning the functional significance of the alveolar lining material.

Macklin (137) postulated that these substances were functionally significant in maintaining alveolar stability, in preventing adhesion of alveolar walls after prolonged lung collapse, in inhibiting bubble formation within alveoli, in trapping and transporting foreign particles, in facilitating gas transport, and in retaining contents of edematous alveolar walls. Although his methods were rather crude, his theories have to a large extent been borne out by time.

Pattle (179) deduced that since bubbles expressed from sectioned lungs failed to shrink in air-saturated saline that the lungs must contain

a powerful surfactant capable of reducing alveolar surface tension to nearly zero. He theoretically explained how the stability of terminal air spaces depended upon a low surface tension lining material. Realizing that water had a surface tension (70 dynes/cm) seven times higher than the lower limiting tension of lung extracts, he proposed that the formation of a water film in terminal air spaces would cause immediate alveolar collapse due to the unbalanced forces. He further explained how widespread distribution of a water film causing extensive atelectasis could be the cause of reduced compliance observed in fluid filled lungs. About the same time, Clements, Brown, and Johnson (45) also predicted that the mechanical behavior of the lungs depended upon the characteristics of a film lining the respiratory surface. They suggested that the stabilizing effect on the stress-strain relationship of alveoli was due to a substance whose surface tension varied as a function of alveolar volume and surface area.

Several years later, Clements (41) developed a mathematical model explaining lung behavior in terms of surfactant characteristics. By simultaneously plotting surface tension against surface area during compression and expansion of normal lung extracts, they found a variable surface tension (5-40 dynes/cm) with marked hysteresis during the cycle. In contrast, extracts treated with a nonionic detergent were found to have a constant surface tension of 32 dynes/cm throughout the cycle. This variation of tension with surface area was expressed as surface elastance

$$(s) = Ad\gamma/dA$$

where (s) is surface elastance, A is surface area, and γ is surface

tension. The inverse of surface elastance provides a coefficient of compressibility, the minimum of which can be used to characterize the type of surface film. Brown et al. (30) determined this value to be between 0.010-0.020 which placed alveolar lining material in the category of liquid films.

In assessing the role of surface tension in producing atelectasis, the work of Levine and Johnson (128) must be included. They made a series of surface tension measurements on a Langmuir-Adam trough of extracts from artificially degassed as well as normally aerated lungs, finding that degassed lungs and saline filled lungs exhibited markedly reduced surface activity, i.e., increased minimal surface tension and reduced hysteresis. Extracts from atelectic lungs of infants experiencing severe respiratory distress have similarly failed to show low surface tensions lending further support to the idea that alveolar stability depends upon the presence of surface active material (10).

Johnson et al. (109) reported that two to six hours after instilling saline into dog lungs, there was a significant negative correlation between maximum inflation volume and maximum surface tension as well as between minimum volume during deflation and minimum surface tension. They concluded that intra-alveolar fluid either inactivated or displaced the surface active material from the alveolar lining. They explained that in the absence of a lining film two results would follow. First, assuming that the surface tension of the lung lining had become comparable to that of blood serum, i.e., 55 dynes/cm, the lung would require a much larger internal pressure to keep it open. Hence, a reduced compliance is apparent. If that pressure were not applied, atelectasis would occur. Secondly, if in the absence of the lining film the lung were kept open by

internal pressure, the surface tension would cause transudation from the blood into the alveoli.

Blood or serum present in alveoli as a result of microvascular transudation in pulmonary edema could theoretically cause destruction, removal, and/or inhibition of the alveolar lining material. Tierney (235) found that the minimum surface tension (0-5 dynes/cm) of rabbit lung extracts was inhibited, i.e., elevated to 15 dynes/cm, when (1) the extract was prepared with distilled water rather than saline, (2) the temperature was elevated from 22° to 42°C, (3) incubation with phospholipase C was carried out, (4) cholesterol or oleic acid was added to the extract, and (5) blood or serum was added to the sample. All of these conditions are potentially present in pulmonary edema.

It is conceivable that alterations in surfactant could be due to changes in electrolyte content of alveoli since changes in the hypophase have been shown to alter surfactant surface tension-surface area curves (208). Variations from normal surface tension characteristics are not always the result of diminution or absence of a specific surface active component but may be due to the interaction of various factors which prevent biosynthesis of surfactants in the presence of adequate substrate.

Composition of Alveolar Lining Material

Early studies by Pattle (182) describe an insoluble lining film about 50 Angstroms thick in contact with the air. Between this layer and the epithelial cells is a saline dispersible layer of approximately 300-

20,000 Angstroms thickness often referred to as the "hypophase" which acts as a reserve of the pulmonary surfactants.

Histochemical characterization by light and electron microscopy of the alveolar lining layer has revealed specific molecular components. The extracellular alveolar lining layer appears to be composed of both a surface film consisting primarily of phospholipids and polysaccharides, and a homogeneous hypophase that occasionally contains tubular myelin figures (80). Whether the surface active phospholipids are free in the alveolar lining or present in chemical combination with other molecules is not definitely known.

The material comprising the alveolar-atmospheric interphase is thought to be composed of at least eight lipid components to which Klaus et al. (120) and Pattle and Thomas (183) have assigned functional roles. The lipids have been categorized as follows: (1) unsaturated phospholipids, predominantly dipalmitoyl lecithin for providing low surface tensions on deflation, (2) nonphosphated lipids to prevent oxidation of the phospholipids, and (3) protein skeletons for providing structural support.

Abrams (2) reported a 40.6% lipid content in mammalian lungs which he further separated into 70% phospholipids, 10% fatty acids, 14% triglycerides, 6% free cholesterol, and less than 0.5% cholesterol esters. Several investigators have reported that phosphatidyl choline (29,120) and sphingomyelin (72) are the specific phospholipids at the alveolar-air interface which are essential for the maintenance of alveolar stability. Clements (44) determined surfactant content and lipid composition of homogenized lungs in 11 vertebrate species and reported that saturated

phosphatidyl choline was directly related to the alveolar surface area. Similar reports by Goerke (83) showed interspecies variation in ^{32}P incorporation into lung phosphatidyl choline which was significantly correlated with alveolar diameter and respiratory rate.

Although there is general agreement that the pulmonary surfactant contains lipids, there is controversy over the protein and carbohydrate content. Macklin (137) and Pattle (180) originally hypothesized the alveolar lining material to be of a mucoprotein nature. Other investigators considered the surface active lining material responsible for alveolar stability to be of a lipoprotein nature (2) with the activity residing in the phospholipid fraction (20,62). In contrast, Scarpelli et al. (208) reported that surfactants in dog and rabbit lung extracts contained lipids and carbohydrates, but no lipoproteins.

Evidence that lung surfactant is a lipoprotein complex is indirect (63,76,114). Pattle and Thomas (183) using infra-red absorption determined that bovine alveolar lining material consisted of approximately 1% protein. Fujiwara and coworkers (78) calculated a stability ratio of 0.82 for bovine lung foam, indicating surface active material. The stability ratio of the same foam after lyophilization was 0.65 and remained constant for 5 days at 37°C in air suggesting to these workers that the alveolar lining material contained an antioxidant. They hypothesized this stability characteristic to be due to the presence of protein in their extracts, since it is known that purified lipids are highly susceptible to atmospheric oxidation (95). The first direct evidence that lung surfactant was a lipoprotein was presented by Abrams (2) who isolated a lipoprotein

from lung homogenate which he reported to be surface active with an electrophoretic mobility of an alpha-globulin. Using lung homogenate, he found that 40 μg of a crude lipoprotein extract lowered surface tension to 8 dynes/cm on compression to 20 cm^2 in a Wilhelmy balance, while separation of purified lipids from the crude extract resulted in a minimum surface tension of only 20 dynes/cm. From this he stressed the importance of the protein interaction in maintaining alveolar stability.

Studies have provided kinetic evidence for intracellular protein transport in the lung (37,139) and glucose incorporation into glycoprotein (255). Several recent biochemical analyses have demonstrated the presence of at least three serum proteins, albumin, IgG globulin, and an $alpha_1$-globulin, in the alveolar lining material (115,119). It is possible that these results represent serum contamination (208), although Bignon et al. (18) suggest that albumin and IgG are autologous proteins and may have a functional role in surfactant stability. Recently two nonserum proteins comprising 10% of the surfactant dry weight, with molecular weights of approximately 11,000 and 34,000 daltons have been isolated from canine surface active material (115). Massaro (138) provided substantial evidence that the intact lung meets all the criterion characteristic of protein secreting cells.

Studies of the turnover rate of surface active material have shown that the lipid and protein components are continuously secreted (184). Young and Tierney (256) made quantitative determinations on the amount of dipalmitoyl lecithin (DPL) in lung tissue and lavage fluid of rats finding that DPL in lavage fluid was 12.1% of the total DPL recovered from lung

tissue plus lavage fluid. Accordingly, Massaro and Massaro (140) found that 12.4% of the total protein in lavage fluid and lung tissue was present in lavage fluid alone. It is unknown if there is a relationship between the distribution and/or synthesis of DPL and protein.

METHODS AND MATERIALS

Design

Nine mongrel dogs (13-20 kg) were obtained from Laboratory Animal Resources (Iowa State University) after routine worming, vaccination, and inoculation. The animals were randomly divided into two groups. Group I consisted of four dogs for alloxan-induced pulmonary edema. Group II consisted of five dogs which served as controls. The animals were anesthetized with sodium pentobarbitol (30 mg/kg, i.v.) initially with subsequent administration of 16 mg doses as required throughout the experiment. Rusch 12-13 mm (i.d.) cuffed endotracheal tubes were used for entubation. The dogs were strapped in dorsal recumbency on a thermal pad. A standard Lead II electrocardiogram was continuously recorded and rectal temperature was determined intermittently. A 45 minute time period was required to surgically prepare the animal, check calibrations of recording devices, and connect the various leads to the animal. Respiratory rate, electrocardiogram, and peripheral signs (palpebral reflex, jaw tone, and withdrawal reflex) were used to determine the level of anesthesia. After all preparations were complete and the animal appeared stabilized, baseline values were determined for pulmonary function, blood gas tensions, electrocardiogram, blood PCV and hemoglobin. Following baseline recordings, the animals in the edema group were injected with alloxan, monohydrate[1] at a rate of 1 mg/kg·s (dose = 140 mg/kg). The control animals

---

[1] J. T. Baker Chemical Co.

were injected with 0.15 M sterile saline at the same rate and volume (1.8 ml/kg) as the alloxan group. Anaerobic arterial and venous blood samples were collected and respiratory parameters at 30, 60, 90, and 120 minutes post-injection of either saline or alloxan. The last recording period was followed by a pulmonary "lobar" lavage technique developed by this laboratory. Lungs were grossly examined and excised for determination of wet weight/dry weight ratios. Specific blocks of tissue were removed from the lungs, pancreas, and cardiac muscle for light and electron microscopic examination. The heart was excised, weighed, and inspected for dirofilaria. One animal was infested with dirofilaria, and was discarded from the study.

Pulmonary Function

Intrapleural pressure was estimated from intraesophageal pressure (P_{es}) relative to atmospheric as measured by an open-end fluid-filled catheter (polyethylene tubing 240) attached to a Statham P23Db pressure transducer. Catheter placement was determined by locating the level of the most negative pressure during inspiration in the absence of cardiac interference. Inspiratory airflow ($\dot{F}_I$) and expiratory airflow ($\dot{F}_E$) were measured in liters/min with a Fleisch #0 pneumotachograph attached to the endotracheal tube. Tidal volume (V_t) was computed on-line by electronic integration of airflow (Appendix A). Inspiratory airway resistance (RAW_I), expiratory resistance (RAW_E), dynamic lung compliance (C_L), and flow-volume ($\dot{F}$-V) curves were simultaneously plotted by a Hewlett-Packard 7035B X-Y recorder (Appendix B).

Blood Collection and Analysis

Forty cm catheters[1] were placed in the femoral artery and femoral vein after surgical exposure for blood collection from the thoracic aorta and inferior vena cava, respectively. Sterile saline (0.15 M) was used to keep catheters patent throughout the experiment. Anaerobic samples were collected in heparinized (1000 I.S.P. units/ml) three ml glass syringes and refrigerated at 4°C for subsequent analysis of oxygen partial pressure (P_{O2}), carbon dioxide partial pressure (P_{CO2}), pH, bicarbonate ion (HCO_3-), and base excess (BE) by a pH/Blood Gas Analyzer 513 (Instrumentation Laboratory). Packed cell volume (PCV) was determined by a microhematocrit method. Hemoglobin (Hgb) in g/100 ml was determined by the cyanomethemoglobin method. Both PCV and Hgb were determined at the beginning and end of each experiment.

Pulmonary Lobar Lavage

Following the last recording period, ca. 120 minutes post-injection, a lobar lavage was performed using 100 ml of sterile saline (0.15 M) as the lavaging fluid. Three Foley catheters attached end-to-end with blunt tip hypodermic needle barrels provided a long tube with a small enough outside diameter to pass down the endotracheal tube to the level of the bronchioles (2-4 mm diameter) for isolating a single area of the lung. Ease of manipulation was aided by inserting a thin guide wire down the length of the catheter. When resistance was encountered while placing the

---

[1] Polyethylene 205 tubing from Intramedic Corp.

catheter, forward motion was stopped, the catheter was retracted approximately 2 cm, and a 3 ml balloon cuff was inflated with saline to secure the catheter in place. The lavaging saline was introduced very slowly in 15 ml aliquots, left in for one minute, and slowly withdrawn. Saline introduced too rapidly or in larger volumes was found to cause alveolar rupture as evidenced by blood in the sample as well as cause mechanical displacement of the lobar catheter. This procedure was adapted in order to eliminate a majority of the contaminants indigenous to the mucociliary lining which are consistently found in standard tracheo-bronchial lavage collections. We generally recovered 80-85% of the original lavaging fluid in control dogs. However, in one case of edematous lungs, lobar fluid could be obtained without the use of a lavaging fluid at all. The lavage fluid was centrifuged at 890 g for 30 minutes for removal of cellular contaminants. The supernatant was dialyzed against distilled water until less than 0.50 ppm could be detected in the dialyzing solution. The dialysate was lyophilized,[1] weighed, and stored in the dark at 4°C until needed.

Lipid Analysis

Total lipids were extracted from the lyophilized lavage material in chloroform/methanol (2:1, v/v) according to Folch, Lees, and Sloane-Stanley (73). The extract was washed with 0.74% aqueous potassium chloride to remove traces of nonlipid contaminants. The isolated chloroform

---

[1] Lyophilized at -75°C, -50 μ pressure in a Lab Con Freeze Dry-5 apparatus.

fraction containing the lipids was gently evaporated at 47°C under a stream of nitrogen. The moist residue was redissolved in 2 ml chloroform/methanol (1:1, v/v) and stored under nitrogen at -20°C for subsequent analysis.

Total lipid determination

An aliquot (0.5-1.0 ml) of the lipid extract was dried (110°C) to constant weight in a tared aluminum pan for gravimetric determination of total lipids.

Quantitative phospholipid identification

Phospholipids were separated by thin layer chromotography on silica gel plates.[1] Chambers were equilibrated for 1 hour prior to plate development in a chloroform/methanol/water (80/25/4, v/v) solvent system. Migration was allowed to proceed to a distance of 14 cm at room temperature (24°C). Phospholipid spots were identified for R_f determinations by iodination and then scraped into storage vials for subsequent phosphorous analysis which was always performed within 24 hours of the elution. Standard lipids[2] were run simultaneously on each plate. Phosphorous content was determined colorimetrically according to the procedure of Morrison (159). Optical density was determined at 822 nm. A standard curve was prepared by spotting known quantities (1-5 μg) of DL-α lecithin on TLC plates, eluting these spots, and determining their phosphorous content.

---

[1] LQD preabsorbant 250 μ thick plates obtained from Kontes.

[2] Lipid standards (>95% pure) obtained from United States Biochemical Corp. included phosphatidyl-L-serine, phosphatidylethanolamine, sphingomyelin, DL-α-lecithin, cholesterol, lysolecithin, and phosphatidyl inositol.

Surface Tension Measurements

Surface activity of lyophilized alveolar lining material (ALM) and lipid extracts (LEX) was determined by means of a modified Wilhelmy surface-balance completely enclosed within two plexiglass dust shields. The ALM was dissolved in 0.15 M sterile saline to a final concentration of 20 µg dry weight per µl. The LEX were dissolved in chloroform/methanol (1:1, v/v). Maximum trough area was 35 cm^2 which was reduced to a minimum surface area of 10 cm^2 upon compression. Surface tension was measured with a platinum plate (2 cm perimeter), connected to the arm of a Grass FT03C force displacement transducer. The signal was displayed on a Hewlett-Packard 7035B X-Y direct writing pen recorder which simultaneously plotted surface tension (Y-axis) versus area of the bath (X-axis). The subphase in the trough consisting of 30 ml 0.15 M saline at room temperature (25°C) was placed in the trough and allowed to equilibrate for 10 minutes. Five compression-expansion cycles were run on saline to insure cleanliness in the system. When hysteresis was apparent, the bath was removed, cleaned, refilled, equilibrated, and cycled again until a straight and repeating pen tracing at 72-75 dynes/cm was effected. The sample was layered on the subphase at maximum surface area by slowly dripping 10-40 µl volumes from the tip of a Hamilton syringe through a small port opening in the dust shield. After a 10 minute equilibration period, ten compression-expansion cycles were performed with a periodicity of 8 seconds. The procedure was repeated at different sample volumes until the lowest minimum surface tension was reached. A duplicate run of the ideal sample volume was then performed to insure repeatability. Maximum and

minimum surface tensions (γ_{max} and γ_{min} respectively) were measured for each sample from which the stability index was calculated as follows:

$$\text{Stability index } (\overline{S}) = 2\ (\gamma_{max} - \gamma_{min})/(\gamma_{max} + \gamma_{min})$$

where surface tension is expressed in dynes/cm. Coefficients of compressibility (k) were calculated for the compression isotherm of cycle 1 as follows:

$$k = dA/Ad\gamma$$

where dA is the change in surface area, $d\gamma$ is the change in surface tension, and A is the maximum surface area (35 cm^2).

Histological Techniques

Blocks of tissue were taken from the left apical, left diaphragmatic, and right cardiac lobes for histological and ultrastructural examination. Tissues were processed for light microscopy by immersion in Bouins fixative at room temperature (25°C) for 16 hours followed by two changes of 50% ethanol (12 hours). Partially dehydrated tissues were further dehydrated in graded ethanols, infiltrated with xylene and embedded in paraffin in an Autotechnicon Model 2A. Tissues for electron microscopy (Appendix D) were fixed in 4% glutaraldehyde, post-fixed in osmium tetroxide, infiltrated with acetone and embedded in an Araldite-Epon mixture. Thin sections were prepared with a Sorvall Porter-Blum MT-2 ultra-microtome. Grids were stained with lead citrate/uranyl acetate and examined with a Hitachi HU-12A electron microscope.

Protein Analysis

Molecular weights of proteins in lyophilized alveolar lavage material were determined by SDS gel electrophoresis as described by Weber, Pringle, and Osborn (242) with some modifications by our laboratory (Appendix C). Buffers, separating gels, and samples were prepared on the same day as the electrophoretic run was made. Triplicate samples (100 µl) were run simultaneously with bovine serum albumin (m.w. 68,000), catalase (m.w. 58,000), and trypsin (m.w. 23,300) standards. Good separation in the molecular weight range 12,000-190,000 was obtained on 7.5% SDS gels.

RESULTS AND DISCUSSION

Immediate Response to Alloxan

The effective dose (140 mg/kg) of alloxan administered at a rate of 1 mg/kg·s was determined in a preliminary set of experiments. The respiratory response following administration of alloxan was highly consistent in all animals studied (Figure 2). Brief periods of apnea, onset 15-20 seconds, duration 10-40 seconds, were followed by dyspneic breathing during the injection and lasted 3-5 minutes after the injection. Thereafter, polypneic breathing (frequency range 37-78) was spontaneously regular. The intrapleural pressure swing monitored by the change in esophageal pressure rapidly increased, but returned toward baseline values within 4-10 minutes after the injection. The maximum ΔP_{es}, invariably reached within the first 2 minutes, averaged 15 cm H_2O. For individual breaths the ΔP_{es} was frequently greater than 21 cm H_2O. Vigorous inspiratory efforts were apparent. Mean inspiratory flow increased from 16.5±3.8 to 24.3±4.2 L/min within two minutes representing a 47% increase, although individual animals often revealed a more marked response. One animal showed a 72% increase in $\dot{V}_I$ from a baseline value of 12.1 to 20.9 L/min within 2 minutes. Expiratory airflow was slightly increased (mean +12%) from a baseline average of 26.3±3.5 to 29.6±8.8 L/min. Tidal volume per kg body weight varied from breath to breath (range 12-19 ml/kg), although always transiently increased during the injection, but just as rapidly began to decline toward baseline value (13±2 ml/kg) within 4

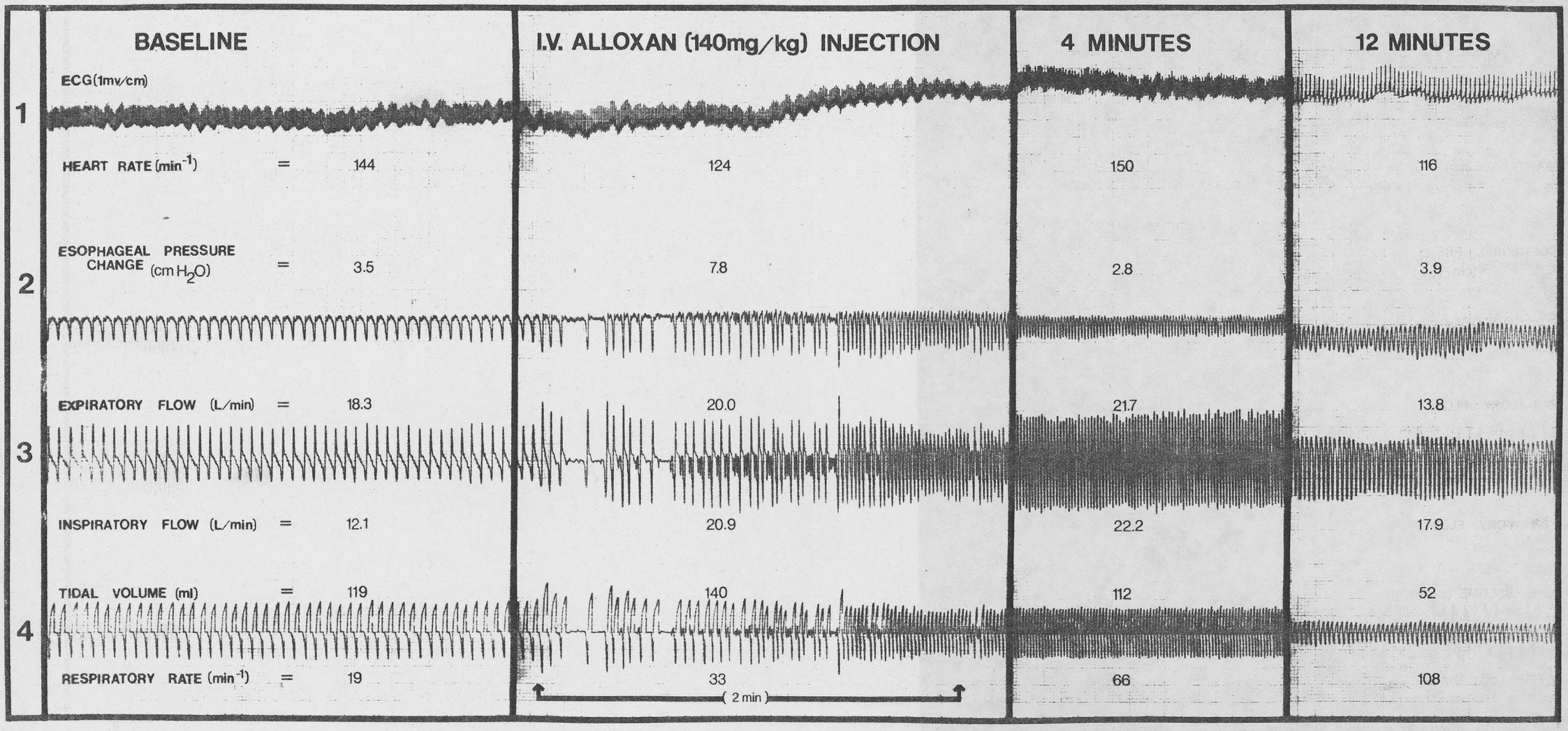

Figure 2. Immediate response to intravenous injection of alloxan monohydrate (140 mg/kg).

minutes after the alloxan was given, and was significantly ($P<0.05$) reduced within 12 minutes to an average value of 9±2 ml/kg.

In a separate series of experiments, arterial and venous blood samples were obtained at 20 second intervals throughout the injection period and at 4 minute intervals for 30 minutes following the alloxan. During the injection, the partial pressure of arterial oxygen increased from 77.9±17.8 (baseline) to 83.1±11.9 torr as expected in light of the ventilatory response. Arterial carbon dioxide partial pressure simultaneously increased from 53.9±8.1 (baseline) to 61.4±18.9 torr during the injection. Carbon dioxide retention in these animals is difficult to explain since it is highly unlikely that diffusion of gases across the blood-air barrier has already been impaired at this point. The pH of the blood entering the lungs was observed to decrease from 7.298±0.02 before injection to 6.757± 0.22 after the injection. In one animal, the pH of arterial blood decreased from 7.422 to 6.230.

The results of these experiments has led us to conclude that the dyspnea observed during the injection was primarily due to metabolic acidosis caused by the alloxan solution with a pH of 2.02 units. When the pH of alloxan was adjusted to 7.2 with either 1 N NaOH or phosphate buffer, the response was similar to that observed following saline injection. Furthermore, .01N HCl injected at a pH of 2.02 was followed by a transient respiratory alkalosis which maintained arterial pH, P_{O_2}, and P_{CO_2} near pre-injection levels. In general it can be stated that 30 minutes after the alloxan injection, only partial recovery had been accomplished. The metabolic acidosis resulting from the alloxan appears to be

specific and in a different category than those of HCl in which excess hydrogen ions stimulate the well-known buffer responses.

Blood-Gas Analysis

Figure 3 graphically illustrates the changes observed in mean values of oxygen partial pressure, carbon dioxide partial pressure, pH, bicarbonate ion concentration, and base excess of arterial blood at 30 minute intervals in control and alloxan treated animals. No significant differences between the two groups for any of these variables were observed during the baseline period, thus a composite of the nine animals is represented by the baseline values shown in Table 2. For mean values obtained from venous samples refer to Appendix E.

Oxygen tension of arterial blood drawn during the baseline period ranged from 79.3 to 98.1 torr with a composite mean of 88.6±8.0. The P_{O_2} values were consistent with the range of expected values for normal dogs (52,189). The P_{O_2} in the control group remained nearly constant throughout the entire experiment ranging from 86.4±6.2 to 90.7±10.5 torr. The P_{O_2} in the alloxan group two minutes after the injection transiently increased to a mean value of 93.1±8.8. Thirty minutes later the mean P_{O_2} was 77.9±9.3 and was followed by a progressive decrease to 74.7±4.4 at 60 minutes, 67.9±7.6 at 90 minutes, and 60.1±10.9 at 120 minutes. These means were significantly different at 60 minutes ($P<0.050$) and at 90 and 120 minutes ($P<0.010$) from control values observed during the same time periods.

The mean partial pressure of arterial carbon dioxide during the baseline period was 50.1±6.8 torr, within the range of values reported for

Figure 3. Changes in mean P_{O_2}, P_{CO_2}, pH, HCO_3-, and BE in arterial blood of control and alloxan treated dogs at timed intervals.

Abbreviations used: Partial pressure of oxygen (P_{O_2}), partial pressure of carbon dioxide (P_{CO_2}), bicarbonate ion (HCO_3-), and base excess (BE). Ordinates are as designated; abscissa is time in minutes. Solid lines represent controls while the broken lines represent the alloxan group. Arrow indicates time of injection.

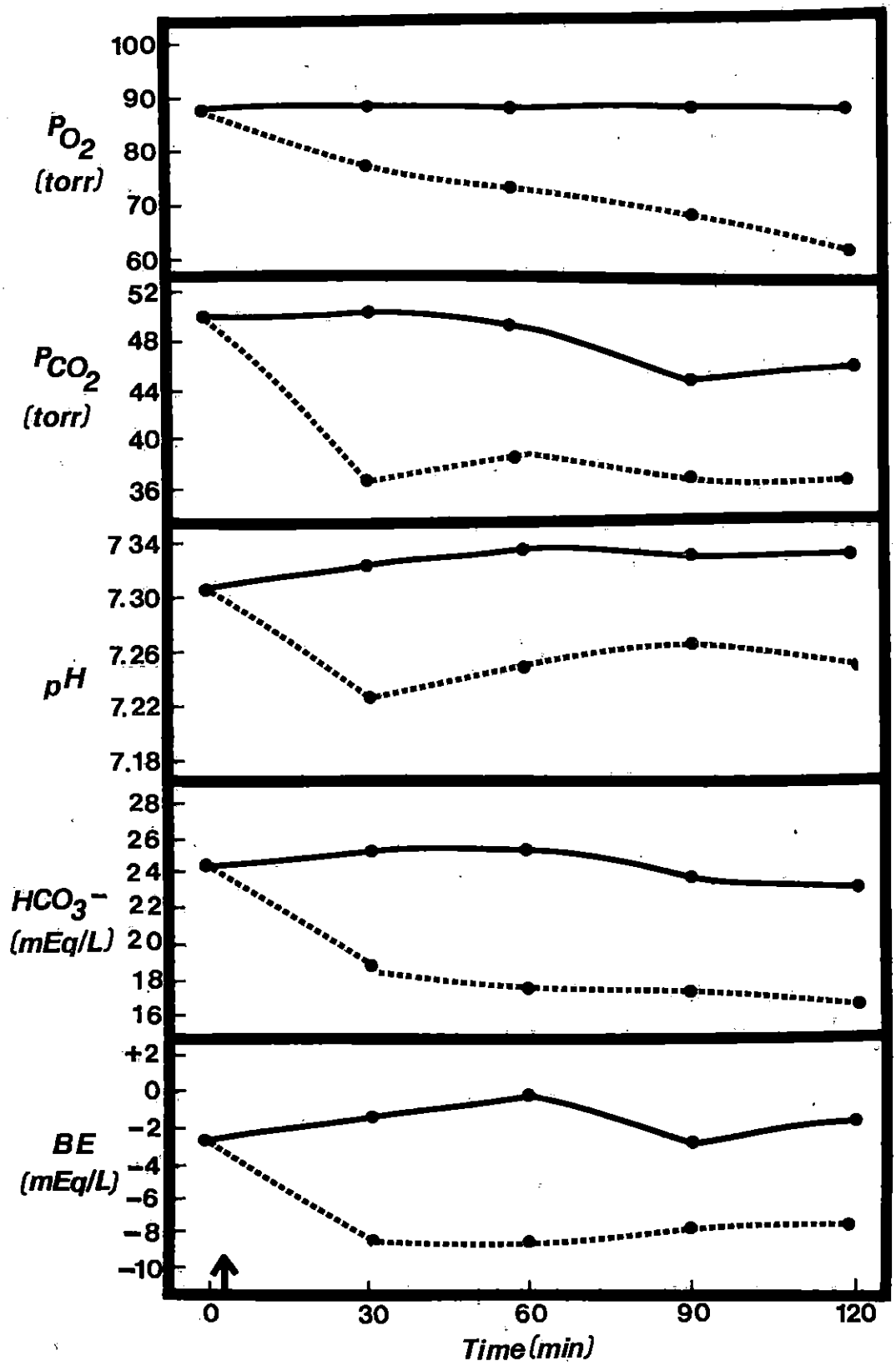
P_{O_2} (torr)
100
90
80
70
60
P_{CO_2} (torr)
52
48
44
40
36
pH
7.34
7.30
7.26
7.22
7.18
HCO_3^- (mEq/L)
28
26
24
22
20
18
16
BE (mEq/L)
+2
0
−2
−4
−6
−8
−10
0
30
60
90
120
Time (min)

Table 2. Summary of arterial P_{O_2}, P_{CO_2}, pH, HCO_3^-, and BE at timed intervals before and after injection of saline (1.8 ml/kg) in 5 control dogs and alloxan (140 mg/kg) in 4 treatment dogs

Variable[a]	Group[b]	Baseline	Time, post-injection			
			30 min	60 min	90 min	120 min
P_{O_2} (torr)	C	88.6±8.0[c]	90.7±10.5	89.8±11.1	89.4±8.5	88.9±10.9
	AE		77.9±9.3	74.7±4.4[d]	67.9±7.6[e]	60.1±10.9[e]
P_{CO_2} (torr)	C	50.1±6.8	50.1±9.3	48.6±12.6	44.8±7.9	45.4±10.4
	AE		36.8±7.1	39.0±6.1	37.1±6.4	37.6±7.3
pH	C	7.306±0.00	7.321±0.05	7.335±0.06	7.332±0.04	7.327±0.04
	AE		7.225±0.05[d]	7.247±0.03[d]	7.257±0.03[d]	7.243±0.04[d]
HCO_3^- (mEq/L)	C	24.4±6.4	25.0±2.8	25.0±3.9	22.5±2.3	23.0±3.5
	AE		17.4±0.8[e]	16.5±1.8[e]	16.1±1.7[e]	15.7±2.0[e]
BE (mEq/L)	C	-2.11±4.1	-0.10±0.6[f]	-0.86±2.6	-3.08±1.2	-2.50±2.2
	AE		-9.10±0.6[f]	-9.60±1.2[f]	-9.60±0.7[f]	-10.00±1.2[f]

[a]Abbreviations: partial pressure of oxygen (P_{O_2}), partial pressure of carbon dioxide (P_{CO_2}), bicarbonate ion (HCO_3^-), and base excess (BE).

[b]Abbreviations: control (C) and alloxan edema (AE).

[c]Values represent mean ± SD.

[d]Significantly different from control value obtained during same time interval ($P<0.050$).

[e]Significantly different from control value obtained during same time interval ($P<0.010$).

[f]Significantly different from control value obtained during same time interval ($P<0.001$).

pentobarbital anesthetized dogs (52). The values obtained thereafter in the control group showed insignificant decreases from the baseline value. Thirty minutes after the alloxan injection in the edema group the mean P_{CO_2} was observed to decrease by 27% to a value of 36.8±7.1 torr and remain relatively steady thereafter. At no time during the experiment were the mean P_{CO_2} values in the alloxan group statistically different from control values measured during the same time period. However, the decreases in P_{CO_2} from baseline in the edema group were significant ($P<0.050$) at 30, 90, and 120 minutes post-injection. The alloxan treated dogs can be considered physiologically hypocapnic.

The mean baseline arterial pH value was 7.306±0.00 which is in the lower range of normal values reported for dogs and may be explained in part by the effects of pentobarbital anesthesia (52). Small but statistically insignificant fluctuations in mean arterial pH were observed in the control group throughout the experiment ranging from 7.321±0.05 to 7.335±0.06. However, in the alloxan treated group the mean arterial pH was significantly ($P<0.050$) lower than the control group during every recording period following the injection. The lowest mean pH observed (7.225±0.05) occurred 30 minutes after alloxan was administered.

Mean arterial bicarbonate was 24.4±6.4 mEq/L during the baseline period and again was within the normal range reported for dogs (52). Control animals maintained constant HCO_3^- ion concentrations throughout the entire experiment, unlike the alloxan group in which we observed a steady decline in mean HCO_3^- during each 30 minute interval reaching the lowest value of 15.7±2.0 mEq/L at 120 minutes. This represented a significant

($P<0.010$) reduction from the baseline value. The mean HCO_3^- values of the alloxan treated animals were significantly lower ($P<0.010$) than the control values obtained during all time intervals following the injection.

The base excess was negative throughout the experiment in both groups as would be expected with pentobarbital anesthesia (52). Statistically insignificant changes were observed in the control group from the baseline mean of -2.1 ± 4.1 to a value of -2.5 ± 2.2 mEq/L at the end of the experiment with the most negative BE occurring at 90 minutes (-3.08 ± 1.2). Mean base excess in the alloxan group showed a significant change ($P<0.001$) 30 minutes after injection of alloxan from a baseline value of -3.5 ± 1.3 to -9.1 ± 0.6 mEq/L. Thereafter, only minor fluctuations were observed. However, the mean BE values of the alloxan group were significantly ($P<0.001$) more negative than the control group at all time intervals following the injection.

It has become apparent that there is a wide spectrum of acid-base disturbances which are associated with acute pulmonary edema (1,8,11,75). The most important cause of these disturbances is thought to be interference with gas exchange due to uneven ventilation-perfusion in edematous lungs (195). The hypoxemia resulting from mismatched ventilation-perfusion ratios normally stimulates the respiratory drive to increase total ventilation such that hypocapnia ensues and arterial oxygen returns toward normal according to the dissociation curves of oxygen and carbon dioxide (93).

Although we did observe a significant hypoxemic ventilatory drive (Figure 4) resulting in a hypocapnic condition, the arterial hypoxemia

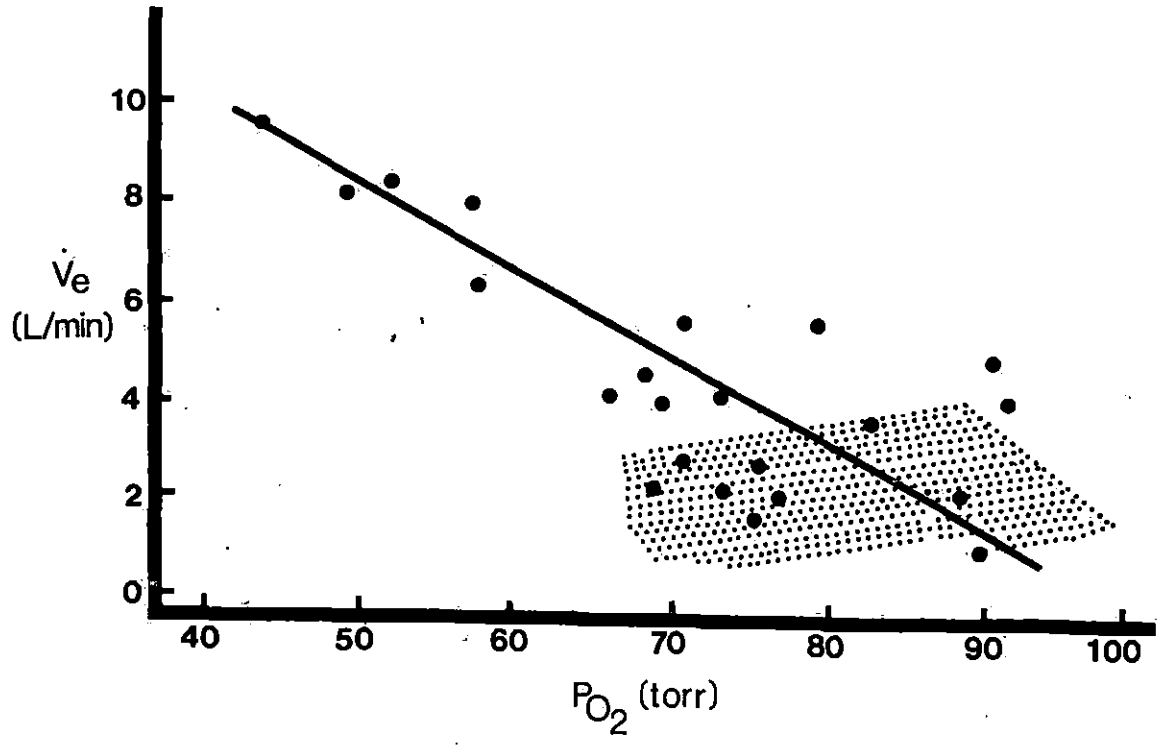

On the ordinate total ventilation and on the abscissa, partial pressure of arterial oxygen. Shaded area represents range of values observed in control dogs. Closed circles represent individual values for edema dogs.

Figure 4. Hypoxemic ventilatory drive observed during alloxan-induced pulmonary edema.

remained and even became more pronounced. The hypocapnic and hydrogen ion ventilatory responses have obviously been blunted. Our results agree with Aberman and Fulop (1) who reported mean arterial P_{O_2} (48 torr) and mean arterial P_{CO_2} (29 torr) in 45 human patients with lung edema. The hypoxemia we observed can be accounted for by one or more of the three primary causes of hypoxemia. They are (1) alveolar hypoventilation, (2) ventilation/perfusion imbalance, and (3) increased venous admixture (right-to-left shunts). Diffusion impairment must also be included in this list, but considered as a subgroup of ventilation-perfusion imbalance. Hypoventilation has been eliminated in our animals as the primary cause. Considering the work of Datta (60) in which it was determined that mismatched ventilation/perfusion in edematous lungs results in carbon dioxide retention, which we did not observe, argues against the presence of severe regional distribution abnormalities in the alloxan treated animals. Although not statistically significant, the marked decrease in arterial P_{CO_2} does hint at the presence of some venous admixture.

The availability of oxygen to the organism is dependent on the quantity brought into the lungs per unit of time (ventilation) and, since oxygen is limited by diffusion, on the internal surface of the lungs. Alloxan has been shown to produce acute pulmonary edema in dogs probably by direct injury to pulmonary capillaries (12,13,27,127). From the foregoing, we suggest that impaired diffusion which is a function of the area and permeability of the air-blood barrier is primarily responsible for the hypoxemia observed in our animals. Partial explanation for selective reduction in oxygen diffusion may be due to the lower "effective" solubility of oxygen in blood (246). It should be noted that low oxygen tension

itself has been shown (125) to promote increased capillary fluid leakage. The additional fluid causes widening of the air-blood barrier, thereby further impeding gas transfer.

Complicating the situation further, the alloxan treated group showed a pronounced increase in the acidity of arterial blood, one of them surviving despite a pH of 7.150. These responses are in contrast to the usual textbook description (75). The decrease in P_{CO_2} coupled with the increased acidity of the blood indicates a shift to the left in the carbon dioxide dissociation equation. The presence of metabolic acidosis was probably due to elevated blood lactate generated by the muscular effort of labored breathing (8) in conjunction with infusion of the acidic (pH = 2.02) alloxan solution. The significant acidity of the alloxan treated dogs may further have implications regarding the surface activity of the alveolar lining material as will be discussed later.

Whether or not hypoxemia coupled with the low arterial pH caused pulmonary vasoconstriction in our animals as observed by others (131,199, 203) cannot be discerned from our study. Cottrell et al. (53) reported normal pulmonary arterial and left atrial pressures during alloxan-induced edema except for a transient (2 min) elevation immediately following the injection. Furthermore, heart rate (Figure 5) and arterio-venous oxygen content differences (Figure 6) remained fairly constant in our alloxan treated dogs. A significant difference ($P<0.050$) between control and edema animals was observed only at the end of the experiment, which infers that changes in cardiac output were not involved in the acid-base disturbances we have reported. Direct measurements by others (12) have

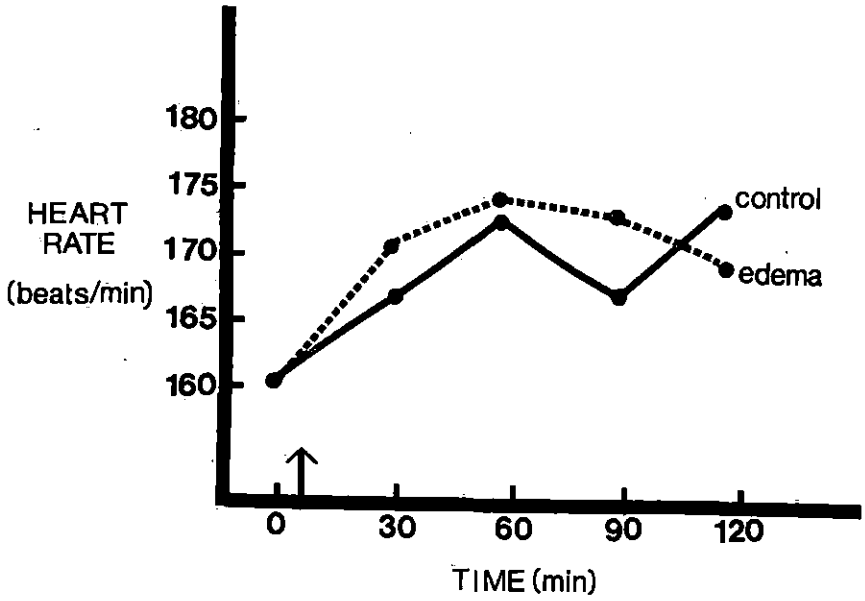

Figure 5. Mean heart rate at 30 minute intervals before and after injection (arrow) of saline (1.8 ml/kg) in 5 control dogs and alloxan (140 mg/kg) in 4 edema dogs.

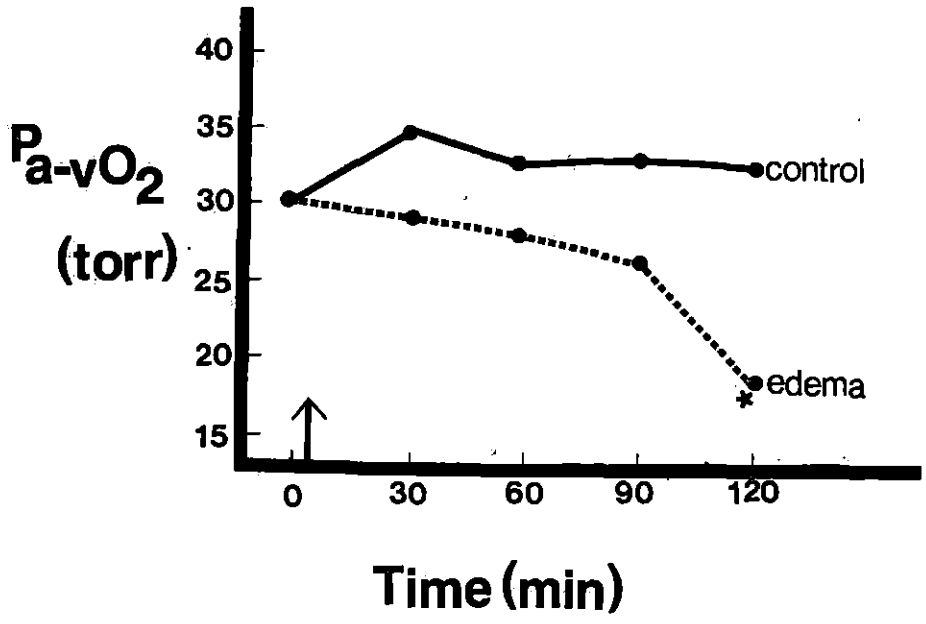

The only significant (P<0.050) difference between group means was observed at 120 minutes post-injection (*). Arrow indicates time of injection.

Figure 6. Mean arterio-venous partial pressure oxygen difference in control and alloxan treated dogs at timed intervals.

revealed no change in cardiac output during alloxan induced pulmonary edema. Collection of alveolar air samples for oxygen and carbon dioxide determination must be undertaken if the hypoxemic-hypocapnic condition in these animals is to be quantitatively partitioned into alterations of diffusion and/or distribution.

Lung Mechanics

Previous studies (86,105,157) have shown that pulmonary edema is accompanied by marked changes in the mechanical properties of the lungs. A summary of the ventilatory parameters and pulmonary mechanics obtained during the baseline period and at four 30 minute intervals after saline (1.8 ml/kg) injection in 5 control dogs, and alloxan (140 mg/kg) in 4 treatment animals is shown in Table 3. Average values for every parameter were obtained during each recording period from measurements of three minute breath-by-breath analysis. In the absence of a significant difference in the baseline values between the control and edema groups a composite population mean ± SD with n = 9 is presented. Tidal volume (V_t), total lung ventilation ($\dot{V}_e$), alveolar ventilation ($\dot{V}_A$), and dead space ventilation ($\dot{V}_\Delta$) are expressed on a per kg body weight basis as suggested by Tenny and Remmers (233).

Though there was some individual variation in the control group, the results obtained during the baseline period and the subsequent 30, 60, 90, and 120 minute intervals were not significantly different from the initial values. Injection of alloxan resulted in a significant ($P<0.010$) three-fold rise within 30 minutes in respiratory frequency from an average

Table 3. Summary of ventilatory parameters and lung mechanics in control (C)[a] and alloxan edema (AE)[b] dogs at time intervals[c]

Variable[d]	Group	Baseline	Time, post-injection			
			30 min	60 min	90 min	120 min
f (BPM)	C	13±4[e]	12±3	14±5	14±5	15±5
	AE		36±10[f]	30±13[g]	33±24	38±30
$\dot{V}_t$ (ml/kg)	C	13±3	14±2	14±2	13±2	14±3
	AE		10±3	10±4	10±4	11±5

[a]The frequency (f, in breaths per minute: BPM) and depth (V_t, ml) of the tidal excursions as measured from the Beckman recording were multiplied to give total ventilation ($\dot{V}_e$, L/min). Alveolar ventilation ($\dot{V}_A$, L/min) was calculated by subtracting the estimated dead space ventilation ($\dot{V}_D$, L/min) from $\dot{V}_e$. All are expressed on a per kg body weight basis. Inspiratory airflow (F_i, L/min) and expiratory airflow (F, L/min) were measured directly from the Beckman recording as was the change in esophageal pressure (ΔP_{es}, cm H_2O). Inspiratory airway resistance (RAW_i, cm H_2O/L·s) and expiratory airway resistance (RAW_e, cm H_2O/L·s) were calculated by dividing the ΔP_{es} by the respective airflow after correction for resistance imposed externally. Dynamic lung compliance (C_L, ml/cm H_2O) was calculated by dividing V_t by ΔP_{es} as obtained from the Beckman recordings. The elastic work component of breathing (W_{El}, kg·m/min/10^{-2}) was calculated from the formula derived by Coebatch (48) as follows: $W_{El} = 0.5\ V_t^2 \times f \times 10^{-3}/C_L$.

[b]Control (C) dogs given 1.8 ml/kg 0.15 M sterile saline.

[c]Edema (AE) dogs given 140 mg/kg alloxan.

[d]Injections performed immediately after baseline recordings were obtained. All parameters were measured again at 30, 60, 90, and 120 minutes after administering saline or alloxan.

[e]Values represent mean ± SD for n = 5 in the control group and n = 4 in the alloxan edema group.

[f]Significantly different from control group ($P<0.010$).

[g]Significantly different from control group ($P<0.050$).

Table 3. (Continued)

Variable	Group	Baseline	Time, post-injection 30 min	60 min	90 min	120 min
$\dot{V}_e$ (ml/min·kg)	C	162±49	163±35	186±49	184±54	195±47
	AE		360±102[h]	288±130	316±236	365±292
$\dot{V}_A$ (ml/min·kg)	C	124±41	127±28	144±36	141±40	151±34
	AE		250±86[i]	197±105	217±176	252±225
$\dot{V}_D$ (ml/min·kg)	C	38±10	36±9	42±15	43±17	45±17
	AE		110±33[h]	91±37[g]	99±69	112±85
$\dot{F}_I$ (L/min)	C	16.5±3.8	14.7±3.1	15.2±2.9	15.2±2.1	15.7±2.7
	AE		21.9±4.1	20.6±6.2[j]	21.2±5.9	22.4±6.2
$\dot{F}_E$ (L/min)	C	26.3±3.5	24.5±4.9	24.5±3.5	24.3±3.6	24.9±3.5
	AE		27.2±3.1	25.7±5.3	27.1±5.1	30.2±4.3
ΔP_{es} (cm H_2O)	C	3.6±1.0	3.8±0.7	3.5±0.9	3.6±0.9	3.6±1.1
	AE		4.0±0.6	4.0±0.9	4.1±1.3	5.4±2.1
RAW_I (cm H_2O/L·s)	C	8.44±3.79	8.00±2.37	7.37±3.07	7.62±2.55	7.07±2.78
	AE		6.27±0.51[i]	6.71±1.38	6.48±0.33	8.92±2.03
RAW_E (cm H_2O/L·s)	C	5.22±2.25	4.94±1.54	4.55±1.59	4.56±1.16	4.35±1.22
	AE		4.98±0.39	5.19±0.48	5.05±0.96	6.33±1.39

[h]Significantly different from control group ($P<0.005$).

[i]Significantly different from control group ($P<0.025$).

[j]Significantly different from control group ($P<0.020$).

Table 3. (Continued)

Variable	Group	Baseline	Time, post-injection			
			30 min	60 min	90 min	120 min
C_L (ml/cm H_2O)	C	56.0±21.6	59.3±14.0	62.5±11.4	59.2±6.9	62.5±11.0
	AE		46.0±14.9[g]	43.8±9.4[f]	45.1±15.1	36.2±19.0[g]
W_{El} (kg-m/min/10^{-2})	C	5.56±2.9	4.99±1.11	5.35±0.93	5.48±1.20	5.74±1.21
	AE		12.58±4.05	10.41±5.56	13.09±11.80	20.66±22.27

baseline value of 13±4 to a value of 36±10 breaths per minute. Tidal volume simultaneously decreased (-23%) from 13±3 to 10±3 ml/kg. The result of these responses was a significant ($P<0.025$) elevation in alveolar ventilation from 124±41 to 250±86 ml/min·kg. During the next 30 minutes, we observed a transient decrease in $\dot{V}_A$ resulting primarily from a 17% reduction in f, since V_t remained essentially constant. During the 90 minute recording period, the increase in alveolar ventilation to 217±176 ml/min·kg was again primarily due to an increase in f, with tidal volume remaining steady. Peak alveolar ventilation (252±225 ml/min·kg) was observed during the 120 minute recording period, but this time was the result of both an increase in frequency as well as an increase in tidal volume. The significant increase in the dead space component of total pulmonary ventilation at 30 minutes ($P<0.005$) and at 60 minutes ($P<0.050$) caused a marked decrease in the efficiency of ventilation in the alloxan treated animals. Efficiency was reduced from 77% (baseline) to 67% following alloxan. Ventilation of poorly perfused areas and/or ventilation of lung areas with impaired diffusion are primarily responsible for the inefficient ventilation and may explain the hypoxemia in these animals.

The demand for ventilation can be partitioned into two components: (1) demand for tidal volume, and (2) the demand for an "instantaneous" frequency. When ventilation was plotted as a function of tidal volume (Figure 7A) the relationship was found to be roughly linear in agreement with the results obtained for humans by Hey et al. (102). The slope of the relationship was greater for all alloxan treated animals. In one edema dog the $\dot{V}_e - V_t$ relation assumed a very steep course when total lung

Figure 7. Ventilation-tidal volume and ventilation-frequency plots of individual data from 5 normal (closed circles) and 4 alloxan treated (open circles) dogs measured at five 30 minute intervals.

A. The $\dot{V}_e - V_t$ relation may be estimated by linear approximation such that $\dot{V}_e = k (V_t - V_o)$ where k is the slope constant and V_o is the value of the intercept. Linearity maintained; the slope of this relationship is somewhat increased in the alloxan treated animals as is indicated by the steep course when $\dot{V}_e$ rises above a critical value of 5 L/min as indicated (x----x).

B. The $\dot{V}_e$ - f plot similarly showed a positive relationship. Point scattering in the alloxan group indicates a deviation from linearity in their ventilatory responses.

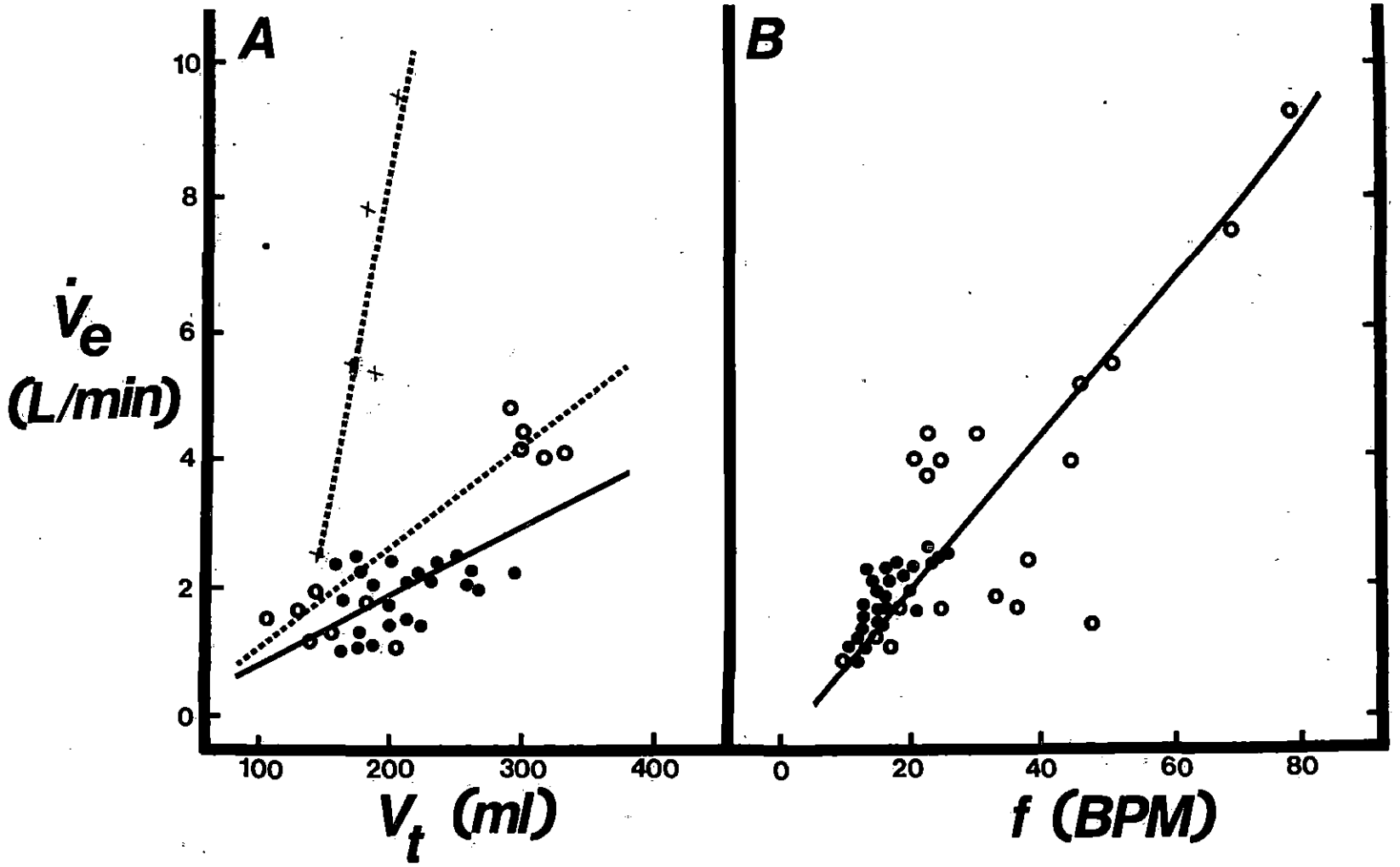
A
B
$\dot{V}_e$ (L/min)
10
8
6
4
2
0
100
200
300
400
V_t (ml)
0
20
40
60
80
f (BPM)

ventilation exceeded an apparently critical value of 5 L/min. The increased ventilation beyond this value was achieved almost entirely by an increase in respiratory rate while tidal volume remained constant. The result of this respiratory pattern was a marked increase in dead space ventilation such that effective alveolar ventilation was compromised. The individual edema dog showing the steep $\dot{V}_e - V_t$ slope was found to be ventilating at 52% efficiency. When tidal volume becomes too small a fraction of lung volume intrapulmonary mixing of the gases will be incomplete with each breath which may further explain the hypoxemia accompanying this type of ventilatory pattern in alloxan-induced pulmonary edema. The corresponding ventilation - frequency plot (Figure 7B) also showed a positive and near linear relationship as expected. The slope of this relationship was not markedly altered in the alloxan treated animals when compared with normal dogs. However, the scattering of points is evidence of nonlinearity in this relationship particularly in pulmonary edema when an increased ventilatory requirement may be affected by variable increases in tidal volume and/or respiratory frequency.

The optimum balance between tidal volume and frequency requires that ventilation be achieved either with a minimal amount of work (174), or with a minimal average force by the respiratory muscles (250). Elastic work of breathing (W_{El}, kg-m/min/10^{-2}) was calculated from tidal volume, respiratory frequency, and compliance according to the formula derived by Colebatch and Halmagyl (48) as follows:

$$W_{El} = 0.5\ V_t^2 \times f \times 10^{-3}/C_L$$

where tidal volume (V_t) is expressed in ml, respiratory frequency (f) in

breaths per minute, and compliance (C_L) in ml/cm H_2O. This is not the total work of respiration, but rather serves as a convenient index of the change in elastic work performed on the lung due to alterations in compliance or tissue elastic recoil and tidal volume. Flow resistive work, inertial tissue and gas forces must be included if the total mechanical work performed by the lungs is to be fully assessed. The average elastic work established in normal dogs during baseline measurements in our experiment was 5.56±2.29 kg-m/min/10^{-2}. During the two hour study period we observed relatively no change in W_{El} in the control group (Figure 8). Although not significant, W_{El} in the alloxan treated animals was greater than the corresponding value calculated for control animals during all recording periods. Peak values (20.66±22.27) representing a 27% increase from baseline were observed 120 minutes after induction of edema. The additional work performed by the edematous lungs to accomplish the ventilatory requirement resulted primarily from an increase in respiratory frequency and a decrease in compliance, the magnitudes of which were too large to be compensated for by the reduction in tidal volume (Figure 9).

The respiratory cycle (inspiration/expiration) requires pressure fluctuations to overcome elastic recoil of lung parenchyma and to overcome resistance to flow in the airways. The change in esophageal pressure observed in the alloxan treated animals, although not significantly different, was larger than the corresponding ΔP_{es} in control animals during all recording periods except baseline (Figure 10). In fact, only minimal fluctuations in ΔP_{es} were observed for both groups throughout the experiment. However, ΔP_{es} markedly increased (+31%) during the last 30 minutes

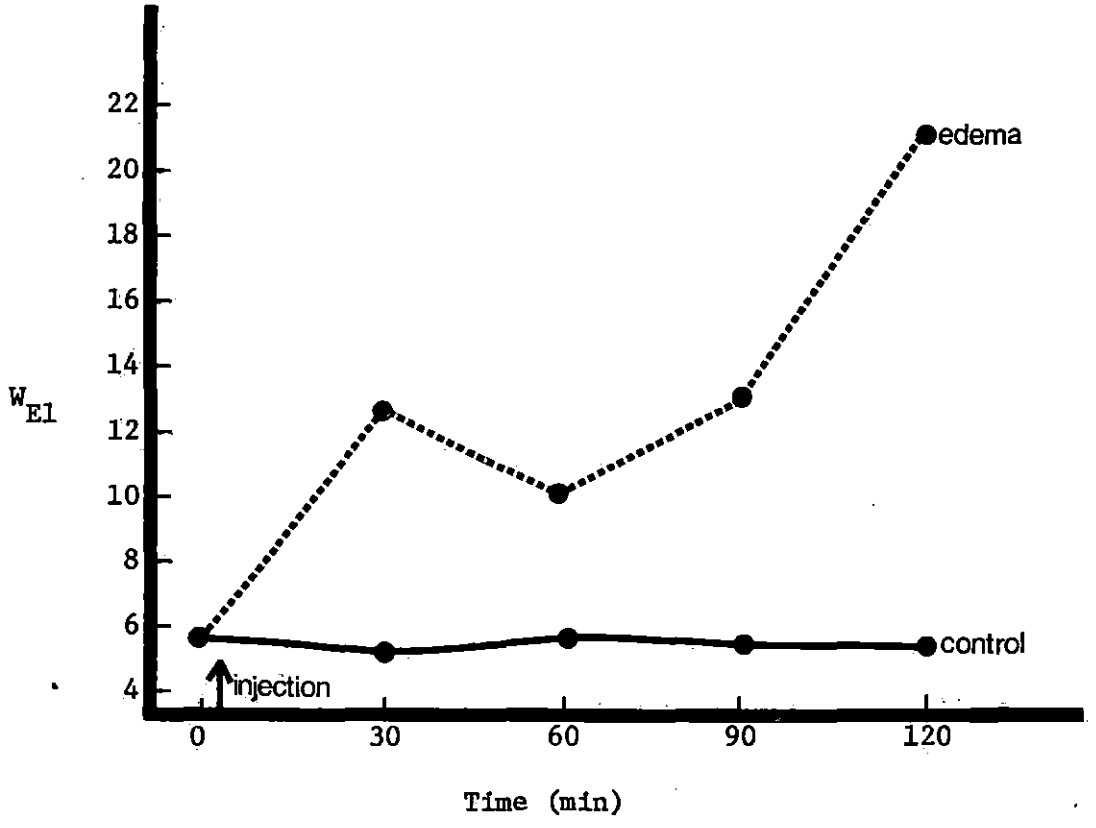

Figure 8. Time course changes in the elastic work component (W_{El}, kg-m/min/10^{-2}) of the respiratory cycle in control and alloxan treated animals.

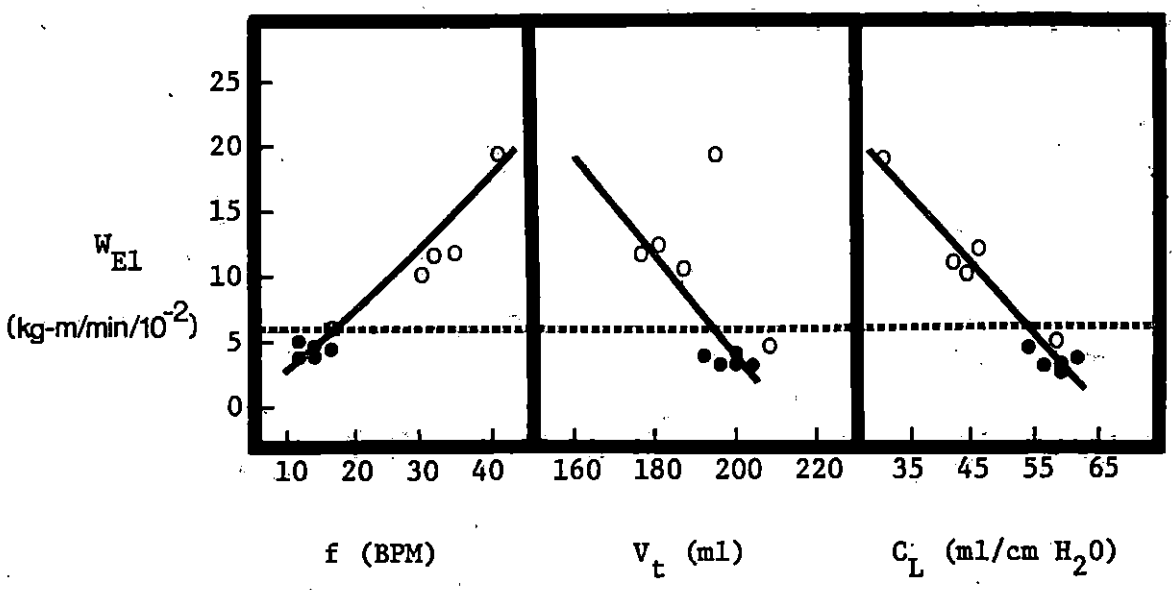

Minimal changes were observed in the mean control values (closed circles) of f, V_t, and C_L obtained during all 5 time intervals. Hence, W_{El} remained less than 6 kg-m/min/10^{-2} and relatively constant. Subsequent to alloxan injection, W_{El} in the edema dogs (open circles) increased during all recording periods. The change resulted primarily from the increased f and reduced C_L.

Figure 9. Graphical presentation of the elastic work component as a function of respiratory frequency, tidal volume, and dynamic lung compliance.

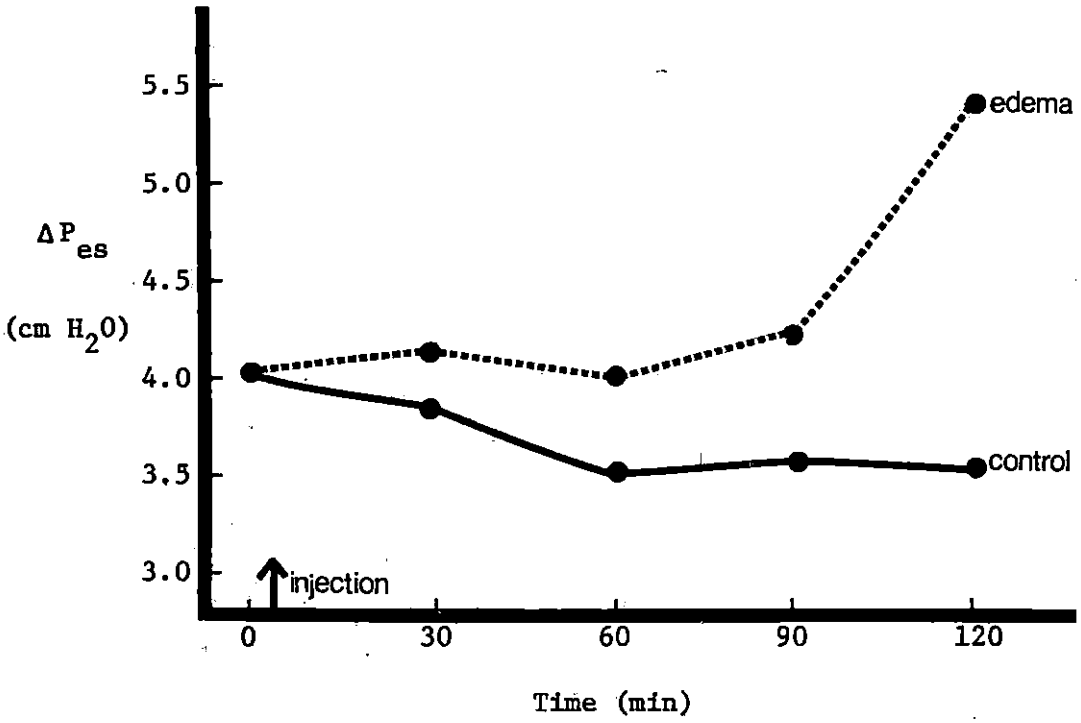

Figure 10. Time course changes in pleural pressure as estimated by intraesophageal pressure changes in control and alloxan treated animals.

of the experiment in the edema dogs from 4.1±1.3 at 90 minutes at 5.41± 2.1 cm H_2O at 120 minutes.

Baseline measurement of inspiratory airflow and expiratory airflow were not significantly different between the control and alloxan treated groups; hence a composite mean ± SD of the nine dogs is represented in Table 7. Baseline $\dot{F}_I$ (16.5±3.8 L/min) was less than $\dot{F}_E$ (26.3±3.5 L/min) as was the case in all succeeding measurements in both groups. There were no significant changes in $\dot{F}_I$ or $\dot{F}_E$ within the control group throughout the course of study. In contrast, both $\dot{F}_I$ and $\dot{F}_E$ increased immediately after administration of alloxan and remained elevated. The only significant difference ($P<0.020$) between control and treated animals occurred 60 minutes post-injection when $\dot{F}_I$ in the edema dogs had increased to 20.6± 6.2 L/min compared to 15.2±2.9 L/min in the control group. The increases in inspiratory airflow observed in the alloxan group were always more marked than the increases in expiratory airflow of the same dogs during the entire experiment. The enhanced airflow, both $\dot{F}_I$ and $\dot{F}_E$, observed in these animals is partially due to the increased respiratory frequency they exhibited in response to alloxan (Figure 11). The range of average frequencies among alloxan treated dogs (13-38 BPM) during the experiment has spread the airflow-frequency ($\dot{F}$ - f) curves out demonstrating a relationship between velocity of airflow and respiratory rate which was not apparent in the control group alone. Discriminate statistical analysis allows us to describe $\dot{F}$ - f curves characteristic of pulmonary edema such that frequencies greater than 20 BPM will produce $\dot{F}_E$ greater than 27 L/min and $\dot{F}_I$ greater than 18 L/min.

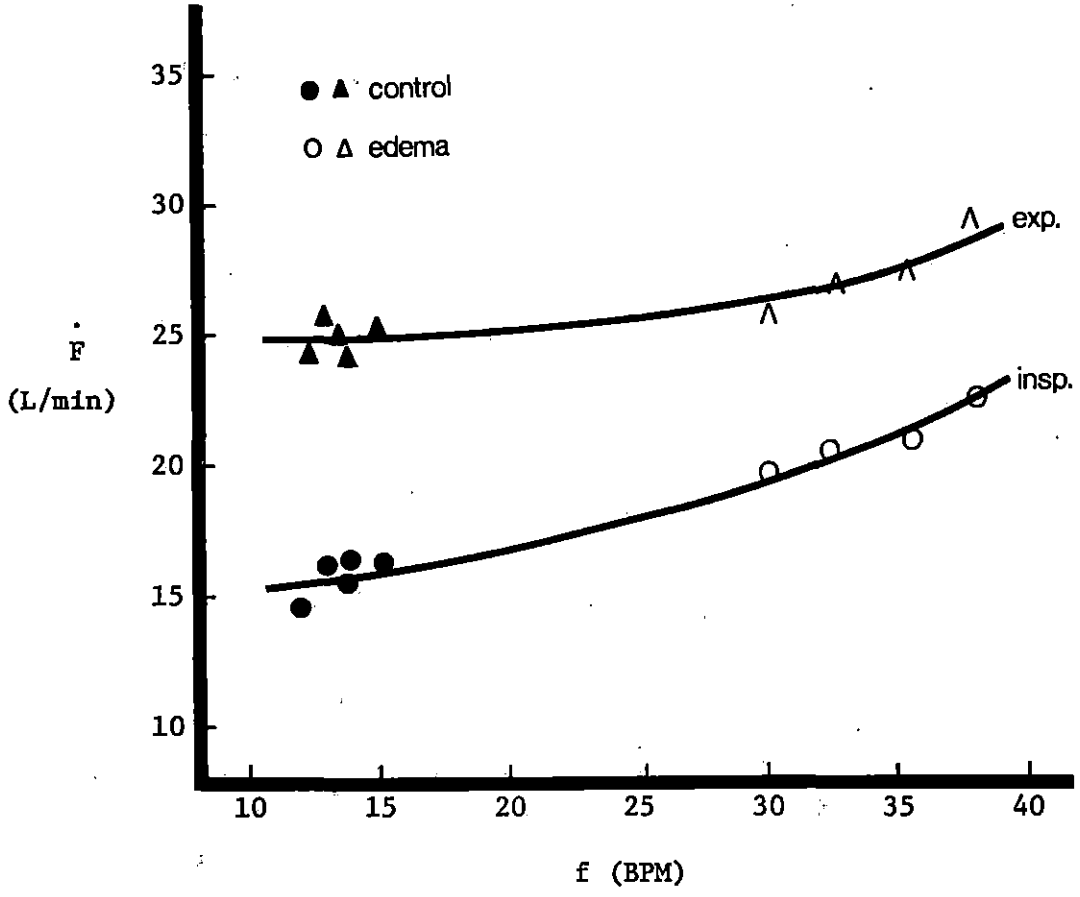

Figure 11. Inspiratory (insp.) and expiratory (exp.) airflow-frequency diagram demonstrating a dependency between these variables.

Lung compliance represents potential energy stored in stretched elastic and collagen tissues which acts as a retractive force during expiration. During inspiration, this elastic recoil as well as gas-liquid surface forces impose hindrances to lung expansion. The force which must be applied to expand the lung must overcome the elastic recoil. Dynamic lung compliance and resistances (inspiratory and expiratory) were measured by relating intrapleural pressure gradients to tidal volume, and flows were measured with a pneumotachograph. The pressure, flow, and volume signals were used to calculate dynamic compliance and resistance.

Dynamic lung compliance, expressed as ml per cm H_2O was obtained by dividing the tidal volume by a simultaneously recorded change in esophageal pressure between points of zero airflow (Appendix B). Measurements obtained during the baseline period averaged 56.0±21.6 ml/cm H_2O in nine dogs. The average increase (+8%) in C_L of the control group from the baseline value was insignificant throughout the experiment. However, the alloxan group showed a significant ($P<0.050$) decrease in dynamic compliance to a value of 46.0±14.9 when compared to the control value (59.3± 14.0) 30 minutes after induction of pulmonary edema. Compliance remained fairly steady for the next hour at which time a second significant decrease ($P<0.050$) to 36.2±19.0 ml/cm H_2O, representing a 55% change from the baseline value was observed in the alloxan treated animals. The changes in compliance were the result of both a reduced tidal volume and an increase in the pleural pressure gradient. The ΔP_{es} observed in the edema animals was greater than corresponding pressure changes in control animals during all recording intervals except the baseline period. During

the respiratory cycle this pressure gradient is produced by a number of factors, including resistance to a airflow, pulmonary and chest-wall compliance and tissue and gas inertia. At points of no flow, which is when we took measurements for our calculations, both resistance to airflow and inertial forces are essentially absent; thus ΔP_{es} becomes a function of compliance alone (Figure 12). We have further calculated from this that an increase of 5% in ΔP_{es} in the alloxan treated animals for inflation in the tidal range corresponds to 8% decreases in compliance when compared to the baseline values. Two "counterbalancing" mechanisms may be operative in our edematous dogs: (1) loss of smooth muscle tone in terminal airways due to hypoxia resulting in increased compliance, and (2) stiffening of lung tissue due to fluid accumulation resulting in decreased compliance. The result of these two actions is physiologically significant, although not always statistically significant as is the case in our data.

Hughes, May, and Widdicombe (105) studying acute lung edema in rabbits and guinea pigs reported that lung compliance decreased by 63% during the course of study. More recently, Muggenberg et al. (163) reported a decrease in C_L from 81.3 to 48.8 ml/cm H_2O just 12 hours after lung lavage in dogs. By studying volume-pressure curves in degassed, excised dog lungs filled with saline before and after edema, Cook et al. (50) demonstrated that the reduced compliance was actually a manifestation of altered surface forces at the air-tissue alveolar interface rather than real elastic tissue property changes. A discussion of this idea as it relates to our study will appear later.

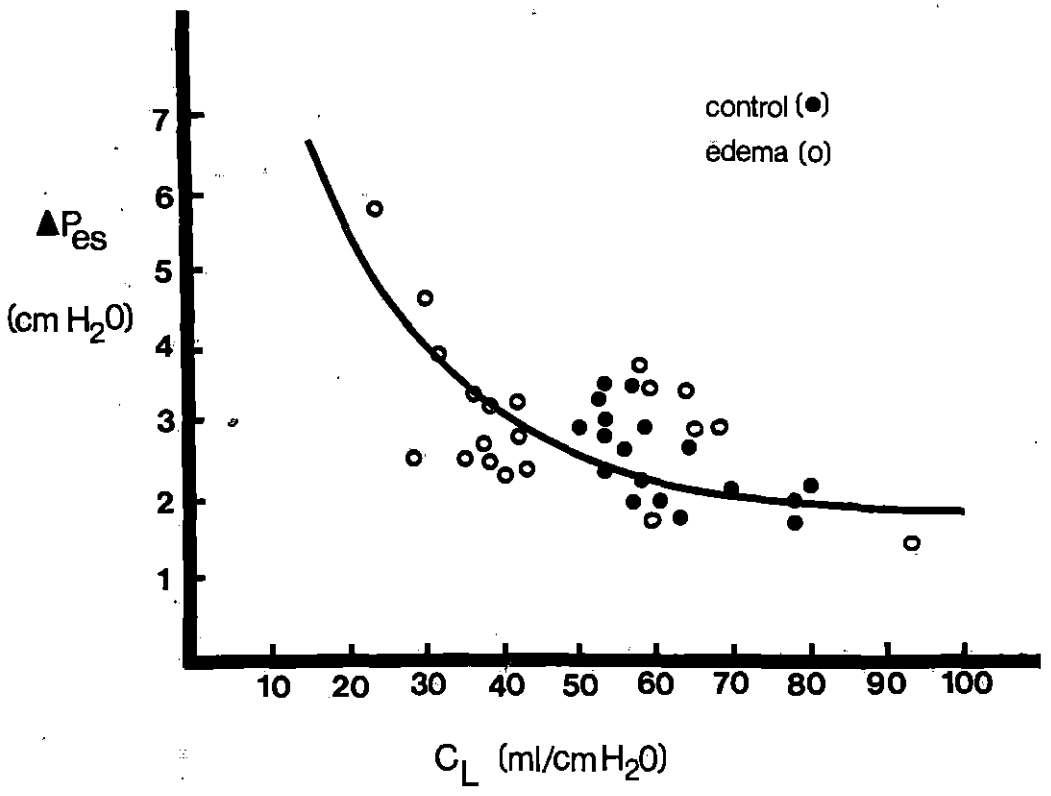

A 5% increase in ΔP_{es} corresponds to an 8% decrease in C_L.

Figure 12. Graph showing the change in esophageal pressure versus dynamic lung compliance.

It has been suggested (133) that compliance is influenced by respiratory frequency. Figure 13 is a plot of the individual pairs of f - C_L values obtained in our experiment from which it can be seen that the range of values for respiratory rate (10-25 BPM) and dynamic lung compliance (45-80 ml/cm H_2O) in normal dogs is narrow. A definitive mathematical relationship in these dogs is difficult to establish. In the edematous lung, both the range of observed respiratory rates (8-75 BPM) and as well as the range of compliances (22-94 ml/cm H_2O) is markedly expanded. There appears to be a wider range of respiratory rates for which a narrow range of compliance values is observed from which we can eliminate frequency dependent compliance as a response to alloxan. However, it should be noted that the f - C_L data points of the alloxan treated animals occur predominantly outside the limits arbitrarily established by discriminate analysis for normal dogs from our experiment.

Care must be taken in the interpretation of volume-pressure curves and the calculated C_L, since any process that reduces the number of air spaces participating in the volume change of the lung will decrease the compliance. Furthermore, it has been suggested that in some respiratory disorders, the position and shape of the V-P curves may be altered, the magnitude of which cannot be detected by simple direct calculations. Atelectasis causes V-P curves to be shifted downward and to the right (133). Hypoxia shifts static deflation V-P isopleths upward with no change in dynamic C_L curves which is interpreted to be the result of the frequency dependent compliance (207). Thus, C_L calculations in our study were compared to the slope determinations of V-P isopleths. These pen

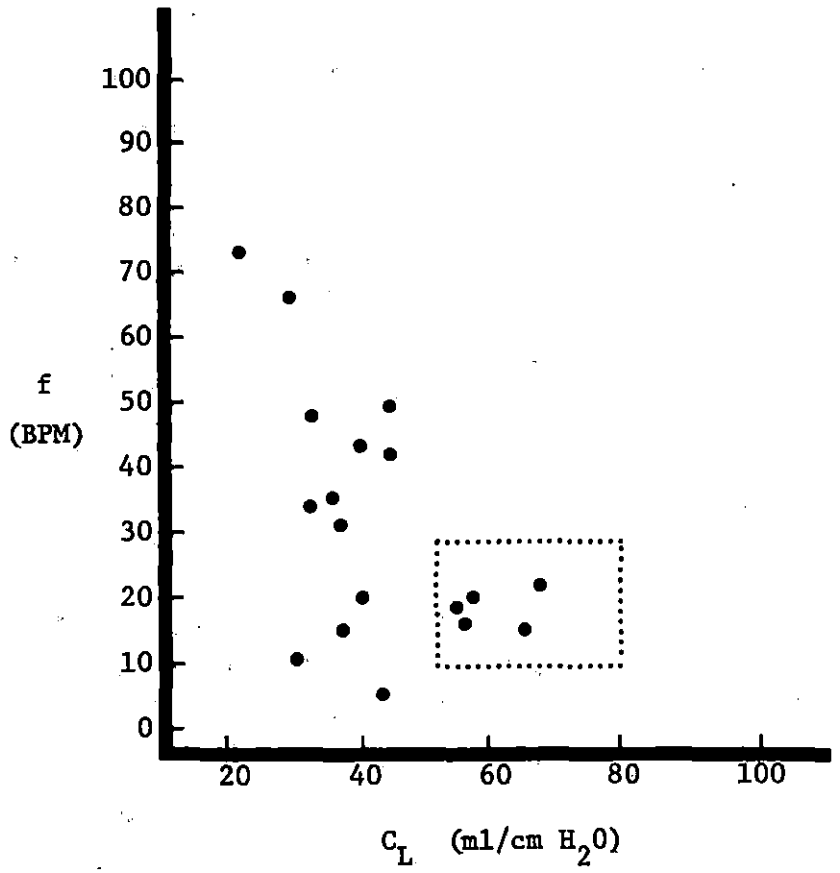

Figure 13. Plotted pairs of frequency-dynamic lung compliance points of alloxan treated (closed circles) and normal dogs (enclosed area) showing that frequency dependent compliance was not symptomatic of alloxan-induced pulmonary edema.

recordings were simultaneously obtained by the X-Y recorder and further analyzed for positional and hysteretic changes. A typical V-P series is shown in Figure 14. The loss of elasticity, i.e., reduced compliance, in the edematous lungs caused both a decrease in the slope of the V-P curves with displacement of the whole curve downward with overlapping of the lower portion of the baseline curve both to the right and to the left. The area of the curves (hysteresis) between the inspiratory and expiratory isopleths was much less in all V-P plots following the alloxan injection. At any given lung volume the elastic recoil pressure is just slightly greater on inflation than on deflation in these curves. However, in the normal animal, the elastic recoil pressure was found to be much greater on inflation than on deflation.

Inspiratory resistance and expiratory resistance expressed in cm $H_2O/L \cdot s$ were calculated separately by dividing the change in esophageal pressure by inspiratory or expiratory airflow respectively. Calculated results were compared with pen tracings of pressure-flow (P-F) curves simultaneously obtained by the X-Y recorder. Resistance was measured as the slope of the inspiratory and expiratory isopleths of these curves (Appendix B). Direct calculations and slope determinations reflected the resistance of the whole system, including endotracheal tube and pneumotachograph connections as well as conducting airways. The results presented in Table 3 are true values of RAW_I and RAW_E after correction for externally imposed resistances.

The RAW_I was always greater than the RAW_E. Inspiratory airway resistance in nine spontaneously breathing dogs averaged 8.44±3.79 cm H_2O L•s

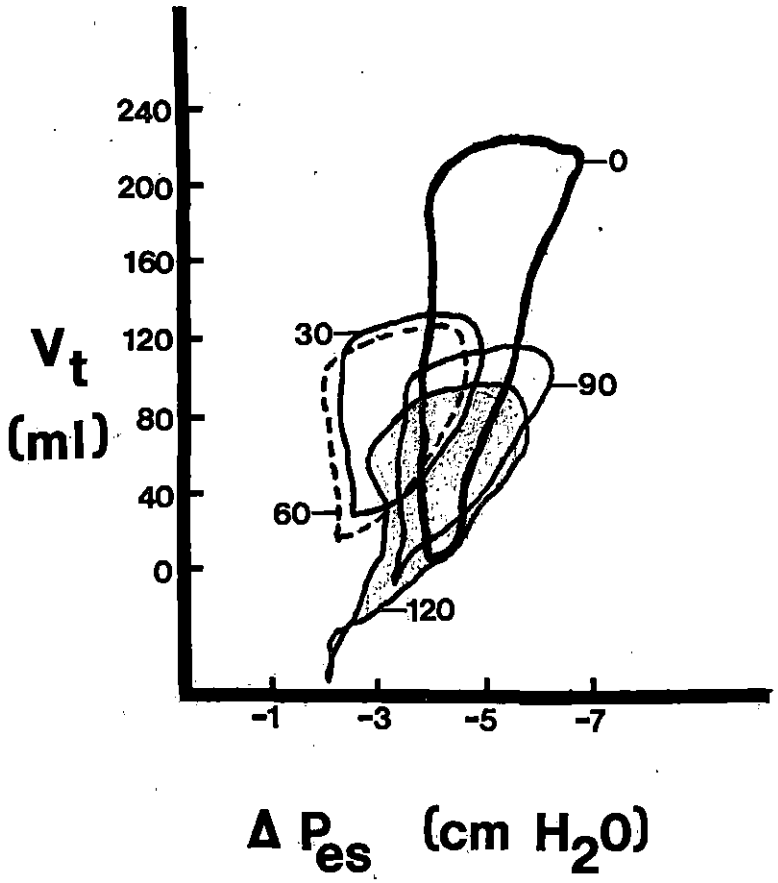

Figure 14. Typical series of V-P curves obtained at 30 minute intervals before and after injection of alloxan.

during the baseline period, while the mean RAW_E at the same time was 5.22± 2.25 cm H_2O/L•s. Though there was some individual variation, the RAW_I and RAW_E obtained at 30, 60, 90, and 120 minutes after saline injection showed only minor decreases, not significantly different from the baseline values. There appears to be a decrease in RAW_I and RAW_E when compared to the population baseline measurement during all recording periods following the alloxan injection; however, this was not actually the case. The value of RAW_I in the alloxan group during the baseline measurement averaged 6.90±2.51 and for RAW_E averaged 4.58±1.06 cm H_2O/L•s. From this it can be seen that RAW_I remained fairly constant until the last 30 minutes of the experiment at which time a significant ($P<0.050$) increase from 6.48±0.33 to 8.92±2.03 cm H_2O/L•s was observed in the edema dogs. The mean RAW_I at 90 minutes (6.48±0.33) and at 120 minutes (8.92±2.03) just failed to reach significance ($P<0.100$) when compared to values obtained during the same time periods in the control group. The RAW_E showed steady but insignificant increases at 30, 60, and 90 minutes post-injection. The value of RAW_E at 120 minutes did approach significance ($P<0.100$) when compared to the control value obtained during the same interval. The increase in RAW_E from 4.56±1.16 (90 min) to 6.33±1.30 cm H_2O/L•s (120 min) was significant ($P<0.050$).

Absolute values for airway resistance in our study are higher than reported by other (22,50). Our resistance values represent individual maximums since they were calculated at peak inspiratory and expiratory flow rates. We can only assume that other authors have calculated resistance values at some predetermined flow which was less than the

maximum, although precise description of their methodology is generally lacking. However, the changes we observed are in agreement with several studies of acute pulmonary edema in man (213) and in dogs (22,50,129) which reported that the changes in total airway resistance were small and inconsistent. Sharp et al. (213) further demonstrated that consistent and substantial increase in airway resistance was observed only when the lung edema was grossly evident, which is in agreement with our findings. Further explanation for the increased airway resistance in the alloxan treated animals at 120 minutes post-injection was initially thought to be related to the increased respiratory frequency these dogs exhibited. Airway resistance is expected to increase with ventilation as flow becomes turbulent (108). This was not found to be the case in our study as can be seen in Figure 15. A linear inverse relationship existed between these variables in normal dogs and during the early stages of edema. However, as inspiratory resistance in the edema dogs approached the minimum value observed in normals, ca. 4.5 cm H_2O/L•s at 90 and 120 minutes post-injection, the relationship between resistance and frequency was no longer associated. Despite the large increase in frequency, resistance remained fairly constant. Similarly, the airflow-resistance diagram (Figure 16) revealed an identical curve as would be expected in view of the fact that frequency and airflow are directly related as was shown earlier (Figure 11). The break point on these curves occurred at approximately 20 L/min and is thought to represent the point at which laminar flow becomes turbulent. Knowing that the force to overcome laminar flow is proportional to the mean forward velocity of flow and for turbulent flow is

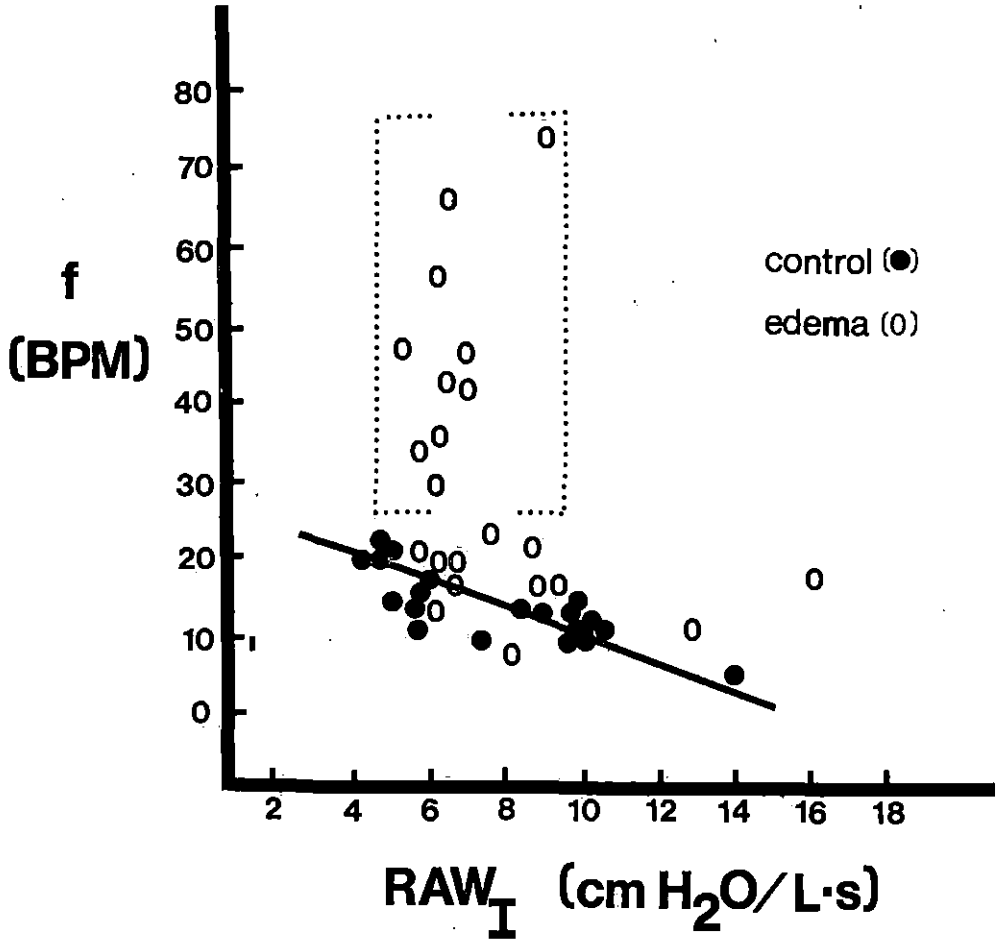

Figure 15. Relationship between respiratory frequency and inspiratory airway resistance in normal dogs and during early edema (solid line) compared to more severe advanced edema (brackets).

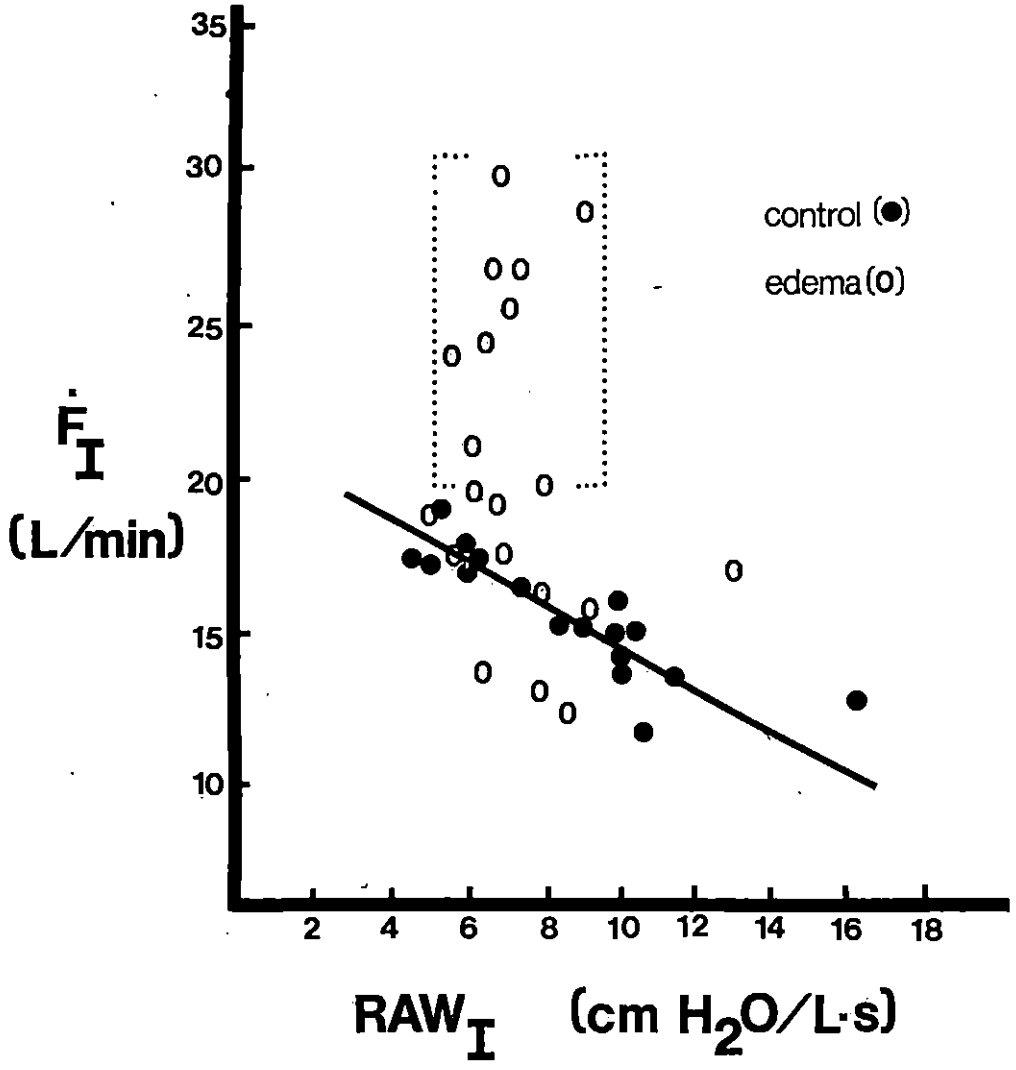

Figure 16. Altered relationship between inspiratory airflow and inspiratory resistance in normal dogs and during early edema (solid line) compared to that observed during the late stages of edema (brackets).

proportional to the square of velocity; we investigated the relationship between flow and pleural pressure (Figure 17). The association between these variables was not as apparent as predicted. Furthermore, normal dogs appeared to expend more force per unit flow at low velocity than at higher velocities. Explanation for these results would be tenacious in light of the small sample size. Regarding the alloxan treated animals we observed two distinct responses during edemagensis. The change in esophageal pressure, i.e., force, required to effect even a small increase in airflow above the hypothesized "critical" airflow of 20 L/min was greatly increased. The presence of the same break point as encountered in the frequency-airflow and frequency-resistance curves lends credence to our explanation of turbulent flow occurring when $\dot{F}_I$ exceeds 20 L/min in acute edema. A comparably large ΔP_{es} was also required at extremely low inspiratory flow rates, which may be a manifestation of the additional inertial air forces which are encountered at low flow rates. The increased resistance to airflow at both extremes of velocity in the alloxan group probably reflects central and peripheral airway obstruction caused by foam production. Mean ΔP_{es} was increased in the edema dogs which has been shown (50) to force open collapsed alveoli with subsequent fluid and gas displacement from alveoli causing formation of bubbles. Rales were heard in most of the alloxan treated animals, although tracheal foam (Figure 18) was evident in only about half of the animals studied.

The hypoxemia observed at 120 minutes is consistent with ventilatory obstruction. The values of both RAW_I and RAW_E during the first 90 minutes are somewhat more difficult to explain in that hypoxemia was apparent more

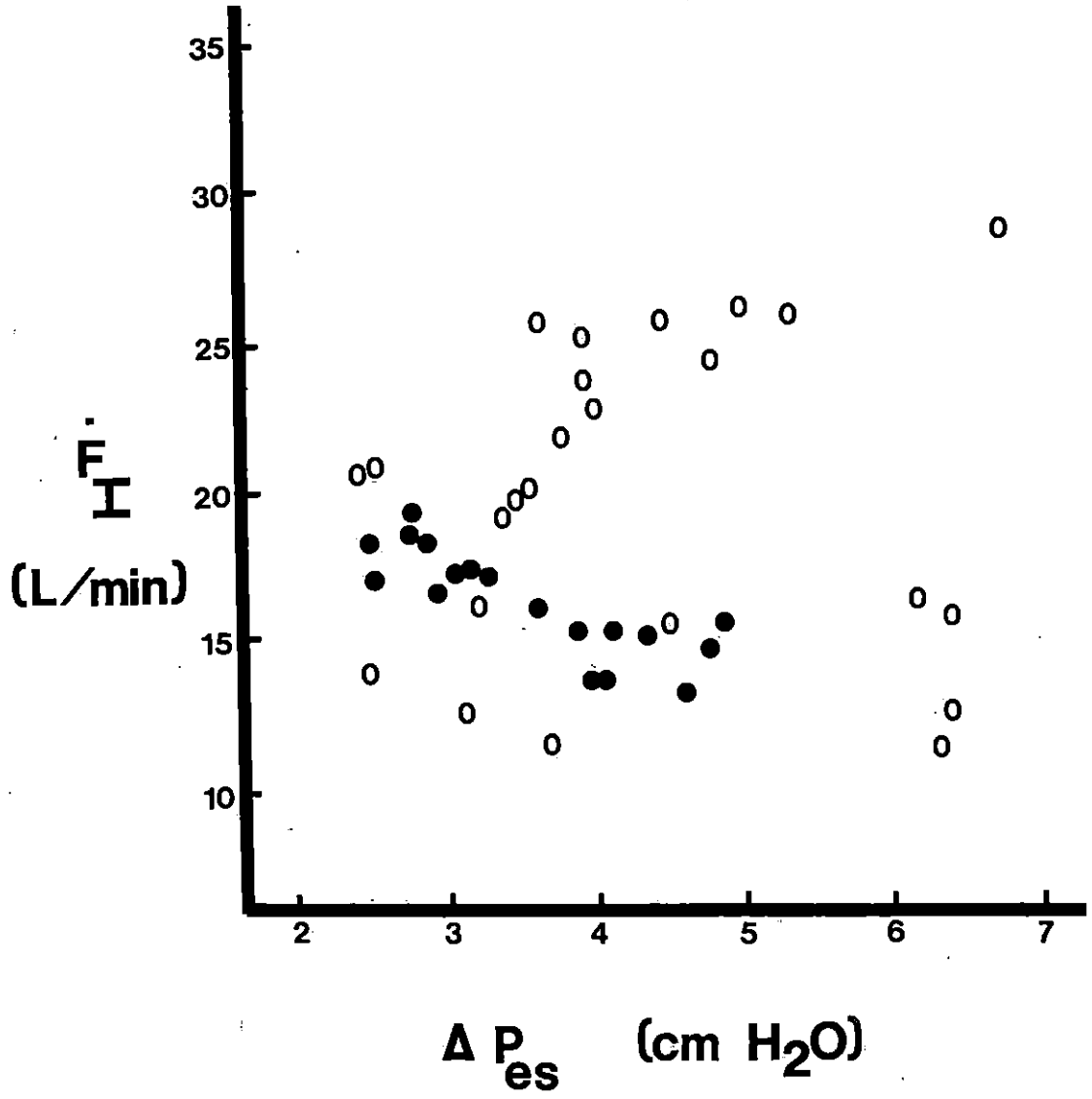

Figure 17. Plot of inspiratory airflow versus the change in esophageal pressure in control (closed circles) and alloxan-edema (open circles) dogs.

Figure 18. Photograph showing the presence of large quantities of foam and discolored lung fluids in the airways of alloxan treated dogs.

than one hour before significant ventilatory obstruction, i.e., increased RAW_I and RAW_E, was apparent. Partial explanation may be afforded by the work of Macklem and Mead (134) and Hogg et al. (103) in which it was demonstrated that small peripheral airways contribute very little to total airway resistance. If such is the case, then massive obstruction of these conducting airways which could markedly impair gas exchange would not be detected in our measurements of total airway resistance. Specific partitioning of peripheral airway resistance as well as total airway resistance will be required to conform these ideas.

Extravascular Water Accumulation

Since pulmonary edema is defined as excess extravascular storage of water in the lung, some method of assessing the amount of water is required. To determine excess extravascular water, we have calculated the total wet lung weight-dry lung weight ratio (W/D), the W/D ratios for the individual lobes, the relative lung weight (RLW) expressed as grams wet lung weight per kg body weight, and the lung weight-heart weight (L/H) (Table 4). There are conflicting ideas in the literature as to which measurement most accurately assesses the degree of edema. We wished to further clarify this matter by making all calculations. The individual lobe W/D ratio determinations were also made in an attempt to localize the edema and relate these findings to the gross and histological evaluations.

The mean W/D ratio for the total lung in the alloxan treated animals (6.2±0.9) was slightly higher than that calculated for the control animals (5.4±0.4). The lack of significance cannot, however, be interpreted to

Table 4. Wet weight-dry weight (W/D) ratios of whole lungs and individual lobes, relative lung weight,[a] and lung weight-heart weight[b] of normal and edematous tissues at autopsy

Variable	Normal	Edema	Probability[c]
Total lung W/D	5.4±0.4[d]	6.2±0.9	0.1282
Right apical W/D	6.0±2.8	5.7±0.8	0.832
Right cardiac W/D	4.1±1.1	5.6±0.9	0.077
Right diaphragmatic W/D	6.1±0.2	6.6±1.7	0.542
Right intermediate W/D	5.8±1.0	7.9±1.5	0.037
Left apical W/D	4.7±0.3	5.6±0.7	0.029
Left cardiac W/D	4.9±0.4	5.3±1.0	0.448
Left diaphragmatic W/D	5.7±1.0	6.2±1.2	0.560
Relative lung weight	8.3±0.8	15.4±4.7	0.012
Lung weight-heart weight	1.21±0.02	2.06±0.22	0.006

[a]Relative lung weight calculated as gram wet lung per kg body weight.

[b]Lung weight-heart weight calculated as gram wet lung per gram heart after heart has been trimmed of the great vessels and pericardium.

[c]Indicates probability that the observed difference between means of the edematous and normal lungs occurred by chance (1-way ANOVA).

[d]Values represent mean ± SD with n = 5 in the normal group and n = 4 in the edema group.

mean that edema was not present. A large degree of variance among animals which has been previously reported (35) is apparent (Figure 19). It is important to note that the mean W/D ratio in every lobe is higher in the edematous lung than in the control lungs, except for the right apical lobe. This can be explained by the fact that the right apical lobe was the lavaged lobe in three of the five control dogs. The wet weight of this lobe in these animals may be biased by absorbed lavage fluid. The

Figure 19. Scattergram of wet lung weight-dry lung weight ratios of individual lobes and total lung of normal and edematous tissue.

Abbreviations used: right apical - RA, right cardiac - RC, right diaphragmatic - RD, right intermediate - RI, left apical - LA, left cardiac - LC, and left diaphragmatic - LD. Individual control values (closed circles) and control means (solid line) as well as values for edematous lobes (open circles) and their means (dotted line) are represented.

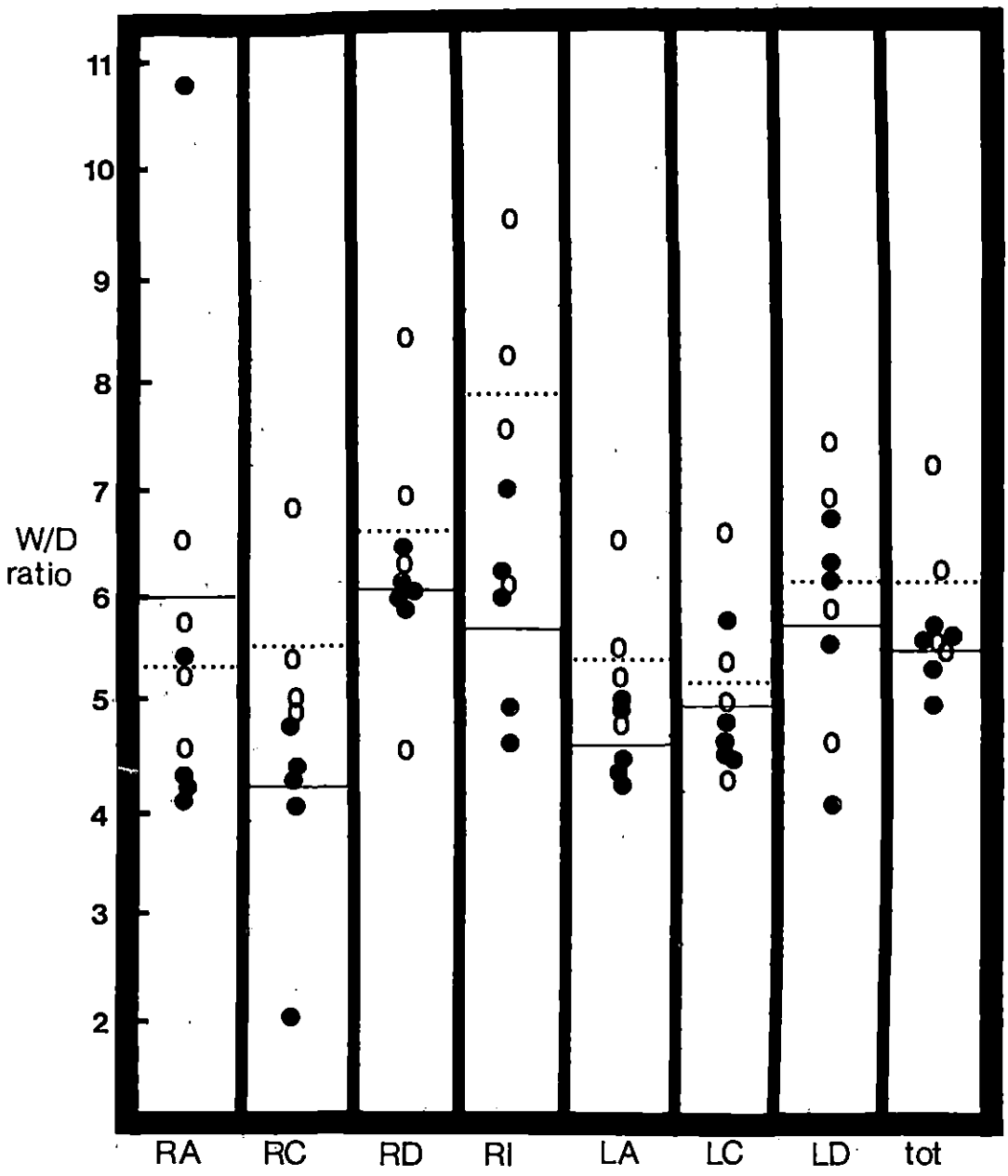
W/D ratio
11
10
9
8
7
6
5
4
3
2
RA
RC
RD
RI
LA
LC
LD
tot

mean W/D ratios in the right intermediate lobe (7.9±1.5) and left apical lobe (5.6±0.7) of the alloxan treated dogs were significantly higher ($P<0.050$) than the corresponding lobe W/D ratios calculated in the control dogs. This was not an artifact due to lavaging, but rather is interpreted as a true indice of the edema, since there two lobes appeared severely damaged when observed grossly and histologically (Figures 23 and 24).

Total lung W/D ratios as we have calculated have previously been reported in normal and edematous lungs. Bredenbe et al. (26) observed an increase from 4.33±0.13 to 5.53±0.24 in hemodynamic pulmonary edema while Glauser et al. (82) observed increased W/D lung weight ratios (4.7 to 6.4) in dogs with pulmonary edema induced by aortic obstruction and fluid overload. Brigham (27) reported a difference of 4.36±0.04 in normal dog lungs and 5.58±0.36 in lungs of dogs with alloxan-induced pulmonary edema. Staub (225) reported the W/D ratios of normal human lungs to be approximately 5.2 compared to 7.6 for edematous lungs.

The relative lung weight in our control group averaged 8.3±0.8 g/kg and corresponds with those reported by Muggenberg et al. (163) ranging from 8.3 to 9.3 in normal mongrel dogs. Relative lung weight in our alloxan group averaged 15.4±4.7 which was significantly larger ($P<0.012$) than the control mean. Our results are almost identical to those of Meyer and Ottaviano (150) who reported RLW values of 10.0±1.5 in normal dogs while alloxan treated animals in their study had RLW values of 15.3±5.7. The change in RLW we observed is comparable to values reported in dogs immediately after undergoing total lung lavage in which it was calculated that the lungs had retained 13 ml lavaging fluid per kg body weight.

Lung weight-heart weight ratios were also significantly higher ($P<0.010$) in the edematous (2.06±0.22) animals compared to the normal dogs (1.21±0.02). Similarly, Cheng et al. (35) calculated the L/H ratio of edematous animals to be 2.4±0.15.

From the foregoing it is evident that W/D ratios alone are not reliable indicators of the degree of pulmonary edema. Lung weight-heart weight and relative lung weight determination appear to provide more accurate indices of the condition. However, the W/D ratios when used in conjunction with histological examination can assist in localizing the most severely impaired areas of the lung. It is further recognized that other means of evaluating the disease must be incorporated if useful information concerning the pathogenesis of lung edema is to be derived from autopsy cases.

Protein Composition

Figure 20 is a photograph of protein electrophoretic patterns representative of those found in the alveolar lining material (ALM) of normal and edematous dog lungs. Excellent band separation was achieved in the molecular weight range of 10,000-200,000 daltons on 10 cm polyacrylamide (7.5%) gels. The increased gel length promoted visual resolution of molecular weight differences between 1500-2000 daltons.

Eight proteins ranging between 15,000 and 98,000 daltons were separated in lyophilized ALM of control animals. Samples collected from the alloxan treated animals revealed 11 proteins in the molecular weight range of 14,500 to 174,000 daltons. Five proteins were common to both groups

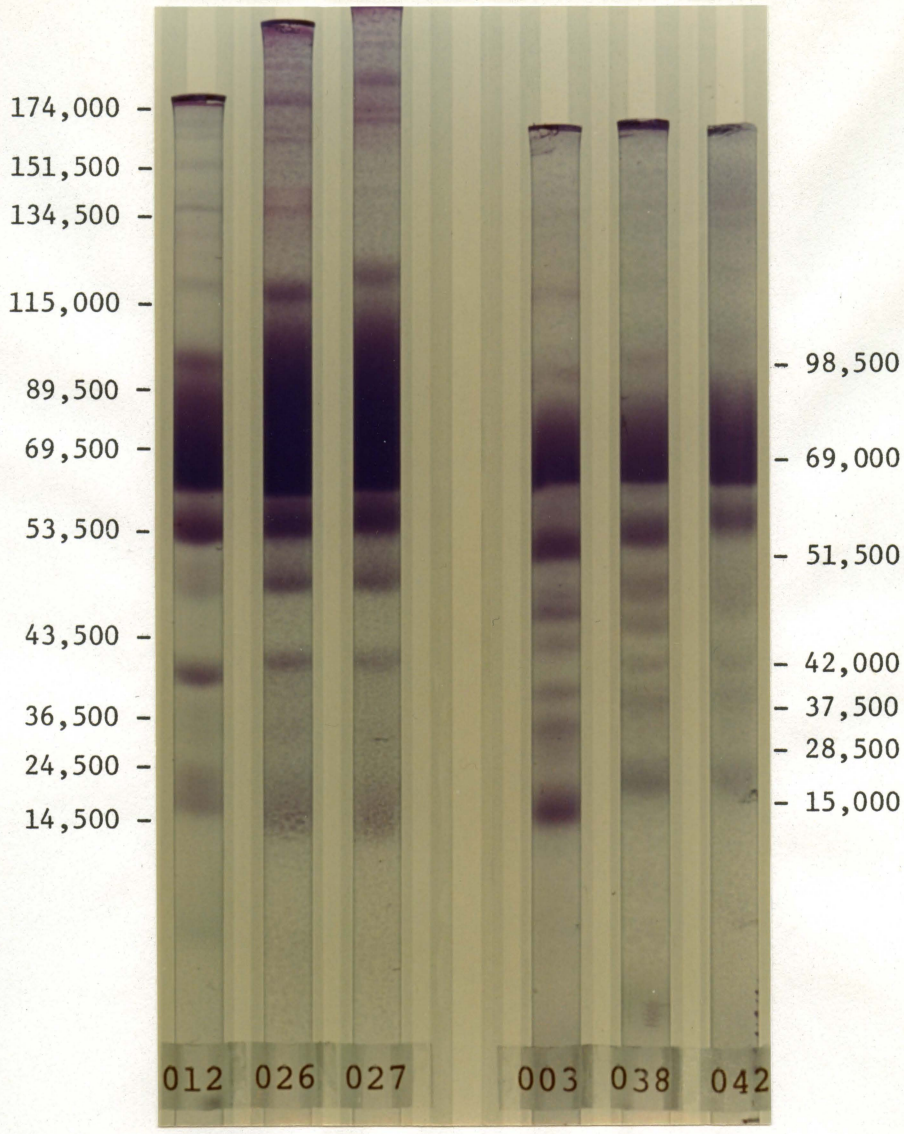

Electrophoresis was carried out on 7.5% polyacrylamide gels in 0.1 M phosphate buffer containing 1% SDS. Proteins were reacted with SDS and β-mercaptoethanol at 100°C before electrophoresis. Gels from control animals are labelled 003, 038, and 042. Gels from alloxan treated dogs are labelled 012, 026, and 027. Molecular weight (daltons) appearing at the margins have been rounded off to the nearest 500.

Figure 20. SDS-acrylamide gel electrophoresis of proteins found in alveolar lining material of normal and edematous dog lungs.

considering the 1500-2000 resolution limitation. Common proteins were isolated at ca. 69,000, 52,000, 43,000, 37,000, and 15,000 daltons. It has been shown that the alveolar membrane is highly impermeable to proteins (65,231). This idea leads us to postulate that the 8 proteins found in lavage fluid of our control group represent autologous proteins in the alveolar lining material. Scarpelli et al. (208) identified five proteins by electrophoresis in tracheal washings obtained from excised dog lungs, although they attributed these to blood contamination rather than to real lung fluid components. Similarly, Klass (119) identified three proteins in pulmonary surface active material by immunological techniques concluding that two of the proteins were probably serum contaminants, while the third protein was unique to the lungs. Along these same lines, Frosolono et al. (76) identified only two proteins by disc electrophoresis. However, they reported that appreciable quantities of material remained at the origin of the gels, indicating to us that other proteins which may have been present in the samples were of molecular weights beyond the capacity of the gels they were using.

Much information concerning lipid components of alveolar lining material has been accumulated, but very little is known about the protein moieties. Conflicting reports have appeared as to the mere presence of proteins in alveolar lining material. Early studies (25,192) reported that normal tracheal fluid contained less than 1% protein, while more recent studies (119) report 10% protein in such fluids. Frosolono et al. (76) reported that isolated surface active material from saline lung lavage fluid of dogs contained significant amounts of protein (0.185±0.022 mg protein/g lung). Radioactive labelling studies (63,138) have revealed

that leucine is actively incorporated into protein found in the surface active fraction of lung washings. Evidence at the electron microscopic level of resolution has provided convincing reports that tubular myelin is normally present in large quantities on the alveolar surface and contains a highly ordered arrangement of albumin, phospholipids, and carbohydrates (80,170).

The six additional proteins found in the edematous lungs of the alloxan treated animals may reflect one or both of the following: (1) increased permeability of the blood-air barrier reported to occur in alloxan induced pulmonary edema (53,69,87), thus allowing plasma contaminants to pass freely into the alveolar lumen, or (2) cellular damage with concomitant release of enzymes. Nitta and Staub (172) reported significant amounts of protein (57%-94% of the plasma level) in alveolar fluid of cats and guinea pigs with ammonium chloride edema which is consistent with Koenig and Koenig's (122) early report of proteinaceous fluid in histologic sections of edematous lungs. Katz and coworkers (112) and Robin et al. (200) reported that airway fluid protein concentration from edematous lungs of humans was identical to the plasma level. Vreim and Staub (240) recently showed that the total protein content of airway fluid was 15% less than alveolar fluid in dogs with alloxan induced pulmonary edema. This finding could help to explain why only two proteins having molecular weights of 35,000 and 10,000 daltons have been identified in adult (113) and puppy (116) lung washings. Our samples were collected by lobar lavage thus representing more true alveolar fluid than those of King's (113) study in which the samples were collected by endobronchial lavage at the

level of bronchi bifurcation. King purified the lavage samples by differential centrifugation in buffered sodium bromide solutions which were designed to exclude small water soluble proteins thought to represent contaminants. The elimination of these polar proteins may provide another explanation for the difference in our results. Although the actual protein isolation in King's study was by SDS polyacrylamide gel electrophoresis on 5.6% gels, similar to ours; they employed fluorescent excitation to visualize the bands in contrast to the highly sensitive and specific Coomassie Blue staining procedure that we used. King reported marked variability in duplicate runs made on the same preparation which may reflect the inadequacy of fluorescent identification. We observed almost no variability among triplicate samples run on the same preparation by our method.

The most striking band occurring in both control and edematous ALM of our animals had a molecular weight of approximately 69,000 daltons and corresponded repeatedly with the bovine serum albumin standard (m.w. 68,000). An intrinsic protein with a molecular weight of 69,000-70,000 daltons has recently been identified as albumin by its immunological properties (116). Assuming the band we identified at 69,000 was albumin, then the quantity of this protein in the ALM from the alloxan treated animals was much greater than that found in the controls. Whether this reflects altered lung metabolism in edema or is merely a consequence of plasma contamination will require radioactive labelling studies.

Lipid Composition of Alveolar Lining Material

Thin-layer chromatograms of lipids visualized by iodination were compared with standards[1] which were simultaneously run on each plate. Discrete separation of individual phosphatides, neutral lipids, and cholesterol was achieved in our system. Neutral lipids appeared as one spot slightly behind the solvent front. Lysophosphatidyl choline (LPC), phosphatidyl serine (PS), sphingomyelin (Sph), phosphatidyl inositol (PI), phosphatidyl choline (PC), unidentified phosphatide (UnP), phosphatidyl ethanolamine (PE), cholesterol (Ch), and neutral lipids (N) were present. The phospholipids we identified in canine ALM are in closest agreement with those reported by Pfleger and Thomas (188) and Harlan et al. (98). Scarpelli et al. (208) reported the presence of neutral lipids, PC, PE, Sph, and an unidentified phosphatide, while Finley et al. (71) described phosphatidic acid, PE, and phosphatidyl methylethanolamine as the major lipid components in dog surfactant. The identity of a phosphatide migrating with an R_f just below phosphatidyl ethanolamine, as had been reported earlier, has recently been characterized as phosphatidyl glycerol (188). It is possible that the unidentified phosphatide we observed was also phosphatidyl glycerol as its R_f (0.302) in our system was slightly behind PE (0.430).

The percent phosphorous contributed by individual lipids to the total recovered phosphorous are presented in Table 5. Sphingomyelin and

---

[1]Standards (>95% pure) were obtained from United States Biochemical and included LPC, PS, Sph, PC, PE, and Ch dissolved in chloroform/methanol (1:1, v/v).

Table 5. Phospholipid composition of alveolar lining material from normal and edematous dog lungs

Phosphatide	R_f[b]	% of total phosphorous[a]	
		Normal (5)	Edema (4)
Lysolecithin	0.064	4.1±3.5[c]	3.1±0.8
Phosphatidyl serine	0.103	5.3±3.2	9.5±6.8
Sphingomyelin and phosphatidyl inositol	0.142-0.158	9.2±3.0	12.8±1.2[d]
Phosphatidyl choline	0.240	60.2±2.8	71.0±4.6[e]
Unidentified phosphatide	0.302	19.5±9.8	Absent
Phosphatidyl ethanolamine	0.403	5.8±2.6	4.7±2.6

[a]Total phosphorous in µg was quantitated by spectrophotometric methods (described in the text) after separation of lipid extracts by TLC in chloroform/methanol/water (80/25/4, v/v).

[b]R_f values were calculated as the distance from the origin to the unknown spot divided by the distance from the origin to the solvent front.

[c]Values represent mean ± SD.

[d]Significantly different from control phosphatide ($P<0.050$).

[e]Significantly different from control phosphatide ($P<0.010$).

phosphatidyl inositol are represented as one component because of their close R_f values. Scraping them from the plate separately was not as reproducible as when they were eluted together, hence we chose the latter procedure. Possible background density resulting from silica gel contamination in our samples was corrected for by eluting blank areas of silica, processing them exactly like the samples for phosphorous analysis,

and using the supernatants for setting infinite absorption on the spectrophotometer.

Phosphatidyl choline was the predominant phosphatide found in both groups, composing 60.2±2.8% in the normal dogs and 71.0±4.6% in the alloxan treated animals. The unidentified phosphatide was the second most abundant phosphatide in the control animals (19.5±9.8%), followed by Sph plus PI (9.2±3.0%), PE (5.8±2.6%), PS (5.3±3.2%), and LPC (4.1±3.5%). The unidentified phosphatide in the controls was not detected in samples from the alloxan treated animals. However, Sph and PI (12.8±1.2%), PS (9.5± 6.8%), PE (4.7±2.6%), and LPC (3.1±0.8%) were present. Significant differences between control and alloxan treated groups were found in phosphatidyl choline ($P<0.010$) and Sph/PI ($P<0.050$) as well as in the unidentified phosphatide found in control samples while absent in all edema fluid lipid extracts.

Table 6 shows that the dry weight recovery of ALM expressed as mg dry weight per 100 ml lavage fluid was significantly ($P<0.010$) greater in the edematous lungs (1083.3±493.6) than in the control lungs (50.3±19.6). However, total lipids expressed as a percent of ALM dry weight were significantly ($P<0.010$) less in the edema group (1.8±0.5) than in the normal animals (10.6±3.7) which is partially due to a dilution factor. We have further found that total phospholipids comprise a significantly ($P<0.010$) larger portion of the total lipids in the alloxan group (82.8±4.8) when compared to the control group (64.2±9.5) without significant changes in relative proportions. The additional weight may be accounted for by any or all of the following: (1) mechanical disruption of the alveolar

Table 6. Total dry weight recovery, percent total lipids, and percent phospholipids in alveolar lining material of normal and edematous canine lungs

Group	Dog No.	Total dry weight recovery (mg/100 ml)	Total lipids (percent dry weight)	Total phospholipids (percent total lipids)
Control	1	72.06	6	77
	2	40.00	12	64
	3	55.56	9	69
	4	22.11	10	59
	5	61.7	16	52
	Mean	50.3	10.6	64.2
	SD	19.6	4.7	9.5
Edema	1	1784.3	2	77
	2	775.5	1	85
	3	703.5	2	81
	4	1069.7	2	88
	Mean	1083.3[a]	1.8[a]	82.8[a]
	SD	493.6	0.5	4.8

[a]Significantly different from control ($P<0.010$).

lining, (2) biosynthesis, and (3) transudation from the vascular system. The magnitude of ALM recovery and the identification of five different proteins from edematous lung fluids leads us to believe that the third mechanism is primarily responsible. Gump et al. (88) similarly reported that increased dry weight recovery of edema fluid was largely due to the presence of proteins. Further evidence for protein accumulation is apparent if the 20-fold dry weight recovery is compared to the 6-fold reduction in total lipid. It is reasonable to expect simultaneous

mechanical disruption occurring in these animals. Physiological studies further suggest that respiratory frequency may be a determinant of the rate at which surface active material is utilized on the alveolar surface (141). The increased ventilatory activity associated with alloxan-induced pulmonary edema in our study may have caused surface absorption of more ALM from the hypophase to the air-interface. It is tempting to speculate that the phospholipids of ALM are not actually "free" in the alveolar lining layer, but instead are present in chemical combination with other molecules rendering them less available by saline lavage in normal dogs. It follows that phospholipid availability from edematous lungs is enhanced either by chemical reactions and/or by mechanical disruption which may further explain why ALM of edematous lungs revealed more phospholipids per gram dry weight than normal lungs.

Our results provide further evidence that phospholipids are the primary class of lipids found in canine alveolar lining material, with phosphatidyl choline being the most predominant, as has been previously reported in several mammalian species (43,76,78,183,208). Harlan et al. (98) studying acute lung edema in dogs isolated the same six phosphatides in tracheal foam that we observed in lobar lavage fluid. Lecithin recovery in their study (57.5%) was less than we have reported (71.0%). However, PE (10.6 vs. 4.7%) and LPC (9.6 vs. 3.1%) were found in larger quantities in their samples than in ours. They further reported that total phospholipids in ALM of the edematous lungs were significantly reduced without alterations in their relative proportions. The physiological significance of compositional changes in alveolar lining material will become more apparent in the discussion of surface behavior that follows.

Surface Characteristics

In describing the physical properties of lung fluids, in vitro surface tension (ST) measurements of monolayers has become a widely used technique. Development and application of the Langmuir-Adam trough and Wilhelmy balance with modifications by individual laboratories has resulted in massive bodies of information concerning the physical characteristics of lung fluids. Of particular interest to pulmonary physiologists and pathologists is the role of surface tension in normal and abnormal respiratory function. Unfortunately, detailed reports of the conditions of the actual surface tension measurements as well as sample preparation are lacking which makes comparisons of absolute values obtained among different laboratories almost impossible. For these reasons, our laboratory performed a series of quality control experiments aimed at developing a reliable and repetitive protocol for measuring surface tension properties of lung fluids (refer to Methods section).

Ten compression-expansion cycles were run on every sample after a 10 minute equilibration period as illustrated in Figure 21. The equilibrium surface tension, i.e., ST obtained at maximum surface area at the start of the first compression cycle, was considered to be the true γ_{max} of each sample. The primary reason for using this value of γ_{max} is because all γ_{max} obtained at the start of subsequent compression cycles were observed to be steadily increased approaching and even overshooting the ST of the saline subphase. Minimum surface tension (γ_{min}) was always obtained during the first cycle and often occurred during the second and third cycle as well. However, γ_{min} recorded during the 4th-10th cycles was

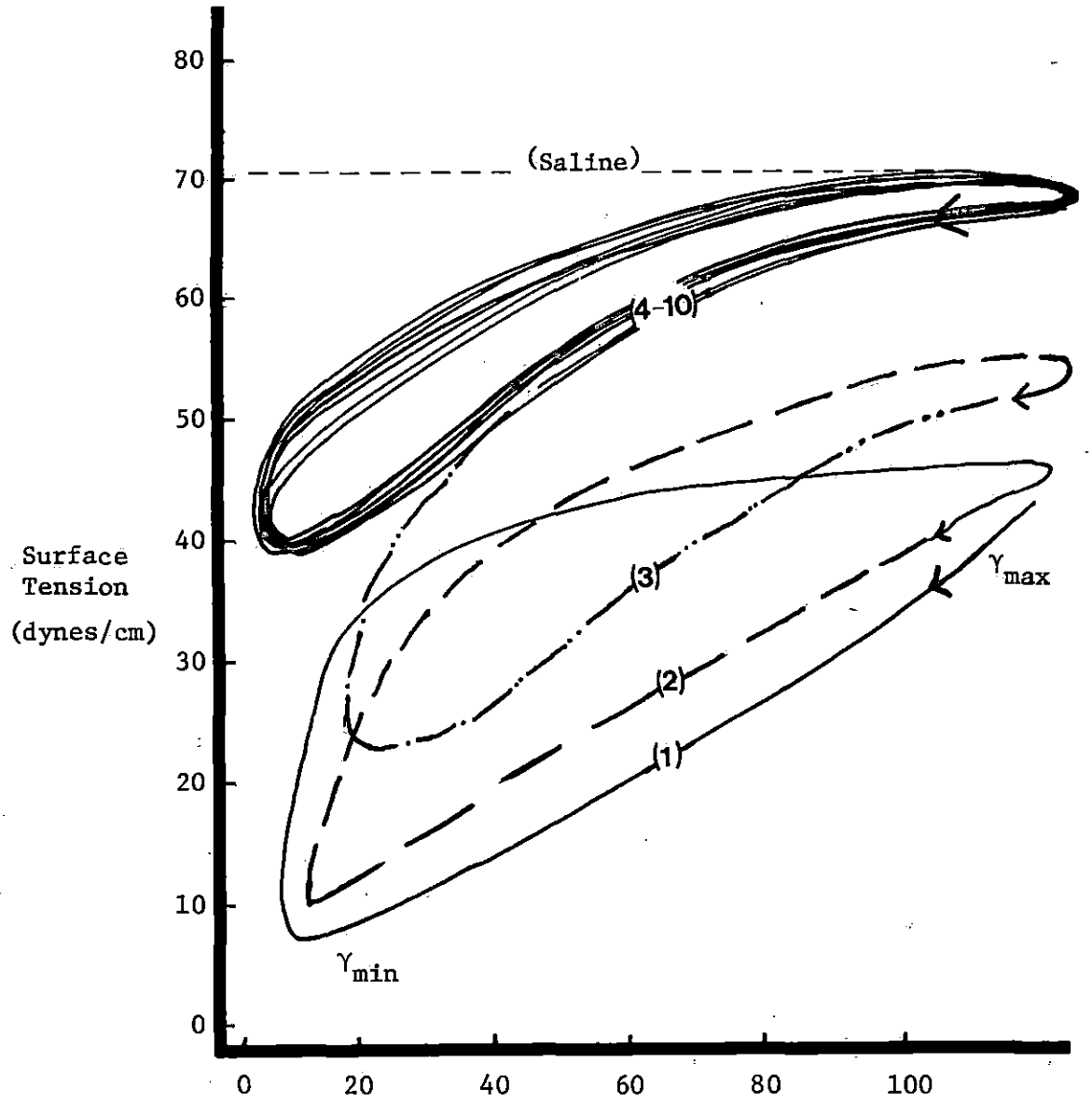

Points where γ_{max} and γ_{min} were measured are marked. Arrows indicate direction of area change.

Figure 21. Typical compression-expansion isotherms obtained during cycle 1-10 on a modified Wilhelmy balance.

usually two to four times higher than that of the first cycle. The ST values at every surface area (SA) of the expansion isotherm were always larger than those of the compression isotherm such that constantly changing open loops were formed during cycle 1-cycle 3. Cycle 4-cycle 10 most often appeared as repeating and closed loops.

Another reason for using cycle 1 values as the most representative of lung liquid surface behavior was that the hysteresis effect was most apparent for these isotherms. The fact that the path of cycle 1 was rarely repeated during cycle 2-cycle 10 probably reflects adhesion of molecules to the platinum strip, evaporation of sample, and/or collapse of the monolayer film. The cycle periodicity (8 sec) used in our experiment corresponds to a respiratory frequency of approximately 8 BPM and is much faster than previous reports in which cycle periodicities range from 3 to 28 minutes. Such slow speeds of compression and expansion hardly mimic physiological in vivo respiratory rates.

Numerical values describing the surface characteristics of reconstituted lyophilized alveolar lining material (ALM) and the corresponding lipid extracts (LEX) are presented in Table 7. Individual values of γ_{max} and γ_{min} represent the mean of duplicate sample runs. The minimum criterion of surface activity used by King and Clements (114) was the ability of the tested material to achieve a surface tension of 10 dynes/cm or less when spread and compressed on a saline surface. Only the lipid extracts from normal dog lung fluids exhibited this characteristic in our experiment. The average γ_{min} on compression in these samples was 4.9±1.8 cynes/cm which was significantly ($P<.001$) lower than the average γ_{min} (22.8±2.6

Table 7. Surface characteristics of reconstituted alveolar lining material[a] and lipid extracts[b] as determined on a modified Wilhelmy balance[c]

Group	Dog No.	γ_{min}[d] (dynes/cm) ALM	γ_{min}[d] (dynes/cm) LEX	γ_{max}[e] (dynes/cm) ALM	γ_{max}[e] (dynes/cm) LEX	$\bar{s}$[f] ALM	$\bar{s}$[f] LEX
Control	1	21.7	7.7	61.6	52.5	0.96	1.49
	2	25.9	3.5	62.3	27.3	0.83	1.55
	3	47.6	3.5	65.1	23.8	0.31	1.49
	4	29.2	6.0	63.6	41.1	0.74	1.49
	5	34.1	4.2	65.0	36.2	0.62	1.58
	Mean	31.4	4.9	63.5	36.2	.69	1.52
	SD	9.9	1.8	1.6	11.4	.25	.04
Edema	1	33.6	25.9	48.3	31.5	0.36	0.19
	2	39.2	20.3	55.3	23.1	0.34	0.13
	3	48.3	23.8	60.2	30.1	0.22	0.23
	4	33.9	21.0	50.4	30.8	0.39	0.38
	Mean	38.8	22.8[g]	53.6[h]	28.8	.33[i]	.23[g]
	SD	6.9	2.6	5.3	3.9	.07	.10

[a] Lyophilized alveolar lining material (ALM) dissolved in 0.15 M saline to a final concentration of 20 µg/µl.

[b] Lipid extracts (LEX) dissolved in chloroform/methanol (1:1, v/v).

[c] Sample monolayers formed by dripping 10-40 µl on a saline subphase (25°C) at maximum surface area, equilibrated 10 min, followed by 10 continuous cycles with a periodicity of 8 sec.

[d] Minimum surface tension (γ_{min}) measured at end of first compression cycle. SA = 10 cm^2.

[e] Maximum surface tension (γ_{max}) measured at start of first compression cycle. SA = 35 cm^2.

[f] Stability index ($\bar{s}$) calculated as: $2(\gamma_{max}-\gamma_{min})/(\gamma_{max}+\gamma_{min})$.

[g] Significantly different from control ($P<0.001$).

[h] Significantly different from control ($P<0.010$).

[i] Significantly different from control ($P<0.050$).

dynes/cm) of lipid extracts from the edematous lung fluids. In contrast, when compression-expansion cycles were performed on whole ALM the average γ_{min} of normal and edematous lung fluids were similar being 31.4±9.9 dynes/cm in the control group and 38.8±6.9 dynes/cm in the alloxan treated group. The average γ_{max} in normal (36.2±11.4 dynes/cm) and edema (22.8± 3.9 dynes/cm) fluid lipid extracts were not significantly different. The same was not true for γ_{max} of the ALM, which was 63.5±1.6 dynes/cm in the control dogs and 53.6±5.3 dynes/cm in the edemic animals, a significant difference ($P<.010$). However, γ_{max} of ALM and LEX, when compared within groups revealed significant ($P<0.001$) differences; with γ_{max} of ALM greater than γ_{max} of the corresponding lipid extracts in all cases.

The stability index ($\bar{s}$) of these samples provides further information regarding the physical nature of lung liquids, both ALM and LEX. Lipid extracts of normal lung fluids revealed the highest $\bar{s}$ of 1.52 which approaches the theoretical $\bar{s}_{max}$ value of 2.0. In contrast, lipid extracts of the edema fluid had the lowest $\bar{s}$ (0.23). Similarly, the average $\bar{s}$ in ALM from normal dogs and the alloxan treated animals were 0.69 and 0.33 respectively. The differences between the mean stability indices of the two groups were statistically significant for ALM ($P<0.050$) as well as LEX ($P<0.001$). Furthermore, $\bar{s}$ of lipid extracts in control dogs was statistically ($P<.001$) greater than the stability index of the corresponding samples of normal ALM. The opposite occurred in the alloxan treated group. The $\bar{s}$ of ALM from edematous lungs was larger than the $\bar{s}$ of corresponding lipid extracts.

Our results are in accord with those of Clements et al. (46) in the original paper describing these measurements in which they reported normal lung fluids having stability indices ranging from 0.80 to 1.82; whereas the value of $\bar{s}$ in detergent treated rat lung fluids was approximately 0.20.

A representation of average surface tension vs. surface area isotherms obtained during the first compression cycle is given in Figure 22. The slope of the LEX compression isotherms in normal dogs was found to be much steeper than that for LEX of edematous lungs. On expansion the LEX of normal lungs showed a much larger increase in surface tension as the surface area was enlarged from 10 to 40% than when enlarged from 40 to 100%. In contrast, the expansion isotherm of the LEX from edematous lungs was essentially linear throughout the entire range of surface areas. Hysteresis was apparent in both sets of data, although the area between the isotherms in the control group was approximately 2.5 times greater than that for the edematous lung fluid. Isotherms obtained from samples of reconstituted ALM are comparable in shape to those obtained from the corresponding LEX within both groups of dogs. The absolute values are larger causing the curves to be shifted upward. However, the change in ST per unit change in SA remains nearly linear in the compression cycles of both groups as well as the expansion cycle of the alloxan treated dogs. The expansion isotherm of lipid extracts from lung fluids of normal dogs is hyperbolic with the breaking point occurring at approximately 35-40% of the maximum surface area. In addition, the hysteresis observed between the isotherms in normal samples is again nearly 2.5 times that obtained for the ALM of edematous lungs.

Figure 22. Tension-area diagram of cycle 1 compression expansion isotherms of alveolar lining material and lipid extracts from normal control and edematous canine lungs.

Each curve represents average values for 5 control or 4 alloxan-edema dogs as indicated. Arrows show the direction of area change during each cycle. Vertical slashes on compression phase represent arbitrary break points used in calculating phase 1 and phase 2 compressibility coefficients appearing in Table 8.

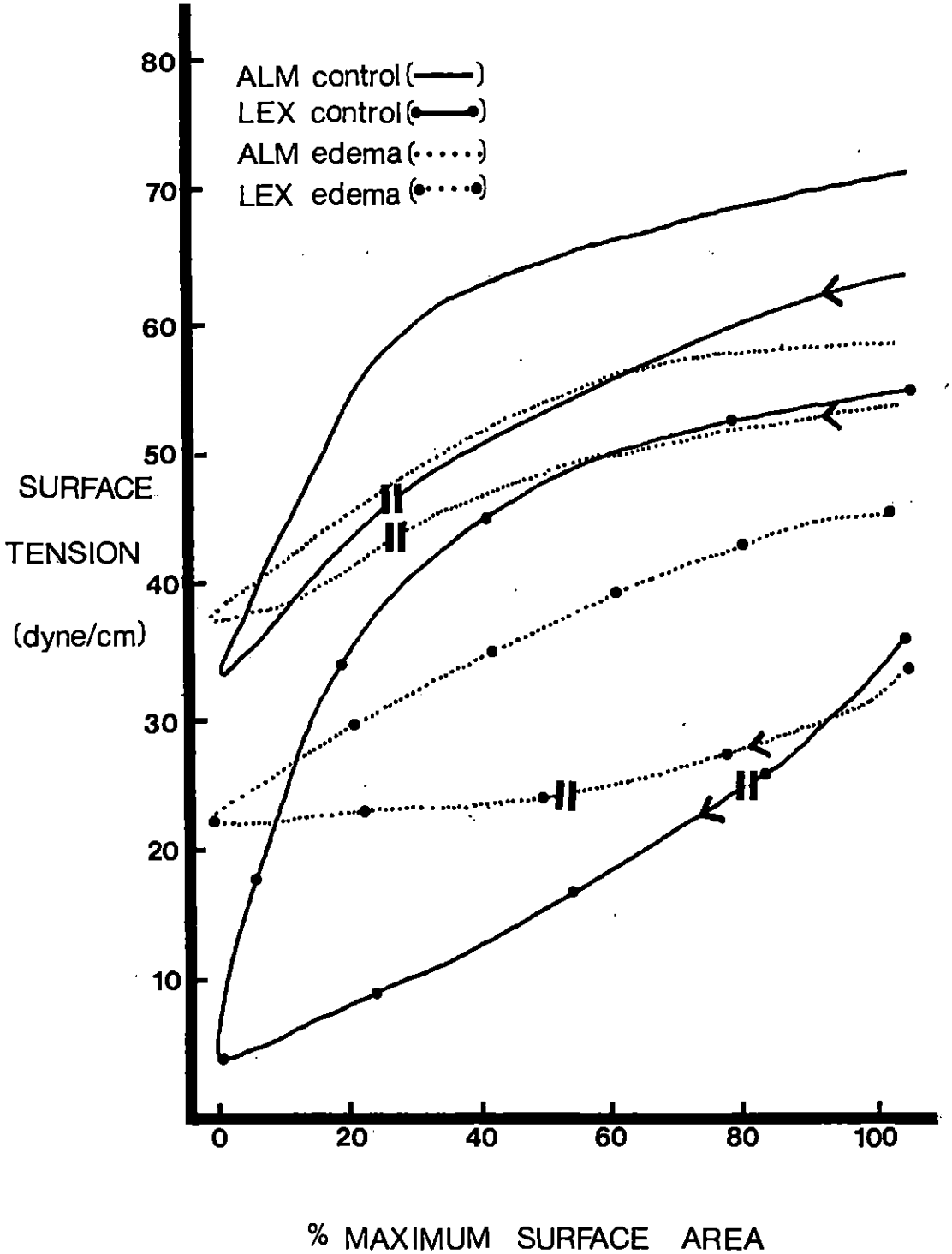
ALM control
LEX control
ALM edema
LEX edema
80
70
60
50
40
30
20
10
SURFACE
TENSION
(dyne/cm)
0
20
40
60
80
100
% MAXIMUM SURFACE AREA

From a plot of surface tension versus surface area, the coefficient of compressibility (k) of the surface film can be calculated which numerically describes the slope of these isotherms and further characterizes the dynamic physical capabilities of these monolayers. Most authors report one single value of k. In studying the loops (Figure 22) formed by our samples we observed the compressibility of these monolayers to vary throughout the compression-expansion cycle. For this reason we have reported the total compression isotherm k as well as the phase changes in k (if apparent) of cycle 1 compression (Table 8). The average coefficient of compressibility calculated for both ALM and lipid extracts of lung fluids from normal dogs was 0.02 (range 0.01-0.03) which characterized these as true liquid films (96). In contrast, k of ALM from the edematous lungs was 0.05 (range 0.03-0.05) which is comparable to values of k for serum reported by Brown et al. (30). Several explanations for this exist. Larger k values may reflect the molecular adhesion and coagulation which was grossly apparent in these samples. The films are apparently rupturing which suggests irreversible solidification of folding on compression. It is suspected that the proteins and/or electrolytes which are present in edema lung fluids are interfering with the normal molecular attraction and repulsion necessary for compression and expansion of these films. Surface tension is inversely related to the concentration of surface active molecules (233). We propose that extracts that develop very low surface tensions rapidly may be those having the highest ratio of surface active substances to contaminants. The γ_{min} of some surface active substances can be raised by mixing them with less surface active substances.

Table 8. Surface compressibility (k)[a] of cycle 1 compression isotherms[b].

Sample		Compression isotherm k[c] Total	Phase 1	Phase 2
Lipid extracts	C	0.02 (100)	0.01 (20)	0.03 (80)
	AE	0.12 (100)	0.07 (50)	0.51 (50)
Reconstituted alveolar lining material	C	0.02 (100)	0.03 (70)	0.01 (30)
	AE	0.05 (100)	0.06 (70)	0.03 (30)

[a]Surface compressibility (k) calculated as $dA/Ad\gamma$ where A is surface area and γ is surface tension.

[b]Values appearing under subheading total refer to an overall k for the entire cycle with dA = 100%. Phase 1 refers to k during the first portion of compression with phase 2 referring to k values of the second portion of the curve.

[c]Value represent mean values derived from the curves generated in Figure 22. Numbers inside parentheses indicate the % change in surface area used for calculation.

Therefore, the ALM, when mixed with blood and tissue elements in pulmonary edema, might not develop as low a surface tension as normally occurs.

Alterations in surfactant physiology have been implicated in various pathological situations, however, distinction between disorders due to underproduction, faulty production, or inactivation of the material have not been made. In view of the fact that alveolar lining material has a turnover time of about 14 hours; the acute nature of our experiment (ca. 3 hours) precludes positively identifying changes in surfactant synthesis in contributing to the altered surface characteristics we have observed in lung fluids obtained from alloxan treated animals. However, it is highly probable that biosynthesis as well as degradation of surfactant are

altered in acute pulmonary edema, primarily as a result of the hypoxia, acidosis, and vasoconstriction that are present during the pathogenesis of lung edema, although the relationships among these variables and surfactant production remain poorly understood. Schaefer et al. (210) found that uncompensated respiratory acidosis in guinea pigs was accompanied by a rise in the minimum surface tension of lung extracts which is similar to what we have observed. The significant acidosis (mean arterial pH = 7.243) we observed in the alloxan treated animals has been shown 99 (147) to interfere with surfactant synthesis. Similar studies by Adams et al. (3) report that specific changes in phospholipid production observed in ligation experiments appear to depend upon changes in the acid-base balance and/or P_{a0_2} levels in fetal lambs. Furthermore, regional changes in blood flow as evidenced by spotty atelectasis in the edematous lungs of our animals is known to cause reduced production of surfactant (36,70) as well as decrease the surface activity (210) in that which is present. In light of the foregoing, it is proposed that the reduction in surface activity, i.e., inhibition, of ALM and lipid extracts of ALM and lipid extracts of ALM obtained from edematous lungs in our experiment is in part a result of the acidosis and hypoxemia accompanying the edema. Furthermore, we postulate that normal synthesis of surfactant has been interfered with and that regardless of the acute nature of our experiments; the initial effects can be included in contributing to the altered surface characteristics of these animals.

Theoretically, the minimum surface tension observed during film compression is indicative of alveolar surface tension during deflation and an

elevation of this value might be expected to augment premature closure. Accordingly, an elevation of γ_{max} might be expected to impede inflation. The higher γ_{min} which is determined by the pressure at which the surface lining films collapses is physiologically significant in the edematous lung. First, it can cause alveolar collapse such that greater pressures would have to be developed for re-expansion and the work of breathing would be increased. We observed both an increase in ΔPes (Figure 10) and in the W_{El} of breathing (Figure 8) as pulmonary edema developed in the alloxan treated group. Secondly, when alveoli were finally opened the pressure balance between the blood and alveoli would be upset promoting further transudation into the alveoli. The latter may partially explain why the alloxan treated animals generally showed a gradual deterioration in both ventilatory and mechanical aspects of respiration.

Microscopic Evidence of Pulmonary Edema

Diagnosis at necropsy revealed swollen and firm lungs (Figure 23). The most marked changes were in the dependent lobes which contained dark purple areas with free fluid and blood exuding from cut surfaces. Hemostatic areas in the upper lobes were most apparent near the hila. Interstitial and septal edema could be recognized by undue prominence of rather gelatinous bands along the pleural surface. Foam and fluid ranging in color from clear to reddish-brown drained from cut surfaces of the bronchi.

Microscopically, the diseased lung presented with capillary congestion, dilated lymphatics, and thickening of the alveolar septum (Figure

Figure 23. Typical appearance of edematous lung. Hemorrhagic areas most pronounced in dependent lobes. Upper lobes swollen and pink with focal loci of hemostasis.

24). Expansion of the perivascular and peribronchiolar connective tissues was evident as has been previously reported (53,166,216). Swirls of thin basophilic strands and cellular material within the bronchial lumen were frequently observed. Alveolar lumen were filled with desquamated pneumocytes and precipitates of edema fluid. Walls of the fluid filled alveoli were usually folded in contrast to the walls of air-filled alveoli which were generally straight and smooth (compare Figures 25A and 25B).

Figures 26 and 27 show that the major ultrastructural changes in the edematous lung were confined to the interstitial portions of the alveolar septum. Preferential thickening of the fluid exchanging side (cf. Figure 1) of the alvolo-capillary barrier was observed. These spaces contained plates of elastic tissue and bundles of collagen fibrils embedded in a slightly electron dense ground substance. The elastic fibers were widely separated from one another in the edematous lung. The endothelial and epithelial basement membranes were intact. Numerous pinocytotic vesicles were present in the attenuated endothelial cells. Mitochondria appeared swollen and often contained internally disrupted cristae. Edema fluid appeared to compete for physical space by causing pneumonocytes to bulge into the alveolar lumen (Figure 27B) eventually leading to unit closure and alveolar collapse (Figure 27C) in extreme cases.

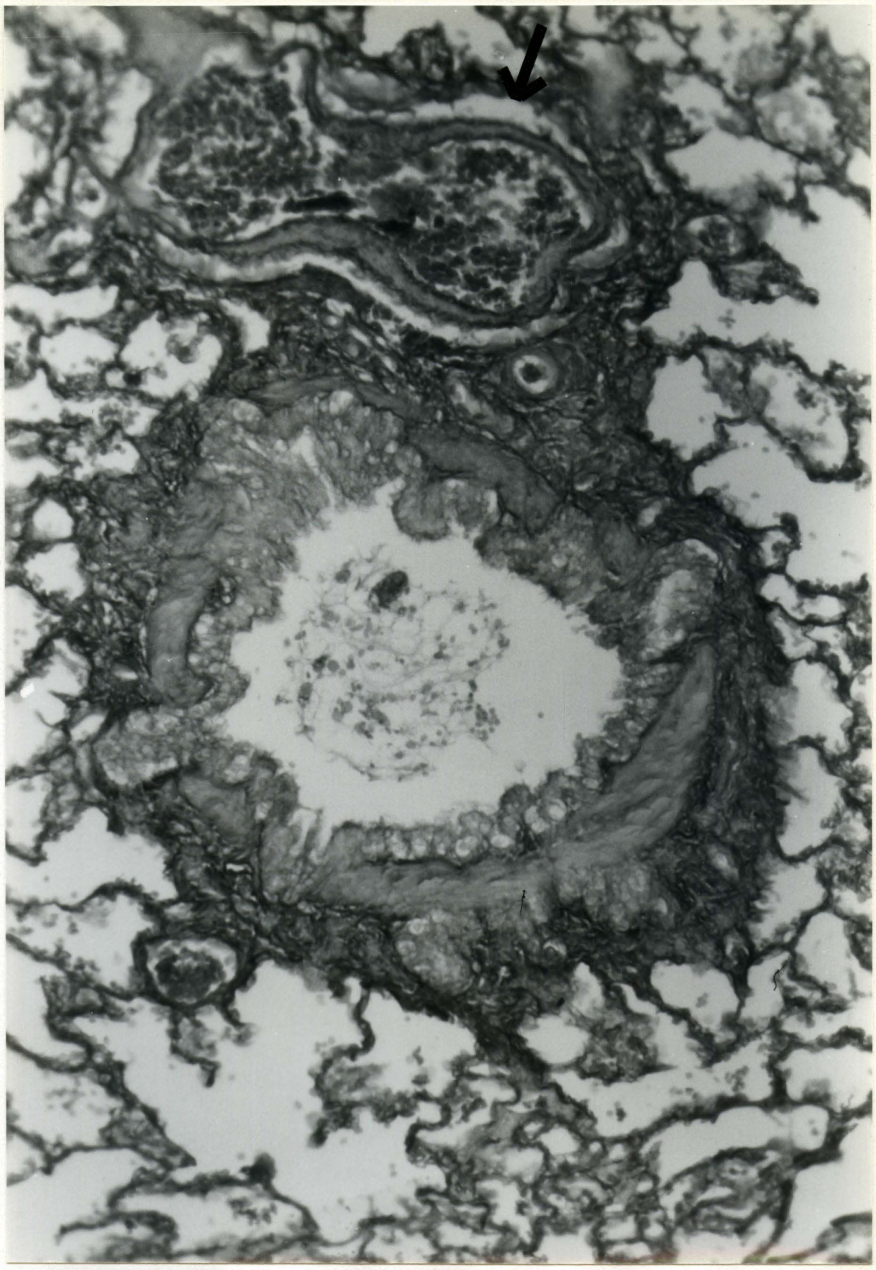

Figure 24. Canine lung three hours after injection of alloxan. Large tertiary bronchus filled with basophilic fibers and desquamated cells associated with blood-filled artery. Perivascular cuffing (arrow) is extensive. Tissue fixed in buions; stained with safranin/fast green/chlorasol black E. (X200)

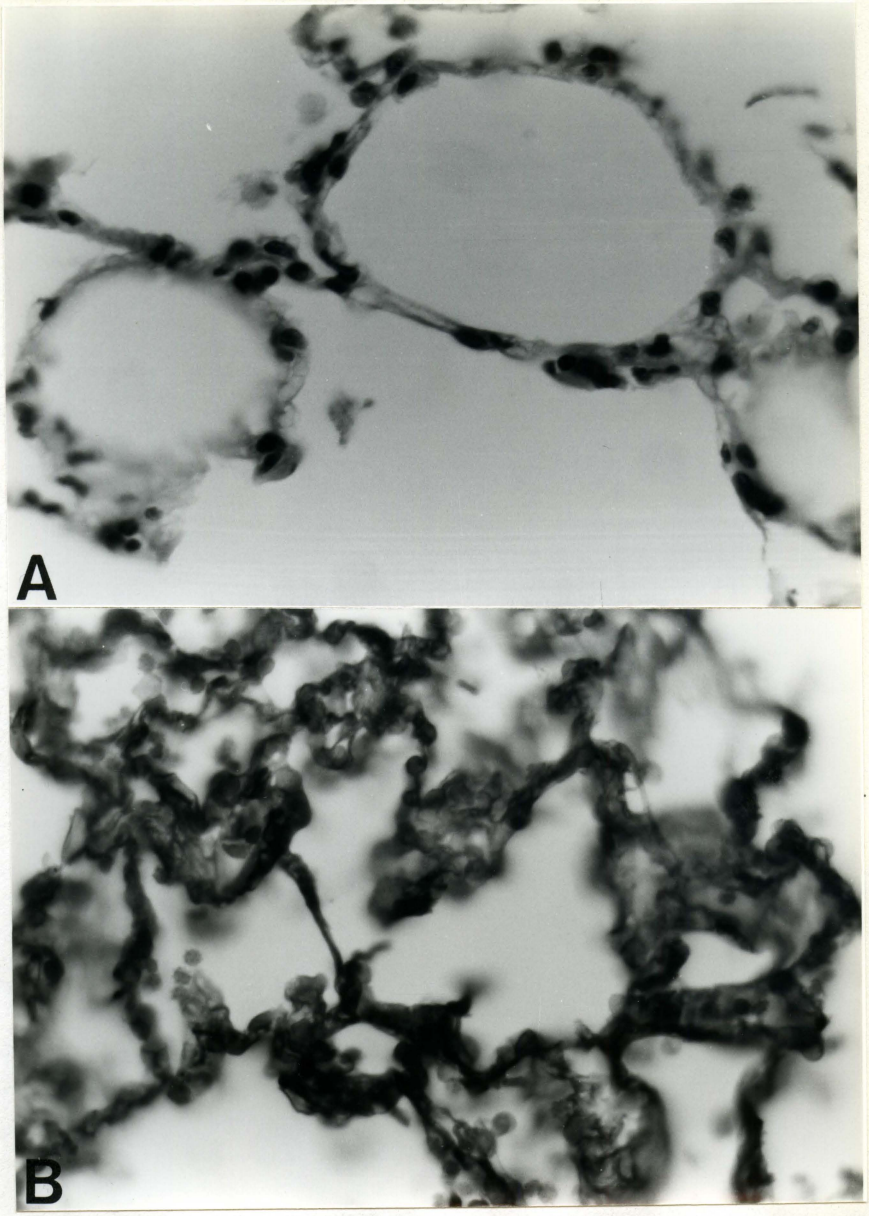

Figure 25. Photomicrograph of canine lung three hours after i.v. alloxan showing normally aerated aleoli (A) adjacent to atelectatic alveoli (B). Tissues fixed in buions; stained with safranin/ fast green/chlorasol black E. (X475)

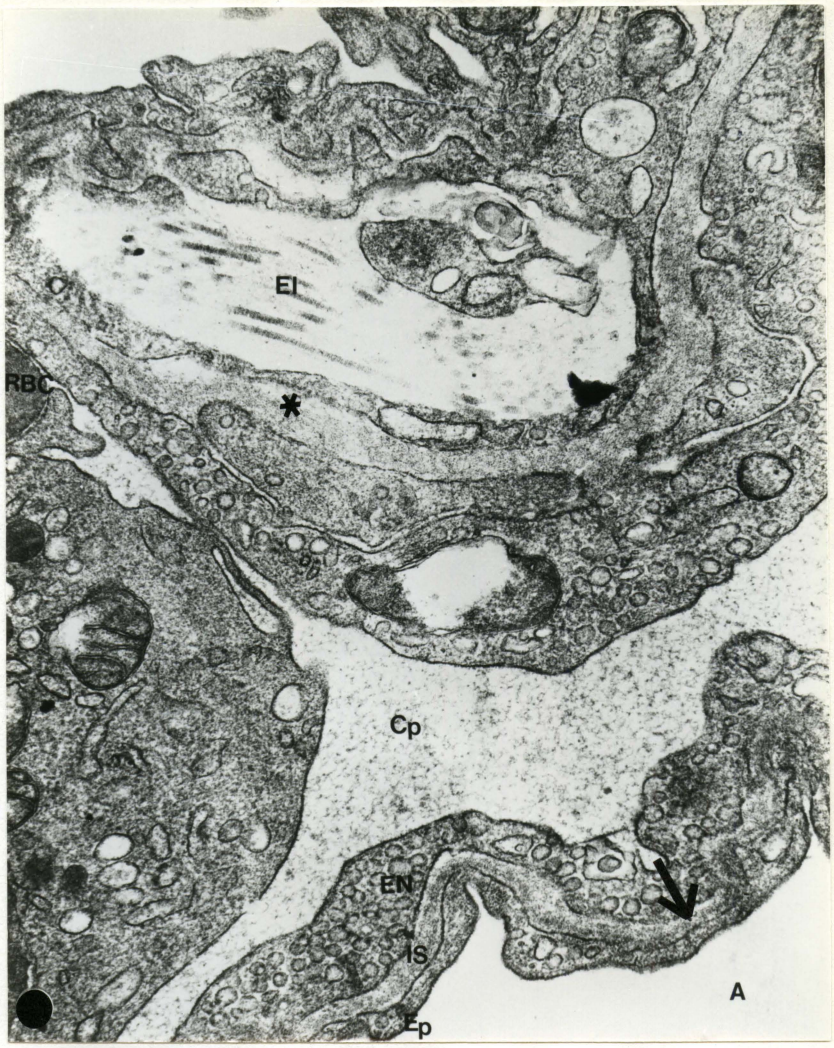

Figure 26. Electron micrograph of canine lung illustrating the thick and thin sides of the alveolo-capillary barrier. The interstitial space on the thin side (arrow) is approximately 90 nm while that on the thick side (*) approaches 200 nm. (X32,500)

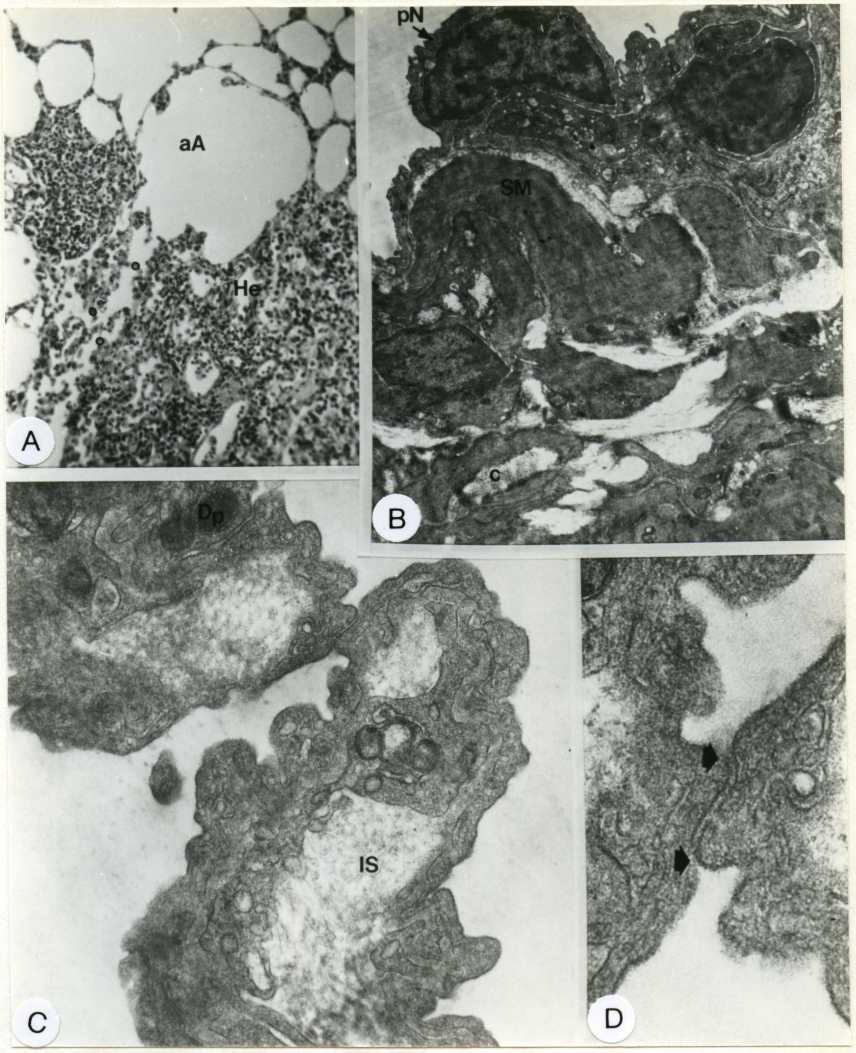

Figure 27. Canine lung edema observed at necropsy. A. Histology, normally aerated alveoli (aA) adjacent to atelectatic area with severe hemostasis (He). (X125) B. Electron micrograph of respiratory bronchiole of same lung showing extravasation of tissue, particularly around smooth muscle bundles (SM) and collagen bands (c). Type II pneumonocyte (pN) bulging into alveolar lumen. (X7,300) C. Marked expansion of interstitial space (IS) by pockets of fluid accumulation. (X34,000) D. Apposition of two sides of a collapsed alveoli resulting from the massive fluid pockets. (X83,000)

SUMMARY

This report deals with the sequelae of events associated with acute pulmonary edema induced by intravenous injection of 140 mg/kg alloxan. Diagnosis of the disease was based on the presence of progressive ventilatory failure coupled with a hypoxemic-hypocapnic condition reflecting a combined respiratory alkalosis and metabolic acidosis. The events leading to this unusual combination can only be surmised. Physiologic measurements show that the lungs are stiff, expending excessive energy and performing inordinate work in breathing. The polypnea cannot be entirely accounted for by changes in arterial P_{O_2} and P_{CO_2} since carbon dioxide levels appeared stabilized 30-60 minutes after injection despite the increasing hypoxemia. The possibility of a central nervous system effect with a blunted response to hydrogen ion concentration seems tenable. Our results are in agreement with the early work of Drinker (64) that the diffusion barrier is the main physiologic abnormality, but is followed by airway obstruction which becomes the second predominant stage. In contrast to Williams (252) and Said et al. (205), we do not feel that alveolar filling is the only physiologically important stage as far as gas exchange is concerned. The interstitial stage of edema prior to the alveolar stage initially alters gas exchange by widening the diffusion barrier. This phase of lung edema is also associated with impaired tissue elasticity such that the required ventilatory movements are accomplished at the expense of large amounts of energy.

Diffuse bilateral rales were present in the four dogs with alloxan-induced pulmonary edema, although the presence of tracheal foam was not a

consistent finding as had been reported by other investigators (12,14,53) using alloxan. It was further shown that the ensuing edema was characterized by small increases in airway resistance and pleural pressure while dynamic lung compliance decreased. We have postulated that excess fluid in lung edema is accommodated at the expense of alveolar volume not only by directly competing for space (reduced tidal volume) and altering tissue distensibility (reduced compliance), but by promoting alveolar closure as the lining material is displaced or rendered inactive.

Part of the discrepant behavior of the lungs with respect to water accumulation seems attributable to the physical and chemical properties of the alveolar lining. It was considered possible that the ventilatory effort temporarily increased the internal surface area of the lungs thereby enhancing absorption of more alveolar lining material to the internal surface which could account for the density and additional dry weight lavage recovery from edematous lungs. However, the fact that such a small area of the lung was lavaged lends more credence to the idea that protein accumulation as well as absorption accounts for the density of fluids obtained from edematous lungs. Coagulation of lung fluids from the alloxan treated animals and electrophoretic identification of several high molecular weight proteins suggests that large alveolo-capillary leaks contribute to the syndrome whereby edema fluid may actually "lift" the alveolar lining. The radius of curvature across the air-liquid interface would then be decreased. By examining the LaPlace equation ($P = 2T/r$), we can see that increased critical interfacial tension (γ_{min}) and decreased curvature in the edematous lung are such that the existing transpulmonary pressure

can no longer hold alveoli in a stable configuration. In view of the fact that lipid extracts from edematous lung fluids had a higher minimal surface tension when surface area was reduced in vitro; the morphological evidence substantiating the predicted atelectasis is readily explained in physical terms.

If we assume a continual turnover of alveolar lining material and that a quantitative relationship between its constituents is responsible for optimum surface activity, then the events of alloxan-induced pulmonary edema can serve as a useful model in studying the contribution of alveolar lining material to lung mechanics. We cannot offer conclusive information as to whether the physio-chemical alterations in the lining material of edematous lungs are a direct consequence of the alloxan itself, serum contamination, metabolic deficiency, hypoxemia, electrolyte imbalance, or acid-base disturbances. However, we are confident in assigning an important role to changes in alveolar lining material in the genesis and development of pulmonary edema.

LITERATURE CITED

1. Aberman, A. and M. Fulop. 1972. The metabolic and respiratory acidosis of acute pulmonary edema. Ann. Intern. Med. 76: 173-184.

2. Abrams, M. E. 1966. Isolation and quantitative estimation of pulmonary surface-active lipoprotein. J. Appl. Physiol. 21(2): 718-720.

3. Adams, F. H., M. Nozaki, N. Chida, A. El Salaway, and A. Norman. 1967. Effects of hypoxia, hypercarbia, acidosis, and reduced pulmonary blood flow on the surfactant of fetal lamb lung. J. Pediatr. 71: 396-403.

4. Adamson, I. Y. and D. H. Bowden. 1973. The intracellular site of surfactant synthesis. Exptl. Mol. Path. 18(1): 112-124.

5. Addington, W. W., D. W. Cugell, and T. R. Westernhouse. 1972. Pulmonary edema of heroine toxicity--example of stiff lung syndrome. Diseases of the Chest 62(2): 199-203.

6. Agostoni, E., F. F. Thimm, and W. O. Fenn. 1959. Comparative features of the mechanics of breathing. J. Appl. Physiol. 14: 679-683.

7. Andersen, O. S. 1961. Acute experimental acid-base disturbances in dogs. Scand. J. Clin. Lab. Invest. 14(Suppl. 66): 1-20.

8. Anthonisen, N. R. and H. J. Smith. 1965. Respiratory acidosis as a consequence of pulmonary edema. Ann. Intern. Med. 62: 991-999.

9. Askin, F. B. and C. Kuhn. 1971. The cellular origin of pulmonary surfactant. Lab. Invest. 25: 260-268.

10. Avery, M. E. and J. Mead. 1959. Surface properties in relation to atelectasis and hyaline membrane disease. Amer. J. Dis. Child. 99: 517-523.

11. Avery, W. G., P. Samet, and M. A. Sackner. 1970. The acidosis of pulmonary edema. Amer. J. Med. 48: 320-324.

12. Aviado, D. M., Jr. 1953. Pathogenesis of alloxan pulmonary edema investigated by phosphorous^{32} and iodine^{131}. J. Pharmacol. Exptl. Therapeutics 12: 299. (Abstr.)

13. Aviado, D. M. 1959. Therapy of experimental pulmonary edema in the dog with special reference to burns of the respiratory tract. Circ. Res. 7: 1018-1030.

14. Aviado, D. M., Jr. and C. F. Schmidt. 1957. Pathogenesis of pulmonary edema by alloxan. Circ. Res. 5: 180-186.

15. Bauman, A. M., M. A. Rothschild, R. W. Yalow, and S. A. Berson. 1955. Distribution and metabolism of I^{131} labeled human serum albumin in congestive heart failure with and without proteinuria. J. Clin. Invest. 34: 1359-1368.

16. Baxter, C. F., G. Rouser, and G. Simon. 1969. Variations among vertebrates of lung phospholipid class composition. Lipids 4: 243-244.

17. Bensch, K. G., E. Dominguez, and A. A. Liebow. 1967. Absorption of intact protein molecules across the pulmonary air-tissue barrier. Science 157: 1204-1206.

18. Bignon, J., M. C. Jaurand, M. C. Pinchon, C. Sadin, and J. M. Warnet. 1976. Immunoelectron microscopic and immunochemical demonstrations of serum proteins in the alveolar lining material of the rat lung. Amer. Rev. Resp. Dis. 113: 109-120.

19. Bohm, G. M. 1973. Changes in lung arterioles in pulmonary oedema in rats by alpha-naphthythiourea. J. Pathology 110(4): 343-345.

20. Bolande, R. P. and M. H. Klaus. 1964. The morphologic demonstration of an alveolar lining layer and its relationship to pulmonary surfactant. Amer. J. Path. 45: 449-462.

21. Bondurant, S., J. Mead, and C. D. Cook. 1960. A re-evaluation of effects of acute central congestion on pulmonary compliance in normal subjects. J. Appl. Physiol. 15: 875-877.

22. Borst, H. G., E. Berglund, J. L. Whittenberger, J. Mead, M. McGregor, and C. Collier. 1957. The effect of pulmonary vascular pressures on the mechanical properties of anesthetized dogs. J. Clin. Invest. 36: 1708-1714.

23. Bouhuys, A. 1974. Breathing. Physiology, environment and lung disease. Grune and Stratton, Inc., New York, N.Y. 511 pp.

24. Bowden, D. H. 1974. Endothelial regeneration as a marker of differential vascular responses in oxygen-induced pulmonary edema. Lab. Invest. 30(3): 350-357.

25. Boyd, E. M., S. Jackson, M. Machlan, B. Palmer, and J. Whittaker. 1974. The lipid, sodium, chloride, and nitrogen content of the respiratory tract fluid of normal animals. J. Biol. Chem. 153: 435-438.

26. Bredenbe, C. E., T. Kazui, and W. R. Webb. 1975. Effect of positive and expiratory pressure on experimental pulmonary edema. Circulation 52: 131-138.

27. Brigham, K. L. and J. D. Snell, Jr. 1973. In vivo assessment of pulmonary vascular integrity in experimental pulmonary edema. J. Clin. Invest. 52(8): 2041-2052.

28. Brown, E. S. 1957. Lung area from surface tension effects. Proc. Soc. Exptl. Biol. Med. 95: 168-170.

29. Brown, E. S. 1964. Isolation of dipalmitoyl lecithin in lung extracts. Amer. J. Physiol. 207: 402-406.

30. Brown, E. S., R. P. Johnson, and J. A. Clements. 1959. Pulmonary surface tension. J. Appl. Physiol. 14(5): 717-720.

31. Brumley, G. W. 1971. Lung development and lecithin metabolism. Arch. Intern. Med. 127: 413-414.

32. Buckingham, S., H. O. Heinemann, S. C. Sommers, and W. F. McNany. 1966. Phospholipid synthesis in the large pulmonary alveolar cell. Amer. J. Pathol. 48: 1027-1041.

33. Byrne-Quinn, E., I. E. Sodal, and J. V. Weil. 1972. Hypoxic and hypercapnic ventilatory drives in children native to high altitude. J. Appl. Physiol. 32: 44-46.

34. Cameron, G. R. and F. C. Courtice. 1946. The production and removal of oedema fluid in the lung after exposure to carbonyl chloride (phosgene). J. Physiol., London 105: 175-185.

35. Cheng, C. D., K. K. Cheng, and J. C. Wang. 1973. Adrenaline induced acute massive pulmonary oedema in dog. Brit. J. Pharmacol. Chemotherapy 49: 728-737.

36. Chernick, V., W. A. Hodson, and L. J. Greenfield. 1966. Effect of chronic pulmonary artery ligation on pulmonary mechanics and surfactant. J. Appl. Physiol. 21: 1315-1320.

37. Chevalier, G. and A. J. Collet. 1972. In vivo incorporation of choline-^{3}H, leucine-^{3}H and galactose-^{3}H in alveolar type II pneumocytes in relation to surfactant synthesis. A quantitative radioautographic study in mouse by electron microscopy. Anat. Rec. 174: 289-310.

38. Chinard, F. P. 1966. The permeability characteristics of the pulmonary blood-gas barrier. Pages 106-147 in C. Caro, ed. Advances in respiratory physiology. Arnold Company, London.

39. Chinard, F. P., W. Perl, R. M. Effros, R. Dumpys, and A. C. Delea. 1969. Lung water: Physiological and clinical significance. Trans. Amer. Clin. Climat. Assoc. 81: 85-97.

40. Clements, J. A. 1956. Dependence of pressure-volume characteristics of lungs on intrinsic surface-active material. Amer. J. Physiol. 187: 592.

41. Clements, J. A. 1957. Surface tension of lung extracts. Proc. Soc. Exptl. Biol. Med. 95: 170-172.

42. Clements, J. A. 1961. Pulmonary edema and permeability of alveolar membranes. Arch. Environmental Health 2: 280-283.

43. Clements, J. A. 1962. Surface phenomena in relation to pulmonary function. Physiologist 5: 11-28.

44. Clements, J. A. 1971. Comparative lipid chemistry of lungs. Arch. Intern. Med. 127: 387-389.

45. Clements, J. A., E. S. Brown, and R. P. Johnson. 1958. Pulmonary surface tension and the mucous lining of the lungs: Some theoretical considerations. J. Appl. Physiol. 12: 262-268.

46. Clements, J. A., R. F. Hustead, R. P. Johnson, and I. Gribetz. 1961. Pulmonary surface tension and alveolar stability. J. Appl. Physiol. 16(3): 444-450.

47. Colacicco, G., A. R. Buckelew, Jr., and E. M. Scarpelli. 1973. Protein and lipid-protein fractions of lung washings: Chemical characterization. J. Appl. Physiol. 34: 743-749.

48. Colebatch, H. J. H. and D. F. J. Halmagyl. 1961. Lung mechanics and resuscitation after fluid aspiration. J. Appl. Physiol. 16: 684-696.

49. Conroe, J. H., Jr. 1970. Physiology of respiration. An introductory text. Year Book Medical Publishers, Inc., Chicago, Illinois. 245 pp.

50. Cook, C. D., J. Mead, G. L. Schreiner, N. R. Frank, and J. M. Craig. 1959. Pulmonary mechanics during induced pulmonary edema in anesthetized dogs. J. Appl. Physiol. 14(2): 177-186.

51. Cook, W. A. and W. R. Webb. 1966. Surfactant in chronic smokers. Annals Thoracic Surg. 2: 327-333.

52. Cotes, J. E. 1975. Lung function. Assessment and application in medicine. 3rd ed. Blackwell Scientific Publications, London. 619 pp.

53. Cottrell, T. S., O. R. Levine, R. M. Senior, J. Weiner, D. Spiro, and A. P. Fishman. 1967. Electron microscopic alterations at the alveolar level in pulmonary edema. Circ. Res. 21: 783-797.

54. Cournand, A. 1950. Some aspects of the pulmonary circulation in normal man and in chronic cardiopulmonary disease. Circulation 2: 641-644.

55. Courtice, F. C. and P. I. Korner. 1952. The effect of anoxia on pulmonary oedema produced by massive intravenous infusions. Australian J. Exptl. Biol. Med. 30: 511-526.

56. Crone, C. and N. A. Lassen, eds. 1970. Capillary permeability. The transfer of molecules and ions between capillary blood and tissue. In Proceedings of the Alfred Benzon Symposium II. Academic Press, New York. 681 pp.

57. Crosby, R. S., E. C. Stowell, W. R. Hartwig, and M. Mayo. 1957. Pulmonary function in left ventricular failure, including cardiac asthma. Circulation 15: 492-501.

58. Cunningham, A. L. and J. V. Hurley. 1972. Alpha-naphthyl-thiourea-induced pulmonary oedema in rat: Topographical and electron-microscopic study. J. Pathol. 106: 25-35.

59. Cunningham, D. J. C. and J. L. H. O'Rierdan. 1957. The effect of a rise in the temperature of the body on the respiratory response to carbon dioxide. Quart. J. Exptl. Physiol. 42: 329-345.

60. Datta, S. K. 1972. Blood gases in pulmonary edema. Annals Intern. Med. 76(6): 1045-1046.

61. Dejours, P. 1975. Principles of comparative respiratory physiology. American Elsevier Publishing Company, Inc., New York. 253 pp.

62. DeSá, D. J. 1965. Microscopy of the alveolar lining layer in newborn infants. Lancet 1: 1369-1370.

63. Dickie, K. J., G. D. Massaro, V. Marshall, and D. Massaro. 1973. Amino acid incorporation into protein of a surface-active lung fraction. J. Appl. Physiol. 34: 606-614.

64. Drinker, C. K. 1945. Pulmonary edema and inflammation. Harvard University Press, Cambridge, Massachusetts. 106 pp.

65. Drinker, C. K. and E. Hardenbergh. 1947. Absorption from the pulmonary alveoli. J. Exptl. Med. 86: 7-18.

66. duNouy, P. L. 1926. Surface equilibria in colloids. Reinhold Publishing Co., New York. 127 pp.

67. Faridy, E. E. and S. Permult. 1971. Surface forces and airway obstruction. J. Appl. Physiol. 30: 319-321.

68. Faulkner, J. M. and C. A. L. Binger. 1927. Oxygen poisoning in cold blooded animals. J. Exptl. Med. 45: 865-872.

69. Fejfar, Z., F. Zajie, and F. Fejfarova. 1959. Alloxan induced experimental pulmonary edema. I. Haemodynamic alterations. Cor Vasa 1: 56-72.

70. Finley, T. N., W. H. Tooley, E. W. Swenson, R. E. Gardner, and J. A. Clements. 1964. Pulmonary surface tension in experimental atelectasis. Amer. Rev. Resp. Dis. 89: 372-378.

71. Finley, T. N., S. A. Pratt, A. J. Ladman, J. Brewer, and M. B. McKay. 1968. Morphological and lipid analysis of the alveolar lining material in dog lung. J. Lipid Res. 9: 357-365.

72. Fishman, A. P. 1972. Pulmonary edema: The water-exchanging function of lung. Circulation 46: 390-408.

73. Folch, J., M. Lees, and G. H. Sloane Stanley. 1957. A simple method for the isolation and purification of total lipides from animal tissues. J. Biol. Chem. 226: 497-509.

74. Frazer, D. G. and K. C. Weber. 1976. Trapped air in ventilated excised rat lungs. J. Appl. Physiol. 40: 915-922.

75. Friedberg, C. K. 1966. Diseases of the heart. 3rd ed. W. B. Saunders Co., Philadelphia. 1787 pp.

76. Frosolono, M. F., B. L. Charms, R. Pawlowski, and S. Slivka. 1970. Isolation, characterization, and surface chemistry of a surface active fraction from dog lung. J. Lipid Res. 11: 349-457.

77. Fujiwara, T., F. H. Adams, and A. Scudder. 1964. Fetal lamb amniotic fluid: Relationship of lipid composition to surface tension. J. Pediatr. 65: 824-830.

78. Fujiwara, T., H. Hirono, and T. Arakawa. 1965. Chemical identification of the surface-active material isolated from calf lung. Tohuku J. Exptl. Med. 85: 33-39.

79. Fujiwara, T., F. H. Adams, A. El-Salawy, and S. Sipos. 1968. "Alveolar" and whole lung phospholipids of newborn lambs. Proc. Soc. Exptl. Biol. Med. 127: 962-969.

80. Gil, J. and E. R. Weibel. 1969/70. Improvements in demonstration of lining layer of lung alveoli by electron microscopy. Resp. Physiol. 8: 13-36.

81. Glauser, F. L., A. F. Wilson, M. Hoshiko, M. Watanabe, and J. Davis. 1974. Pulmonary parenchymal tissue (V_T) changes in pulmonary edema. J. Appl. Physiol. 36: 648-652.

82. Glauser, F., K. Rupnik, and I. Wells. 1975. Histamine concentrations and endotoxin-induced pulmonary-edema-role of cromolynsodium. Amer. Rev. Respt. Dis. 111: 940-949.

83. Goerke, J. 1974. Lung surfactant. Biochimica et Biophysica Acta 344: 241-261.

84. Goetzman, B. W. and M. Visscher. 1969. The effects of alloxan and histamine on the permeability of the pulmonary alveolocapillary barrier to albumin. J. Physiol. 704: 51-61.

85. Gorlin, R., B. M. Lewis, F. W. Hayes, R. J. Spiegl, and L. Dexter. 1951. Factors regulating pulmonary "capillary" pressure in initial stenosis. Amer. Heart J. 41: 834-854.

86. Greene, D. G., J. T. Sharp, R. E. Reisman, and W. J. Westinghouse. 1955. Evaluation of pulmonary edema. Amer. J. Physiol. 183: 622. (Abstr.)

87. Gruhzit, C. C., B. Peralta, and G. K. Moe. 1951. The pulmonary arterial pressor effect of certain sulfahydryl inhibitors. J. Pharmacol. Exptl. Therap. 101: 107-111.

88. Gump, F. E., Y. Mashima, S. Jorgensen, and J. M. Kinney. 1971. Simultaneous use of three indicators to evaluate pulmonary capillary damage in man. Surgery 70: 262-270.

89. Guyton, A. C. and A. W. Lindsey. 1959. Effect of elevated left atrial pressure and decreased plasma protein concentration on the development of pulmonary edema. Circ. Res. 7: 649-657.

90. Guyton, A. C., H. J. Granger, and A. E. Taylor. 1971. Interstitial fluid pressure. Physiol. Rev. 51: 527-563.

91. Haddy, F. J., G. S. Campbell, and M. B. Visscher. 1950. Pulmonary vascular pressure in relation to edema production by airway resistance and plethora in dogs. Amer. J. Physiol. 161: 336-341.

92. Haddy, F. J., A. L. Ferrin, D. W. Hannon, J. F. Aden, W. L. Adams, and I. D. Baronofsky. 1953. Cardiac function in experimental initial stenosis. Circ. Res. 1: 219-225.

93. Haldane, J. S., ed. 1922. Respiration. Yale University Press, Newhaven, Connecticut. 427 pp.

94. Hamilton, R. W., Jr., R. F. Hustead, and L. F. Peltier. 1964. Fat embolism: The effect of particulate embolism on lung surfactant. Surgery 56: 53-56.

95. Hanahan, D. J., ed. 1960. Lipide chemistry. Wiley and Sons, Inc., New York. 330 pp.

96. Handbook Chemistry and Physics. 1968-1969. 49th ed. Edited by Robert C. Weast. The Chemical Rubber Co., Cleveland, Ohio.

97. Harken, A. H. and N. E. O'Connor. 1976. The influence of clinically undetectable pulmonary edema on small airway closure in the dog. Ann. Surg. 184: 183-188.

98. Harlan, W. R., S. I. Said, and C. M. Banerjee. 1966. Metabolism of pulmonary phospholipids in normal lung and during acute pulmonary edema. Amer. Rev. Respir. Dis. 94: 938-947.

99. Harrison, L. A., J. J. Beller, L. B. Hinshaw, J. J. Coalson, and L. J. Greenfield. 1969. Effects of endotoxin on pulmonary capillary permeability, ultrastructure and surfactant. Surg. Gynecol. Obstet. 129: 723-733.

100. Hayak, H. von. 1960. The human lung. [Translated by V. E. Krahl.] Hafner Publishing Co., New York. 197 pp.

101. Hendley, E. D. and A. A. Schiller. 1954. Change in capillary permeability during hypoxemic perfusion of rat hindlimbs. Amer. J. Physiol. 179: 216-220.

102. Hey, E. N., B. B. Lloyd, D. J. C. Cunningham, M. G. M. Jukes, and D. P. G. Bolton. 1966. Effects of various respiratory stimuli on the depth and frequency of breathing in man. Respir. Physiol. 1: 193-205.

103. Hogg, J. C., J. B. Agarawal, W. H. Palmer, and P. T. Macklem. 1972. Distribution of airway resistance with developing pulmonary edema in dogs. J. Appl. Physiol. 32: 20-24.

104. Howell, J. B. L., S. Permutt, D. F. Proctor, and R. L. Riley. 1961. Effects of inflation of the lung on different parts of the pulmonary vascular bed. J. Appl. Physiol. 16: 71-76.

105. Hughes, R., A. J. May, and J. G. Widdicombe. 1958. Mechanical factors in the formation of oedema in perfused rabbits lung. J. Physiol. 142: 292-305.

106. Hyman, A. L., D. G. Pennington, and W. E. Jaques. 1972. Pulmonary vascular responses to alloxan. J. Pharmacol. Exptl. Therapeutics 181: 92-97.

107. Iliff, L. D. 1971. Extra-alveolar vessels and edema development in excised dog lungs. Circ. Res. 28: 524-532.

108. Jaeger, M. J. and A. B. Otis. 1964. Measurement of airway resistance with a volume displacement body plethysmograph. J. Appl. Physiol. 19: 813-820.

109. Johnson, J. W. C., S. Permutt, J. H. Sipple, and E. S. Salem. 1964. Effect of intra-alveolar fluid on surface tension properties. J. Appl. Physiol. 19: 769-777.

110. Jones, J. G., R. Lemen, and P. D. Graf. 1974. "Airway closure" in alloxan induced pulmonary oedema and raised left atrial pressure. Brit. J. Anesth. 46: 321. (Abstr.)

111. Karliner, J. S., A. D. Steinberg, and M. H. Williams, Jr. 1969. Lung function after pulmonary edema associated with heroin overdose. Arch. Intern. Med. 124: 350-353.

112. Katz, S., A. Aberman, U. I. Frand, I. M. Stein, and M. Fulop. 1972. Heroine pulmonary edema. Evidence for increased pulmonary capillary permeability. Amer. Rev. Respir. Dis. 106: 472-474.

113. King, R. J. 1974. The surfactant system of the lung. Fed. Proc. 33: 2238-2247.

114. King, R. J. and J. A. Clements. 1972. Surface active materials from dog lung. II. Composition and physiological correlations. Amer. J. Physiol. 223: 715-726.

115. King, R. J., D. J. Klass, E. G. Gikas, and J. A. Clements. 1973. Isolation of apoproteins from canine surface active material. Amer. J. Physiol. 224: 788-795.

116. King, R. J., H. Martin, D. Mitts, and F. M. Holmstrom. 1977. Metabolism of the apoproteins in pulmonary surfactant. J. Appl. Physiol. 42: 483-491.

117. Kisch, B. 1958. Electron microscopy of lungs in acute pulmonary edema. Exptl. Med. Surg. 16: 17-28.

118. Kistler, G. S., P. R. B. Caldwell, and E. R. Weibel. 1967. Development of fine structural damage to alveolar and capillary lining cells in oxygen-poisoned rat lungs. J. Cell Biol. 32: 605-628.

119. Klass, D. J. 1973. Immunochemical studies of the protein fraction of pulmonary surface active material. Amer. Rev. Respir. Dis. 107: 784-789.

120. Klaus, M. H., J. A. Clements, and R. J. Hauel. 1961. Composition of surface-active material isolated from beef lung. Proc. Nat. Acad. Sci. 47: 1858-1859.

121. Kleiner, J. P. and W. P. Nelson. 1975. High-altitude pulmonary-edema-rare disease. J. Amer. Med. Assoc. 234(N5): 491-495.

122. Koenig, H. and R. Koenig. 1949. Studies on the pathogenesis of ammonium chloride pulmonary edema. Amer. J. Physiol. 158: 1-15.

123. Kuenzig, M. C., R. W. Hamltion, Jr., and L. F. Peltier. 1965. Dipalmitoyl lecithin: Studies on surface properties. J. Appl. Physiol. 20: 779-782.

124. Lakshminarayan, S. and D. J. Pierson. 1975. Recurrent high-altitude pulmonary-edema with blunted chemosensitivity. Amer. Rev. Respir. Dis. 111: 869-872.

125. Landis, E. M. 1928. Micro-injection studies of capillary permeability. III. The effect of lack of oxygen on the permeability of the capillary wall to fluid and to the plasma proteins. Amer. J. Physiol. 83: 528-542.

126. Landis, E. M. and J. R. Pappenhermer. 1963. Exchange of substances through capillary walls. Pages 961-1034 in Handbook of physiology, circulation, Sect. 2, Vol. II. American Physiological Society, Washington, D.C.

127. Lemen, R., J. G. Jones, P. D. Graf, and G. Cowan. 1975. "Closing volume" changes in alloxan-induced pulmonary edema in anesthetized dogs. J. Appl. Physiol. 39: 235-241.

128. Levine, B. E. and R. P. Johnson. 1964. Surface activity of saline extracts from inflated and degasses normal lungs. J. Appl. Physiol. 19: 333-334.

129. Levine, O. R., R. B. Mellins, and A. P. Fishman. 1965. Quantitative assessment of pulmonary edema. Circ. Res. 17: 414-426.

130. Levine, O. R., R. B. Mellins, R. M. Senior, and A. P. Fishman. 1967. The application of Starling's law of capillary exchange to the lungs. J. Clin. Invest. 46: 934-944.

131. Lloyd, T. C. 1966. Influence of blood pH on hypoxia pulmonary vasoconstriction. J. Appl. Physiol. 21: 358-364.

132. Longmore, W. J., C. M. Niethe, D. J. Sprinkle, and R. I. Godinez. 1973. Effect of CO_2 concentration on phospholipid metabolism in the isolated perfused rat lung. J. Lipid Res. 14: 145-151.

133. Macklem, P. T. 1973. Current concepts. New tests to assess lung function. New Engl. J. Med. 293: 339-342.

134. Macklem, P. T. and J. Mead. 1967. Resistance of central and peripheral airways measured by a retrograde catheter. J. Appl. Physiol. 22: 395-401.

135. Macklin, C. C. 1939. Transport of air along sheaths of pulmonic blood vessels from alveoli to mediastinum. Arch. Intern. Med. 64: 913-926.

136. Macklin, C. C. 1954. Pulmonary sumps, dust accumulations, alveolar fluid and lymph vessels. Acta Anat. 23: 1-33.

137. Macklin, C. C. 1954. The pulmonary alveolar mucoid film and the pneumocytes. Lancet 1: 1099-1104.

138. Massaro, D. 1975. In vivo protein secretion by lung. J. Clin. Invest. 56: 263-271.

139. Massaro, D., H. Weiss, and M. R. Simon. 1970. Protein synthesis and secretion by lung. Amer. Rev. Respir. Dis. 101: 198-206.

140. Massaro, G. D. and D. Massaro. 1972. Granular pneumocytes. Electron microscopic radioautographic evidence of intracellular protein transport. Amer. Rev. Respir. Dis. 105: 927-931.

141. McClenahan, J. B. and A. Urtnowski. 1967. Effect of ventilation on surfactant and its turnover rate. J. Appl. Physiol. 23: 215-220.

142. McHugh, J. R., J. S. Forrester, L. Adler, P. Zion, and H. J. C. Swan. 1972. Pulmonary vascular congestion in acute myocardial infarction: Hemodynamic and radiologic correlations. Ann. Intern. Med. 76: 29-33.

143. Mead, J. 1956. Measurement of inertia of the lungs at increased ambient pressure. J. Appl. Physiol. 9: 208-212.

144. Mead, J. and C. Collier. 1959. Relation of volume history of lungs to respiratory mechanics in anesthetized dogs. J. Appl. Physiol. 14: 669-678.

145. Meban, C. 1972. Localization of phosphatidic acid phosphatase activity in granular pneumocytes. J. Cell Biol. 53: 249-252.

146. Mellins, R. B., O. R. Levine, R. Skalak, and A. P. Fishman. 1969. Interstitial pressure in the lungs. Circ. Res. 24: 197-212.

147. Merritt, T. A. and P. M. Farrell. 1976. Diminished pulmonary lecithin synthesis in acidosis: Experimental findings as related to the respiratory distress syndrome. Pediatrics 57: 32-40.

148. Meth, R. F., D. P. Tashkin, K. S. Hansen, and D. H. Simmons. 1975. Pulmonary-edema and wheezing after pulmonary embolism. Amer. Rev. Respir. Dis. 111: 693-698.

149. Meyer, E. C. and R. Ottaviano. 1972. Pulmonary collateral lymph flow: Detection using lymph oxygen tensions. J. Appl. Physiol. 32: 806-811.

150. Meyer, E. C. and R. Ottaviano. 1973. The effect of fibrin on the morphometric distribution of pulmonary exudative edema. Lab. Invest. 29: 320-328.

151. Meyer, E. C., E. A. M. Dominguez, and K. G. Bensch. 1969. Pulmonary lymphatic and blood absorption of albumin from alveoli. Lab. Invest. 20: 1-8.

152. Meyrick, B., J. Miller, and L. Reid. 1972. Pulmonary oedema induced by ANTU, or by high or low oxygen concentrations in rat - an electron microscopic study. Brit. J. Exptl. Pathol. 53: 347-358.

153. Milic-Emili, J. and F. Ruff. 1971. Effects of pulmonary congestion and edema on the small airways. Bull. Physio-pathol. Respir. 7: 1181-1196.

154. Milic-Emili, J., J. Mead, and J. M. Turner. 1964. Topography of esophageal pressure as a function of posture in man. J. Appl. Physiol. 19: 212-216.

155. Miller, W. S. 1947. The lung. 2nd ed. Thomas Publishing Co., Springfield, Illinois. 222 pp.

156. Miller, W. F. and B. T. Sproule. 1959. Studies on the role of intermittent inspiratory positive pressure oxygen breathing (IPPB/ I-O_2) in the treatment of pulmonary edema. Dis. Chest 35: 469-479.

157. Moore, J. C. and M. S. Sexter. 1956. Changes in lung compliance during development of ANTU pulmonary edema. Fed. Proc. 15: 132-133.

158. Morgan, T. E., T. N. Finley, and H. Fialkow. 1965. Comparison of the composition and surface activity of "alveolar" and whole lung lipids in the dog. Biochimica et Biophysica Acta 106: 403-413.

159. Morrison, W. R. 1964. A fast, simple and reliable method for the microdetermination of phosphorous in biological materials. Analytical Biochem. 7: 218-224.

160. Morrison, N. S., S. Wetherill, and J. Zyroff. 1970. The acute pulmonary edema of heroin intoxication. Radiology 97: 347-351.

161. Moss, G. S. 1972. Pulmonary involvement in hypovolaemic shock. Annu. Rev. Med. 23: 201-228.

162. Moylan, F. M. B., K. C. Oconnel, I. D. Todres, and D. C. Shannon. 1975. Edema of pulmonary interstitium in infants and children. Pediatrics 55(6): 783-788.

163. Muggenberg, B. A., J. L. Mauderly, J. A. Pickrell, T. L. Chiffelle, R. K. Jones, U. C. Luft, R. O. McClellan, and R. C. Pfleger. 1972. Pathophysiologic sequelae of bronchopulmonary lavage in the dog. Amer. Rev. Respir. Dis. 106: 219-232.

164. Naimark, A. 1973. Cellular dynamics and lipid metabolism in the lung. Fed. Proc. 32(9): 1967-1971.

165. Nairn, R. C. 1964. Fluorescent protein tracing. 2nd ed. Williams & Wilkins, Baltimore. 335 pp.

166. Nash, G., F. D. Foley, and P. C. Langlina. 1974. Pulmonary interstitial edema and hyaline membranes in adult burn patients. Electron microscopic observations. Human Path. 5: 149-160.

167. Nasr, K. and H. O. Heinemann. 1965. Lipid synthesis by rabbit lung tissue in vitro. Amer. J. Physiol. 208: 118-121.

168. Nicolaysen, G. 1971. Intravascular concentrations of calcium and magnesium ions and edema formation in isolated lungs. Acta Physiol. Scand. 81: 325-339.

169. Nicoloff, D. M., H. M. Ballin, and M. B. Visscher. 1969. Hypoxia and edema of the perfused isolated canine lung. Proc. Soc. Exptl. Biol. Med. 131: 22-26.

170. Nir, I. and D. C. Pease. 1976. Polysaccharides in lung alveoli. Amer. J. Anat. 147: 457-463.

171. Nissell, O. 1950. The action of oxygen and carbon dioxide on the bronchioles and vessels of the isolated perfused lungs. Acta Physiol. Scand. 23(Suppl.):

172. Nitta, S. and N. C. Staub. 1973. Lung fluids in acute ammonium chloride toxicity and edema in cats and guinea pigs. Amer. J. Physiol. 224: 613-617.

173. Opdyke, D. E., J. Duomarco, W. H. Dillon, H. Schreiber, R. C. Little, and R. D. Seeley. 1948. Study of simultaneous right and left atrial pressure pulses under normal and experimentally altered conditions. Amer. J. Physiol. 154: 258-272.

174. Otis, A. B., W. O. Fenn, and H. Kahn. 1950. Mechanics of breathing in man. J. Appl. Physiol. 2: 592-607.

175. Otis, A. B., C. B. McKerrow, R. A. Bartlett, J. Mead, M. B. McIlroy, N. J. Selverstone, and E. P. Redford, Jr. 1956. Mechanical factors in distribution of pulmonary ventilation. J. Appl. Physiol. 8: 427-443.

176. Paintal, A. S. 1969. Mechanism of stimulation of type J pulmonary receptors. J. Physiol. 203: 511-532.

177. Parenti-Castelli, G., E. Bertoli, A. M. Sechi, M. G. Silvestrini, and G. Lenaz. 1974. Effect of soluble and membrane proteins upon diethyl ether extraction of aqueous phospholipid dispersions. Lipids 94: 221-228.

178. Patel, R., N. Janakira, and R. Johnson. 1973. Pulmonary edema from perchloroethylene. J. Amer. Med. Assoc. 223(13): 1510.

179. Pattle, R. E. 1955. Properties, function, and origin of the alveolar lining layer. Nature 175: 1125-1126.

180. Pattle, R. E. 1956. A test of silicone anti-foam treatment of lung oedema in rabbits. J. Pathol. Bacteriol. 72: 203.

181. Pattle, R. E. 1960. The cause of the stability of bubbles derived from the lung. Physiol. Med. Biol. 5: 11-26.

182. Pattle, R. E. 1965. Surface lining of lung alveoli. Physiol. Rev. 45(1): 48-79.

183. Pattle, R. E. and L. C. Thomas. 1961. Lipoprotein composition of the film lining the lung. Nature 189: 844.

184. Pawlowski, R., M. F. Frosolono, B. L. Charms, and R. Przybylski. 1971. Intra and extracellular comparmentalization of the surface-active fraction in dog lung. J. Lipid Res. 12: 538-544.

185. Pearce, M. L. 1969. Sodium recovery from normal and edematous lungs studied by indicator dilution curves. Circ. Res. 24: 815-820.

186. Pearce, M. L., J. Yamashito, and J. Beazell. 1965. Measurement of pulmonary edema. Circ. Res. 16: 482-488.

187. Permutt, S. 1965. Effect of interstitial pressure of the lungs on pulmonary circulation. Med. Thoracalis. 22: 118-131.

188. Pfleger, R. C. and H. G. Thomas. 1971. Beagle dog pulmonary surfactant lipids: Lipid composition of pulmonary tissue, exfoliated lining cells, and surfactant. Arch. Intern. Med. 127: 863-872.

189. Pickrell, J. A., S. E. Dubin, and J. C. Elliott. 1971. Normal respiratory parameters of unanesthetized beagle dogs. Lab. Anim. Sci. 21: 677-679.

190. Pietra, G. G., J. P. Szidon, M. M. Leventhal, and A. P. Fishman. 1971. Histamine and interstitial pulmonary edema in the dog. Circ. Res. 29: 323-337.

191. Plestina, R. and H. B. Stoner. 1972. Pulmonary oedema in rats given monocrotaline pyrrole. J. Pathol. 106: 235-249.

192. Potter, J. L., L. W. Matthews, J. Lemm, and S. Spector. 1965. Human pulmonary secretions in health and disease. Ann. N.Y. Acad. Sci. 106: 692-695.

193. Rabinovitch, W., R. F. Robertson, and S. G. Mason. 1960. Relaxation of surface pressure and collapse of unimolecular films of stearic acid. Can. J. Chem. 38: 1881-1890.

194. Rahn, H. 1949. A concept of mean alveolar air and ventilation-bloodflow relationships during pulmonary gas exchange. Amer. J. Physiol. 158: 21-30.

195. Rahn, H. and W. O. Fenn. 1955. A graphical analysis of the respiratory gas exchange. The O_2-CO_2 diagram. American Physiological Society, Washington, D.C.

196. Rech, P. H. and H. L. Borison. 1962. Vagotomy induced pulmonary edema in the guinea pig. Amer. J. Physiol. 202: 499-504.

197. Reichsman, F. 1946. Studies on the pathogenesis of pulmonary edema following bilateral vagotomy. Amer. Heart J. 31: 590-616.

198. Riley, R. L. and A. Cournand. 1951. Analysis of factors affecting partial pressures of oxygen and carbon dioxide in gas and blood of lungs: Theory. J. Appl. Physiol. 4: 71-101.

199. Rivera-Estrada, C., P. W. Saltzman, D. Singer, and L. N. Katz. 1958. Action of hypoxia on the pulmonary vasculature. Circ. Res. 6: 10-14.

200. Robin, E. D., L. C. Carey, A. Grenvik, F. Glauser, and R. Gaudio. 1972. Capillary leak syndrome with pulmonary edema. Arch. Intern. Med. 130: 66-71.

201. Robin, E. D., C. E. Cross, and R. Zelis. 1973. Medical progress: Pulmonary edema. New Engl. J. Med. 288: 239-304.

202. Rossier, P. H., A. A. Buhlman, and K. Wiesinger. 1960. Respiration: Physiologic principles and their clinical applications. The C. V. Mosby Co., St. Louis. 505 pp.

203. Rudolph, A. M. and S. Yuan. 1966. Response of the pulmonary vasculature to hypoxia and H+ ion concentration changes. J. Clin. Invest. 45: 399-411.

204. Ryan, S. F., A. L. Loomis Bell, Jr., and C. Redington Barrett, Jr. 1975. Experimental acute alveolar injury. Circulation 52: 130.

205. Said, S. I., J. W. Longacher, Jr., R. K. Davis, C. M. Banerjee, W. M. Davis, and W. J. Wooddell. 1964. Pulmonary gas exchange during induction of pulmonary edema in anesthetized dogs. J. Appl. Physiol. 19: 403-407.

206. Said, S. I., M. E. Avery, R. K. Davis, C. M. Banerjee, and M. El-Gohary. 1965. Pulmonary surface activity in induced pulmonary edema. J. Clin. Invest. 44: 458-464.

207. Saunders, N. A., M. F. Betts, L. D. Pengelly, and A. S. Rebuck. 1977. Changes in lung mechanics induced by acute isocapnic hypoxia. J. Appl. Physiol. 42: 413-419.

208. Scarpelli, E. M., B. C. Clutario, and F. A. Taylor. 1967. Preliminary identification of the lung surfactant system. J. Appl. Physiol. 23: 880-886.

209. Schaaf, J. T., M. L. Spivack, G. S. Rath, and G. L. Snider. 1973. Pulmonary edema and adult respiratory distress syndrome following methadone abuse. Amer. Rev. Respir. Dis. 107: 1047-1051.

210. Schaefer, K. E., M. E. Avery, and K. Bensch. 1964. Time course of changes in surface tension and morphology of alveolar epithelial cells in CO_2-induced hyaline membrane disease. J. Clin. Invest. 43: 2080-2093.

211. Schultz, H. 1959. The submicroscopic anatomy and pathology of the lung. Springer-Verlag, Berlin. 108 pp.

212. Sexton, J. D. and D. L. Beckman. 1975. Neurogenic influence on pulmonary surface tension and cholesterol in cats. Proc. Soc. Exptl. Biol. Med. 148: 679-681.

213. Sharp, J. T., G. T. Griffith, I. L. Bunnell, and D. G. Greene. 1958. Ventilatory mechanics in pulmonary edema in man. J. Clin. Invest. 37: 111-117.

214. Sharp, J. T., I. L. Bunnell, G. T. Griffith, and D. G. Greene. 1961. The effects of therapy on pulmonary mechanics in human pulmonary edema. J. Clin. Invest. 40: 665-672.

215. Singer, D., C. Hesser, R. Pick, and L. N. Katz. 1958. Diffuse bilateral pulmonary edema associated with unilobar miliary pulmonary embolization in the dog. Circ. Res. 6: 4-9.

216. Slavin, G., L. Kreel, A. Herbert, and B. Sandin. 1975. Pulmonary oedema at necropsy: A combined pathological and radiological method of study. J. Clin. Path. 28: 357-366.

217. Smith, U. and J. W. Ryan. 1973. Electron microscopy of endothelial and epithelial components of the lungs: Correlations of structure and function. Fed. Proc. 32: 1957-1966.

218. Snedecor, G. W. and W. G. Cochran, eds. 1972. Statistical methods. 6th ed. Iowa State University Press, Ames.

219. Sobonya, R. E. and J. Kleinerman. 1973. Recurrent pulmonary edema induced by alpha-napthyl-thiourea. Amer. Rev. Respir. Dis. 108: 926-932.

220. Sorenson, S. C. and J. W. Severinghaus. 1968. Irreversible respiratory insensitivity to acute hypoxia in man born at high altitude. J. Appl. Physiol. 25: 217-229.

221. Starling, E. H. 1896. On the absorption of fluids from the connective tissue spaces. J. Physiol. 19: 312-326.

222. Staub, N. C. 1963. The interdependence of pulmonary structure and function. Anesthesiology. 24: 831-854.

223. Staub, N. C. 1966. Effects of alveolar surface tension on the pulmonary vascular bed. Jap. Heart J. 7(4): 386-399.

224. Staub, N. C. 1971. Steady state pulmonary transvascular water filtration in unanesthetized sheep. Circ. Res. 1(Supp. 28/29): 135-139.

225. Staub, N. C. 1974. "State of the art." Review. Pathogenesis of pulmonary edema. Amer. Rev. Respir. Dis. 109: 358-372.

226. Staub, N. C., H. Nagano, and M. L. Pearce. 1967. Pulmonary edema in dogs, especially the sequence of fluid accumulation in lungs. J. Appl. Physiol. 22: 227-240.

227. Staub, N. C., M. Gee, and C. Vreim. 1976. Mechanism of alveolar flooding in acute pulmonary oedema. Excerpta Medica 38: 255-272.

228. Suzuki, Y., T. Takeda, C. S. Yao, and R. Tabata. 1976. Studies of factors influencing alveolar lining layer formation in lung homogenate: Further isolation and identification of interfering materials. Japan. J. Exptl. Med. 46: 51-57.

229. Szidon, J. P., G. G. Pietra, and A. P. Fishman. 1972. The alveolar-capillary membrane and pulmonary edema. New Engl. J. Med. 286: 1200-1204.

230. Takino, M. 1935. Über die Innervation der Lungeng efässwand, besonders über das Vorkommen der Ganglienzellen an der Gefässwand der Venae pulmonales und über die Verbreitungsyustünde der Lungenblutgefassnerven bei der Fledermaus. Acta Sch. Med. Univ. Kioto 15: 303-307.

231. Taylor, A. E. and R. A. Gaar, Jr. 1970. Estimation of equivalent pore radii of pulmonary capillary and alveolar membranes. Amer. J. Physiol. 218: 1133-1140.

232. Taylor, A. E., W. H. Gibson, H. J. Grangen, and A. C. Guyton. 1973. The interaction between intracapillary and tissue forces in the overall regulation of interstitial fluid volume. Lymphology 6: 192-208.

233. Tenny, S. M. and J. E. Remmers. 1963. Comparative quantitative morphology of the mammalian lung: Diffusing area. Nature 197: 54-56.

234. Teplitz, C. 1968. The ultrastructural basis for pulmonary pathophysiology following trauma. J. Trauma 8: 700-703.

235. Tierney, D. F. 1965. Pulmonary surfactant in health and disease. Dis. Chest 47: 247-253.

236. Tierney, D. F. and R. P. Johnson. 1965. Altered surface tension of lung extracts and lung mechanics. J. Appl. Physiol. 20: 1253-1260.

237. Visscher, M. B., F. J. Haddy, and G. Stephens. 1956. The physiology and pharmacology of lung edema. Pharmacol. Rev. 8: 389-434.

238. Viswanathan, R., S. K. Jain, S. Subramanian, T. A. V. Subramanian, G. L. Dua, and J. Giri. 1969. Pulmonary edema of high altitude. II. Clinical, aerodynamic and biochemical studies in a group with history of pulmonary edema at high altitude. Amer. Rev. Respir. Dis. 100: 334-341.

239. Von Neergard, K. 1929. Neue Auffassungen über einen Grundbegriff der Atemmechanic: Die Retraktionskraff der Lunge, abhangig von der Oberflachenspannung in den Alveolen. Z. Gesamte Exptl. Med. 66: 373-394.

240. Vreim, C. E. and N. C. Staub. 1976. Protein composition of lung fluids in acute alloxan edema in dogs. Amer. J. Physiol. 230: 376-379.

241. Warren, M. F., D. K. Peterson, and C. K. Drinker. 1942. The effects of heightened negative pressure in the chest, together with further experiments upon anoxia in increasing the flow of lung lymph. Amer. J. Physiol. 137: 641-648.

242. Weber, K., J. R. Pringle, and M. Osborn. 1972. Measurement of molecular weights by electrophoresis on SDS-acrylamide gel. Methods in Enzymology 26: 3-27.

243. Weibel, E. R. 1973. Morphological basis of alveolar-capillary gas exchange. Physiol. Rev. 53: 419-495.

244. Weibel, E. R. and J. Gil. 1968. Electron microscopic demonstration of an extracellular duplex lining layer of alveoli. Respir-Physiol. 4: 42-57.

245. Welch, W. H. 1878. Zur Pathologie des Lungenödems. Virchows Arch. 72: 375-412.

246. West, J. B. 1971. Causes of carbon dioxide retention in lung disease. New Engl. J. Med. 284: 1232-1236.

247. West, J. B., C. T. Dollery, and A. Naimark. 1964. Distribution of blood flow in isolated lung, relation to vascular and alveolar pressure. J. Appl. Physiol. 19: 713-724.

248. West, J. B., C. T. Dollery, and B. E. Heard. 1965. Increased pulmonary vascular resistance in the dependent zone of the isolated dog lung caused by perivascular edema. Circ. Res. 17: 191-206.

249. Whayne, T. F., Jr. and J. W. Severinghaus. 1968. Experimental hypoxic pulmonary edema in the rat. J. Appl. Physiol. 25: 729-732.

250. Widdicombe, J. G. and J. A. Nadel. 1963. Airway volume, airway resistance, and work and force of breathing: Theory. J. Appl. Physiol. 18: 863-868.

251. Wilen, S., J. Rubin, and H. Lyons. 1975. Vascular leakage of protein in non-cardiac and cardiac pulmonary-edema. Circulation 52: 130.

252. Williams, M. H., Jr. 1953. Effect of ANTU-induced pulmonary edema on the alveolar-arterial oxygen pressure gradient in dogs. Amer. J. Physiol. 175: 84-86.

253. Wood, J. E. and S. B. Roy. 1970. The relationship of peripheral venomotor responses to high altitude pulmonary edema in man. Amer. J. Med. Sci. 259: 56-65.

254. Woolcock, A. J., N. J. Vincent, and P. T. Macklen. 1969. Frequency dependence of compliance as a test for obstruction in small airways. J. Clin. Invest. 48: 1097-1106.

255. Yeager, H., Jr. and D. Massaro. 1972. Glucose metabolism and glycoprotein synthesis by lung slices. J. Appl. Physiol. 32: 477-482.

256. Young, S. L. and D. F. Tierney. 1972. Dipalmitoyl lecithin secretion and metablism by the rat lung. Amer. J. Physiol. 222: 1539-1544.

257. Zinberg, S., Nudell, G., Kubicek, W. G., and Visscher, M. B. 1948. Observations on the effects on the lungs of respiratory air flow resistance in dogs with special reference to vagotomy. Amer. Heart J. 35: 774-779.

APPENDIX A: TYPICAL BECKMAN RECORDING OBTAINED DURING THE BASELINE PERIOD

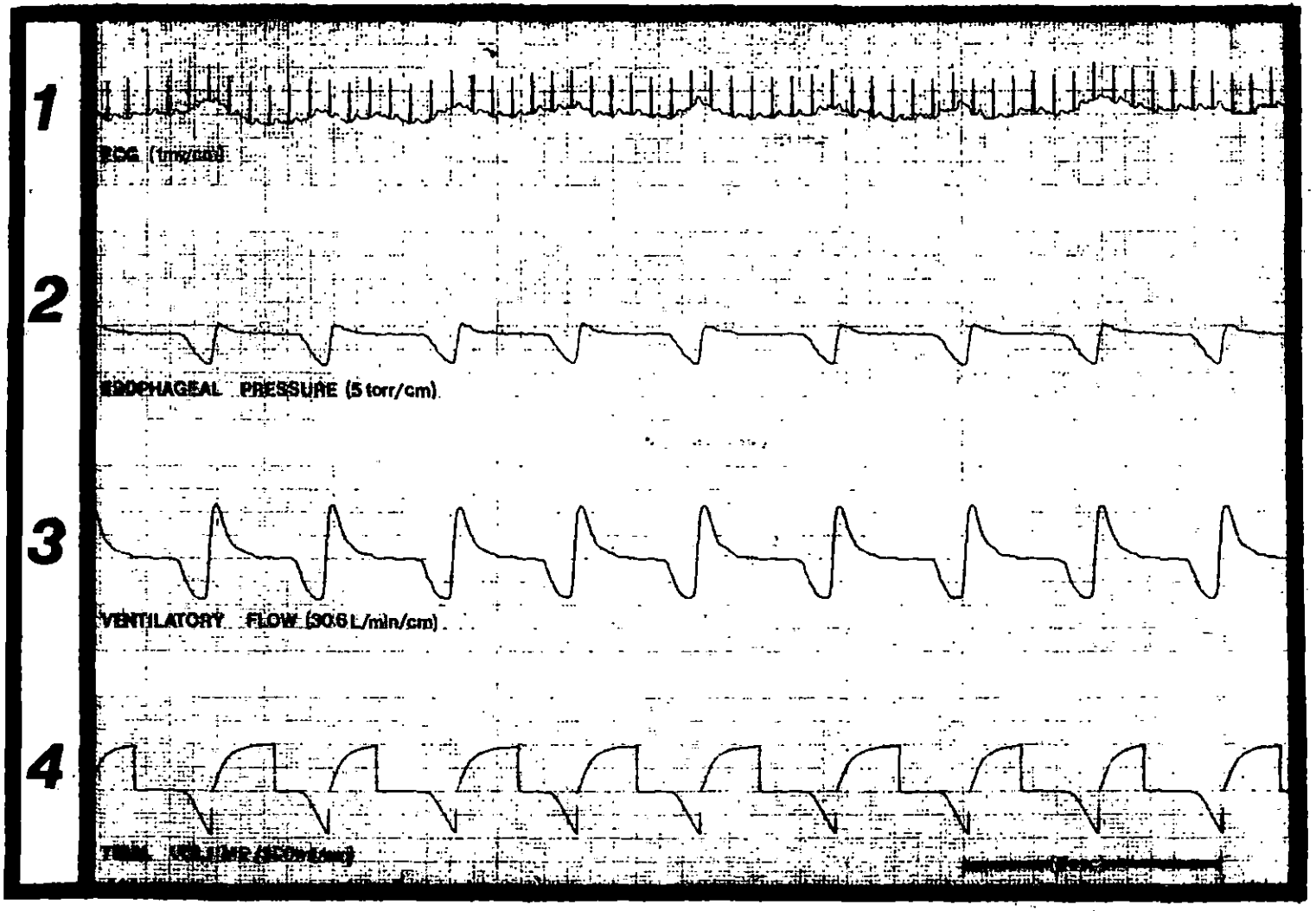

Figure 28. Tracing is continuous from right to left showing simultaneous recordings of a Lead II electrocardiogram (channel 1), esophageal pressure (channel 2), ventilatory flow (channel 3), and tidal volume (channel 4). The inspiratory phase of the respiratory cycle is represented by downward deflections on channel 2, 3, and 4.

APPENDIX B: TYPICAL INSPIRATORY AND EXPIRATORY ISOPLETHS GENERATED BY AN X-Y RECORDER FROM SPECIFIC PLOTS OF RESPIRATORY VARIABLES AS RECORDED BY A DYNOGRAPH

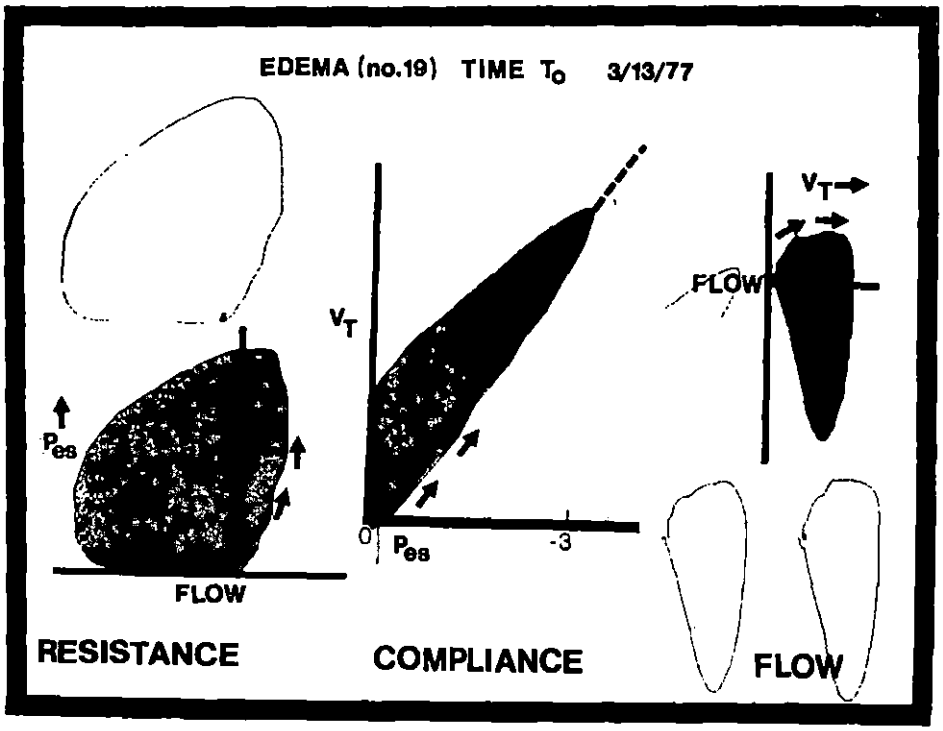

Abbreviations used: esophageal pressure (P_{es}, cm H_2O), tidal volume (V_T, ml). Flow is measured as L/min. Arrows indicate beginning of inspiratory phase of the respiratory cycle.

APPENDIX C: MOLECULAR WEIGHT DETERMINATION OF PROTEINS BY SDS GEL ELECTROPHORESIS

(cf. Weber et al. (242))

Reagents:

1. Acrylamide - Ames Co.
2. N,N'-methylenebisacrylamide H.P. - Conalco Inc.
3. N,N,N',N'-tetramethylethylenediamine (TEMED) - Conalco Inc.
4. Sodium dodecyl sulfate (SDS) - Fisher Scientific Co.
5. β-mercaptoethanol - Aldrich Chemical Co.
6. Ammonium persulfate - Conalco Inc.
7. Bromophenyl blue - Matheson Coleman and Bell
8. Sucrose crystals - Fisher Scientific Co.
9. Coomassie Brilliant Blue R-250 - Bio-Rad Laboratories
10. Methanol - Fischer Scientific Co.
11. Sodium phosphate, diabasic ($NA_2HPO_4 \cdot 7H_2O$) - Fisher Scientific Co.
12. Sodium phosphate, monobasic ($NaH_2PO_4 \cdot H_2O$) - Fisher Scientific Co.
13. Glacial acetic acid

Solutions:

1. Acrylamide stock: 22.2 g acrylamide, 0.6 g methylenebisacrylamide H.P., water to 100 ml. (Dissolve acrylamide (120°C) before adding methylenebisacrylamide. Filter through glass wool. Store 1 month in dark at 4°C.)
2. Gel buffer, 0.2 M, pH 7.2: 7.8 g $NaH_2PO_4 \cdot H_2O$, 38.6 g $Na_2HPO_4 \cdot 7H_2O$, 2.0 g SDS, water to 1000 ml.
3. Ammonium persulfate: 15 mg, water to 1 ml. (Use immediately.)

4. Separating gel, 7.5%, pH 7.0: 10 ml acrylamide solution, 3.4 ml distilled water, 15.0 ml gel buffer, 0.7 ml ammonium persulfate, 0.025 ml TEMED.
5. Reservoir buffer: 1 part gel buffer, 1 part water.
6. Sample buffer, 0.01 M, pH 7.0: 1.38 g $NaH_2PO_4 \cdot H_2O$, 2.68 g $Na_2HPO_4 \cdot H_2O$, adjust pH with 5 N NaOH, water to 1000 ml.
7. Working buffer, 0.01 M, pH 7.0 containing 1% SDS and 1% β-mercaptoethanol: 1.38 g $NaH_2PO_4 \cdot H_2O$, 2.68 g $Na_2HPO_4 \cdot 7H_2O$, 1g SDS, 1 ml β-mercaptoethanol, water to 100 ml.
8. Tracking dye: 50 mg bromophenyl blue, sample buffer to 100 ml.
9. Staining solution: 91 ml methanol, 9 ml glacial acetic acid, 250 mg Coomassie Blue. (The methanol permits staining and gel fixation to occur simultaneously.)
10. Destaining solution: 5 ml methanol, 7.5 ml glacial acetic acid, 87.5 ml distilled water.

Apparatus:

1. Ames Model 1200 Electrophoresis Bath Assembly.
2. Ames Model 1400 Electrophoresis Power Source.
3. Multi-purpose Rorator Model 150V (Scientific Industries Inc.).
4. Ames Model 1801 Quick Gel Destainer.

Procedures:

1. Preparation of separating gel: Acrylamide stock solution (10 ml) was brought to room temperature and carefully added to 3.4 ml distilled water and 15 ml gel buffer in a 50 ml volumetric vacuum flask. The solution was de-aerated for 2 minutes under vacuum with gentle

continuous swirling. Ammonium persulfate (0.7 ml) and 0.025 ml TEMED were added down the sides of the flask to hinder bubble formation. The final solution was again de-aerated with gentle swirling for one minute.

2. Pre-siliconized glass tubes (150 mm x 6 mm, o.d.) were filled with separating gel to a height of 120 mm with a long 14 gauge blunt-tip needle attached to a 10 cc glass syringe.
3. Gels were quickly layered with distilled water (5 mm) to remove the gel meniscus.
4. Polymerization at room temperature was complete within 1 1/2 hours, although gels were allowed to set for 5 hours before use.
5. Sample preparation: lyophilized lavage material (20 mg dry weight) was dissolved in 0.5 ml sample buffer.
6. The reconstituted sample was added to 4.5 ml hot (100°C) working buffer in a 15 ml glass stoppered centrifuge tube.
7. The tubes were capped and the reaction allowed to proceed for 6 minutes with intermittent shaking.
8. The tubes were removed from the boiling water bath and allowed to cool to room temperature for approximately 45 minutes during which further incubation was allowed to proceed.
9. An aliquot (1 ml) of the cooled protein solution was added to a glass culture tube (75 mm x 10 mm, o.d.) containing 80 µl tracking dye, 40 sucrose crystals, and 60 µl β-mercaptoethanol.
10. The final mixture was vortexed (3-5 min) until sucrose crystals were dissolved.

11. Triplicate gels of 100 µl samples were applied by microsyringe to the top of the polymerized gels and filled to the top with reservoir buffer.
12. The upper and lower bath of the electrophoresis apparatus were filled to maximum capacity with reservoir buffer.
13. Electrophoresis was carried out at 5 mAmp/gel for 12 hours or 8 mAmp/gel for 6 hours at which time the tracking dye was 10-15 mm from the bottom of the tube. Migration distances were identical regardless of the running conditions.
14. Gels were carefully removed from the tubes and migration of the tracking dye was marked by penetrating the gel with indigo ink.
15. Gels were placed directly into 20 ml glass tubes filled with staining solution containing fixative.
16. Three hours at room temperature was required for optimal staining at which time the gels were rinsed with distilled water and placed into the destaining solution.
17. Diffusion destaining was accomplished by constant motion at 5 rpm for 72 hours with the destaining solution being changed three times.
18. The gels were placed in the quick gel destaining chamber in the same destaining solution for 10 minutes or until destaining was complete.
19. Migration distances of unknown proteins and tracking dye were measured from the top of each gel. Mobilities were calculated directly as follows:

$$\text{Mobility} = \frac{\text{Distance traveled by unknown band}}{\text{Distance traveled by tracking dye}}$$

Actual molecular weight (dependent variables) were determined from the regression line determined by the mobilities of the bovine serum albumin, catalase, and trypsin standards of each electrophoretic run. The line of best fit was computed by the semi-logarithmic regression equation as follows:

$$Y = A + B_{Log_{10}} x$$

where Y is the molecular weight of the unknown band, A is the ordinate intercept, B is the regression function, and x is the mobility of the unknown protein band.

APPENDIX D: PREPARATION OF TISSUES FOR ELECTRON MICROSCOPY

Reagents:

1. Sodium phosphate, diabasic ($Na_2HPO_4 \cdot 7H_2O$) - Fisher Scientific Co.
2. Sodium phosphate, monobasic ($NaH_2PO_4 \cdot H_2O$) - Fisher Scientific Co.
3. Ethanol (100%) - Fisher Scientific Co.
4. Acetone (100%) - Fisher Scientific Co.
5. Glutaraldehyde (50%) - Fisher Scientific Co.
6. Osmium tetroxide (OsO_4) - Electron Microscopy Sciences.
7. Epon 812 resin - Electron Microscopy Sciences.
8. Araldite 502 resin - Ciba Products Inc.
9. Dodecenyl succinic anhydride (DDSA) - Ernest F. Fullam Inc.
10. Dimethylaminomethylphenol (DMP-30) - Ernest F. Fullam Inc.
11. Uranyl acetate [$UO_2(C_2H_3O_2)_2 \cdot 2H_2O$] - Mallinckrodt Chemical Works.
12. Lead citrate.

Solutions:

1. Buffer A: 30.32 g/1000 ml monobasic phosphate crystals.
2. Buffer B: 28.32 g/1000 ml diabasic phosphate crystals.
3. Stock buffer, 0.2 M, pH 7.4: 19 ml A, 81 ml B.
4. Fixative, 4% in 0.1 M buffer at pH 7.4: 25 ml stock buffer, 10 ml 50% glutaraldehyde, 21 ml distilled water.
5. Wash: stock buffer/distilled water (1:1, v/v).
6. Post-fix: stock buffer/0.2 M OsO_4 (1:1, v/v).
7. Resin: 15.85 g DDSA, 1.4 g Araldite 502, 9.85 g Epon 812, 0.65 g DMP-30.

8. Uranyl acetate stain, pH 3.7: 0.2 g uranyl acetate, 40 ml distilled water. Vigorously shake (ca. 10 min) until solution clears.
9. Lead citrate stain. 100 ml distilled water, 0.4 g lead citrate, 1.0 ml 10 N sodium hydroxide. Shake vigorously in an air-tight vial.

Procedures:

1. Fix fresh tissue blocks (<1 mm^3) at 4°C for 12 hours.
2. Wash 3X (5 min).
3. Post-fix at 4°C for 1 1/2 hours.
4. Wash in distilled water 3X (5 min).
5. Dehydrate:
   a. 3X (5 min) in 70% ethanol.
   b. 1X (15 min) in 95% ethanol.
   c. 3X (20 min) in 100% ethanol.
6. Infiltrate:
   a. 3X (20 min) in 100% acetone.
   b. 2 hours in mixture resin/acetone (1:3, v/v).
   c. 2 hours in mixture resin/acetone (1:1, v/v).
   d. 4 hours in mixture resin/acetone (3:1, v/v).
   e. 6 hours in pure resin.
7. Embed in pure resin in aluminum weighing pans.
8. Polymerize at 65°C for 48 hours.

APPENDIX E: SUMMARY OF VENOUS P_{O_2}, P_{CO_2}, pH, HCO_3^-, AND BE AT TIMED INTERVALS BEFORE AND AFTER INJECTION OF SALINE (1.8 ML/KG) IN 5 CONTROL DOGS AND ALLOXAN (140 MG/KG) IN 4 TREATMENT DOGS

Table 9. Summary of venous P_{O_2}, P_{CO_2}, pH, HCO_3^-, and BE at timed intervals before and after injection of saline (1.8 ml/kg) in 5 control dogs and alloxan (140 mg/kg in 4 treatment dogs

Variable	Group	Baseline	Time, post-injection			
			30 min	60 min	90 min	120 min
P_{O_2} (torr)	C	57.8±7.3[a]	55.4±4.5	57.1±6.8	56.2±9.9	56.8±7.3
	AE	59.8±3.2	48.0±7.1	47.9±3.3[b]	43.6±6.0[b]	40.7±11.1[b]
P_{CO_2} (torr)	C	56.9±7.4	55.3±8.1	51.4±11.7	50.9±11.4	49.1±10.0
	AE	50.6±6.8	47.2±5.5	48.4±6.3	46.4±7.6	44.6±6.3
pH	C	7.314±0.05	7.305±0.02	7.331±0.04	7.311±0.03	7.319±0.04
	AE	7.203±0.04	7.189±0.07[c]	7.215±0.04[c]	7.218±0.02[c]	7.216±0.05[c]
HCO_3^- (mEq/L)	C	25.6±4.2	26.9±3.1	25.4±3.8	24.9±4.3	24.1±3.4
	AE	23.5±4.4	17.6±2.2[c]	19.0±1.2[b]	18.4±2.3[b]	17.5±1.2[b]
BE (mEq/L)	C	-0.7±2.6	0.1±2.9	-0.7±2.0	-1.3±3.0	-2.3±2.6
	AE	-1.1±1.8	-9.8±2.9[c]	-8.0±1.0[c]	-8.3±1.7[c]	-8.8±0.9[c]

[a]Values represent mean ± SD.

[b]Significantly different from control value obtained during same time interval ($P<0.05$).

[c]Significantly different from control value obtained during same time interval ($P<0.01$).